PROLIFERATION RESISTANCE OF UTILIZING ENRICHED REPROCESSED URANIUM: INVESTIGATION OF ENRICHED REPROCESSED URANIUM FUEL FOR INHERENT PROTECTION OF URANIUM AND PLUTONIUM AGAINST PROLIFERATION

A Thesis

by

SAEHYUN CHOI

Submitted to the Graduate and Professional School of
Texas A&M University
in partial fulfillment of the requirements for the degree of

MASTER OF SCIENCE

Chair of Committee,	Sunil S. Chirayath
Committee Members,	John Ford
	Brent Miller
Head of Department,	Michael Nastasi

August 2021

Major Subject: Nuclear Engineering

Copyright 2021 Saehyun Choi

ABSTRACT

The proliferation resistance (PR) of enriched reprocessed uranium (ERU) was investigated. The inherent intrinsic proliferation resistance to production of a uranium or plutonium based nuclear explosive device (NED) is the focus of this study. This study is expected to encourage the employment of closed nuclear fuel cycle employing light water reactors (LWRs), in order to efficiently use uranium resources and reduce the deep geological repository as well.

Reprocessed uranium (RepU), compared to natural uranium contains higher concentration of ^{234}U and other uranium isotopes, such as ^{232}U, ^{233}U, and ^{236}U. The presence of minor isotopes affects the uranium enrichment process and in turn the composition of used fuel discharged from a power reactor. As reprocessing recycling of discharged uranium is repeated, the minor uranium isotopes tend to accumulate more in ERU. ^{238}Pu renders plutonium less attractive for a NED and its buildup is enhanced by the increase of ^{236}U. When ERU is used as fuel in an LWR, ^{238}Pu content in plutonium can easily exceed 6.2% and is expected to provide high intrinsic PR, because it is an undesired isotope of plutonium in a NED due to its high decay heat and spontaneous fission rate.

Besides denaturing plutonium with ^{238P}Pu, RepU holds advantage over natural uranium in terms of discouraging production of highly enriched uranium (HEU). Uranium enrichment process is to preferentially enrich ^{235}U using a physical enrichment method and a gas centrifuge enrichment plant is a commercial means to enrich uranium in bulk. However, the presence of minor uranium isotopes ^{232}U, ^{234}U, and ^{236}U in the discharged fuel complicates this selective ^{235}U enrichment process. ^{232}U complicates the enriched uranium product and the enrichment facility with high γ-radiation, whereas ^{234}U and ^{236}U are neutron poisons.

A matched-abundance ratio cascade (MARC) model was applied to accurately estimate the enrichment of the multi-isotope uranium. The MARC was followed by Monte Carlo N-Particle Transport (MCNP) to simulate the burnup of ERU fuel in a conventional LWR. Both codes were successful in verifying the PR of ERU. After 3 fuel cycles, whereby discharged uranium was reprocessed, enriched, and recycled twice, denatured plutonium was attained and after the 4^{th} fuel cycle, denatured uranium was also attained. Nevertheless, ERU became contaminated with ^{232}U and ^{234}U and the maximum burnup or the amount of electricity generation diminished after 3 fuel cycles. Therefore, further uranium recycling was impractical past that point.

The potential of applying RepU regeneration technique was raised. While this technique can prolong the uranium recycling period, proliferators may acquire the technique to reverse the isotopic denaturing. Thus, further study can be done to enhance the PR of RepU regeneration technique.

ACKNOWLEDGEMENTS

I would like to thank my committee chair, Dr. Chirayath, and my committee members, Dr. Ford, and Dr. Miller, for their guidance and support throughout the course of this research. Thanks also go to my wonderful friends and colleagues I have made at this university for making my time at Texas A&M University a great experience. Finally, thanks to wife, Dayeong Kim, for her encouragement, patience and love.

CONTRIBUTORS AND FUNDING SOURCES

Contributors

This work was supervised by a thesis committee consisting of Professor Sunil S. Chirayath and John Ford of the Department of Nuclear Engineering and Professor Brent Miller of the Department of Geology and Geophysics.

The initial idea for this project was conceived by Professor Sunil S. Chirayath of the Department of Nuclear Engineering.

All other work conducted for the thesis was completed by the student independently.

Funding Sources

Graduate study and thesis research were supported by a fellowship from Republic of Korea Army.

NOMENCLATURE

ENU	Enriched normal uranium
ERU	Enriched reprocessed uranium
HEU	Highly enriched uranium
HLW	High-level waste
HNED	Hypothetical nuclear explosive device
IAEA	International Atomic Energy Agency
LEU	Low enriched uranium
MA	Minor actinide
MARC	Matched-abundance ratio cascade
MCNP	Monte Carlo N- Particle transport
MIST	Minor Isotope Safeguards Techniques
NED	Nuclear explosive device
Pu	Pu
PR	Proliferation resistance
RepU	Reprocessed uranium
RGPu	Reactor grade Pu
SNM	Special nuclear material
U	Uranium
WgNU	Weapon-grade natural uranium
WgRU	Weapon-grade reprocessed uranium

WgU	Weapon-grade uranium
^{232}U	Uranium-232
^{233}U	Uranium-233
^{234}U	Uranium-234
^{235}U	Uranium-235
^{236}U	Uranium-236
^{238}U	Uranium-238
^{238}Pu	Plutonium-238
^{239}Pu	Plutonium-239
^{240}Pu	Plutonium-240
^{241}Pu	Plutonium-241
^{242}Pu	Plutonium-242

TABLE OF CONTENTS

Page

LIST OF FIGURES

FIGURE Page

Page

Page

LIST OF TABLES

1. INTRODUCTION

1.1 Objective

The objective of this project was to study enhanced production of ^{238}Pu, a major proliferation resistance isotope of plutonium (Pu) in used fuel due to the presence of ^{236}U in enriched reprocessed uranium (ERU) as fresh fuel. The second objective was to investigate the proliferation resistance of reprocessed uranium (RepU) due to the presence of minor uranium (U) isotopes such as ^{234}U and ^{236}U as an inhibitor to the production of highly enriched uranium (HEU). The results of the study can be used to support the idea of using ERU in light water reactors (LWRs) to safeguard special nuclear material (SNM), thereby result in efficiently using U resources and reducing the volume of deep geological repository. The enrichment product of RepU and the difficulties associated with the process are assessed using the matched-abundance ratio cascade (MARC) model. Following the MARC model, the production of ^{238}Pu is estimated through simulations of fuel burnup in an LWR using Monte Carlo N- Particle Radiation Transport (MCNP) code.

1.2 Background

Nuclear energy is used throughout the world providing about 10% of the world's electricity from about 440 power reactors and is expected to grow further. One of the distinct features that makes nuclear energy production different from that of traditional fossil fuel energy production is its long-term radioactive waste after the fuel is used. Unlike the fossil fuels, when nuclear fuel is discharged, they are physically in the same shape and about the same weight as when they were fresh. Additionally, the discharged nuclear fuel still contains more than 90% of U that was originally in the fresh fuel and about 1% of the discharged nuclear fuel is Pu [1]. The growth of

nuclear electricity production involves accumulation of Pu in used fuel and increment of separated Pu (Fig. 1.1).

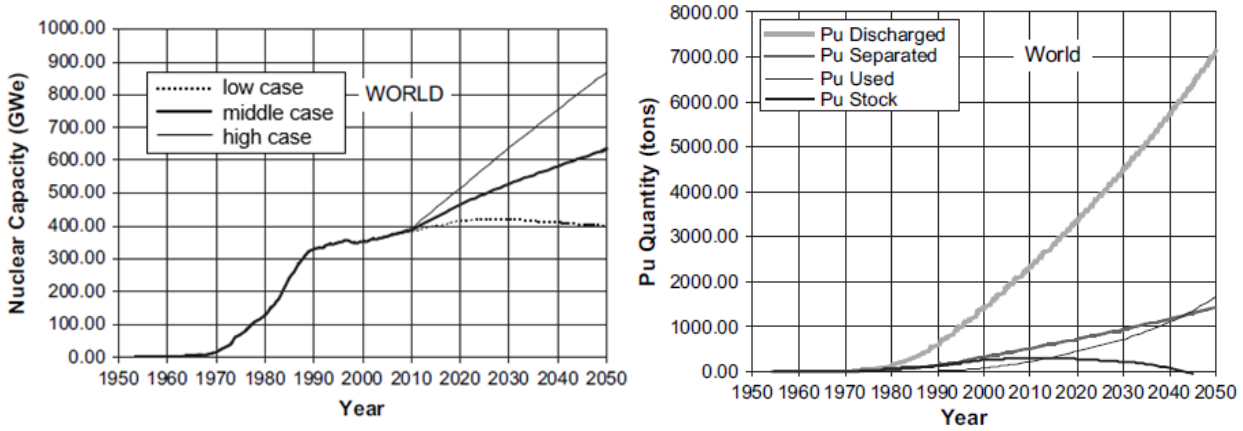

(a) (b)

Figure 1.1. Growth of (a) nuclear electricity production capacity in the world and (b) Pu inventories in various stage of the world. [2]

There exist two options for handling the used nuclear fuel; One is disposal in a deep geological repository and the other is its reprocessing and recycling in nuclear reactors. These options are referred to as open and closed fuel cycles, respectively. Historically, a majority of acquisition paths for the proliferating states involves the back end of the fuel cycle, or more specifically, reprocessing the used fuel for Pu extraction [3, 4]. Due to its inherent risk of nuclear proliferation, many studies have warned the proliferation risk of reprocessing and U.S. President Gerald Ford suspended the domestic commercial reprocessing process in the United States through a Presidential directive [5]. Subsequently his successor, U.S. President Jimmy Carter banned the reprocessing of civilian used nuclear fuel and tried to persuade other nations to follow the U.S. example. In spite of the efforts made, other nations, such as France, the United Kingdom, Russia, Japan, India, Pakistan, and North Korea continued the reprocessing of used nuclear fuel and are now reprocessing approximately 4,200 metric tons of used nuclear fuel per year [6]. The major reasons for choosing the option of reprocessing have been the efficient utilization of U resources

and the reduction of the volume of high-level radioactive waste (HLW) to about one-fifth [7]. In the future, the competitiveness of reprocessed-and-recycled U fuel to natural U fuel will increase even taking the increment of the fuel burnup into consideration [8].

Thus, the intrinsic and extrinsic barriers to proliferation play important roles in the reprocessing of used fuel. Denaturing of a fissile material, such as U or Pu, is one of the intrinsic barriers that renders the fissile material less suitable and less attractive for nuclear explosive device (NED) but does not affect its value as a source of nuclear energy for civilian energy uses. Isotopic denaturing using even-numbered isotopes is known to be less reversible than chemical denaturing because isotopic separation capability is required to obtain weapons-grade material. Isotopic denaturing can directly influence the fission-explosive potential of fissionable materials by (1) increasing the mass and radius of a critical configuration, (2) introducing extraneous sources of radiation and heat, and (3) influencing neutron interactions in the critical assembly [9]. The International Atomic Energy Agency (IAEA) defined that Pu containing more than 80% ^{238}Pu can be exempted from safeguards. This is the only official criterion with respect to the isotopic barrier of Pu, which is based on the characteristic of Pu such as critical mass, heat-generation rate, spontaneous neutron generation, and radiation [10]. Recent studies for quantitative approaches to assess the denatured Pu suggest that Pu, of which ^{238}Pu fraction exceeding 6.2% or higher, would cause a nuclear explosive device to fizzle or pre-detonate due to ^{238}Pu spiking [11 - 15]. Besides the ^{238}Pu spiking, the high specific alpha radiation activity of ^{238}Pu deteriorates the re-enrichment of denatured Pu. Plutonium hexafluoride, a molecule in gaseous form at enrichment phase, is decomposed into plutonium tetrafluoride and free fluorine gas when it is exposed to intensive alpha radiation. The decomposition, ultimately, leads to the almost insurmountable barrier to undoing the Pu denaturing [16]. Such proliferation resistant Pu can be produced by employing ERU or

minor actinides (MAs). Specifically, the ^{238}Pu level is artificially boosted by introducing ^{238}Pu precursors such as ^{236}U, ^{237}Np, ^{241}Am, and ^{242}Cm into a fuel.

ERU contains relatively higher ^{234}U in addition to the other U isotopes, ^{232}U and ^{236}U, compared to natural U. Estimating the ^{236}U fraction in ERU after enrichment is necessary to assess the level of ^{238}Pu production after irradiation since ^{236}U is enriched along with ^{235}U. However, the theory of separation of binary isotope mixtures is inadequate to identify the isotopic concentration of ERU. Moreover, ERU is produced only with gas centrifuge enrichment technology due to its advantage: modular cascade, relatively short equilibrium time, and low inventory [17]. Thus, the calculation of multicomponent isotope separation in matched abundance cascades, composed of stages with large stage separation factors, is required to accurately estimate the ^{236}U fraction in ERU. Additionally, the neutron poisoning effect of ^{236}U must be taken into consideration when operating the reactor with ERU. Otherwise, it must be compensated with higher ^{235}U concentration to produce ERU fuel with equivalent criticality similar to that of a usual low enriched uranium (LEU) fuel. The additional ^{235}U, termed the ^{236}U compensation or penalty factor, ranges from 0.25 to 0.33: that is, 0.25 to 0.33 units of additional ^{235}U to compensate for 1 unit of initial ^{236}U in the RepU [18-25]. The ^{236}U compensation factor depends on fuel burnup, power plant, initial enrichment, and etc., and thus it is necessary to determine the specific value for each case. [26].

In addition to the contribution of higher ^{238}Pu production, RepU itself can be considered as denatured. In order to produce HEU, the valve setting of a cascade should be modified to prevent the enrichment of ^{236}U, which leads to larger time consumption. Not only ^{236}U, but also ^{232}U hinders the production of HEU. ^{232}U is one of the strongest alpha-emitter and thus 1% ^{232}U in 20% enriched U would destroy around 48% of uranium hexafluoride molecules to low uranium fluorides and free fluorine which will create insurmountable difficulties for the re-enrichment

process [27]. Besides the high-energy alpha particles, the daughter products of ^{232}U, ^{208}Ti and ^{212}Bi, emit high-energy gamma radiation that improves the detectability and increase the difficulty of handling the uranium, which are good proliferation resistance metrics.

1.3 Previous Work

The practical value of producing denatured Pu through the so call Protected Plutonium Production (PPP) to obtain high concentration of ^{238}Pu was introduced by Union Carbide staff members [28]. The early concept of producing a high deterrence Pu focused on the doping of ^{237}Np or blending of reprocessed U with enriched U [9, 29]. Later, J. V. Massey tried to quantify the amount of ^{237}Np and ^{236}U required to induce the heat spiking [30]. In the recent study by Broeders [31], he compared the contribution of different fuel types with different compositions—reprocessed U, reprocessed U blended with Pu, reprocessed U blended with Pu and minor actinides, reprocessed U blended with thorium, Pu, and other minor actinides—for the production of denatured Pu. However, his reprocessed U enrichment calculation was based on the rule of thumb; the ratio of ^{235}U and ^{236}U enrichment chosen as 4:3. K. Fukuda extensively studied the contribution of ^{236}U and minor actinides by manipulating the fuel burnup and the composition of ERU blended with minor actinides [32]. In his study, ERU is possible to have a buildup of 6% ^{238}Pu in the total Pu at high burnup. Nevertheless, the enrichment of the reprocessed U was computed using the equation proposed by M. Benedict which does not account for ^{232}U and ^{234}U [33]. In the same sense, E.F. Kryuchkov *et al.,* estimated the proliferation resistance effect of ^{232}U by doping U with ^{232}U not by re-enriching RepU [27].

The multicomponent mixture enrichment calculation is the missing link between reprocessed U to enriched reprocessed U. Introduced by A. de la Garza, the matched-abundance ratio cascade (MARC) is suitable for an enrichment facility simulation with a low stage separation

factor [34, 35]. Later his work was advanced by E. von Halle to be applied in an enrichment plant with an arbitrary separation factor larger than 1 [36]. Based on their works, the theory of estimating various properties of multiple streams with multicomponent mixtures using MARC were improved by many researchers such as H. G. Wood, G. A. Sulaberidze, V. D. Borisevich, and A. M. Shephard [37 - 42]. J.R. Coleman *et al.*, G.D. Del Cul *et al.*, and A. Y. Smirnov *et al.*, investigated the recycling of reprocessd U using the MARC model [43 - 45]. Nonetheless, the focus of their studies was on the sustainability of ERU blended with natural U not the proliferation resistance of ERU itself.

1.4 Scope

This project focuses on the verification of the proliferation resistance (PR) of the LWR spent fuel that underwent multiple reprocessing and recycling. PR was examined from two points of view. First, the contribution of ^{236}U to the buildup of ^{238}Pu and even-numbered Pu isotopes. Next, the impracticability of producing weapon-grade U by re-enrichment of used fuel after multiple recycling.

1.5 Methodology

This research is to investigate the contribution of ERU to the production of denatured Pu. The MARC model, or MSTAR calculation [46, 47], was used to determine the isotopic assay of ERU. The enrichment process is assumed to be carried out at a matched-abundance ratio cascade with a relatively large stage separation factor namely, a gas centrifuge enrichment plant. In addition to the U enrichment calculation, the MCNP criticality calculation is performed to determine the equivalent ^{235}U enrichment of ERU compared to usual LEU. Following the multicomponent enrichment calculation, a single Westinghouse PWR AP1000 fuel assembly is modelled using

MCNP 6.2 code [48] to assess the buildup of ^{238}Pu in the irradiated fuel. Finally, the PR of the reprocessed Pu and U was evaluated.

This MS thesis was completed as follows:

1. Simulated the burnup of a single fuel assembly of Westinghouse AP1000 with 5.0 wt% ^{235}U usual enriched normal uranium (ENU) fuel using MCNP6.2 code to estimate the U composition of a used fuel at the end of burnup. The burnup simulations are carried out at an assembly power level of 21.75 MWth until it reaches 42,000 MWd/MTU. Reflecting boundary conditions is applied on the four lateral sides of the fuel assembly and at the top and bottom of the assembly a vacuum boundary condition is assumed. Assuming 100% power, the fuel is irradiated without an intermediate shutdown as with one batch core, the Pu composition of the discharged fuel is acquired. The discharged fuel is simulated for a cooling period of 5 years by setting the reactor power to 0 and the U isotopic composition of reprocessed U obtained from the discharged fuel is estimated.
2. Estimated the composition of ERU fuel by enriching the reprocessed U that is obtained from MCNP simulation. In this process, it is assumed that the ERU fuel is fabricated from reprocessed U without any time delay so that no decay products of minor U isotopes are formed in the fuel. Since the reprocessed U contains minor isotopes in addition to ^{235}U and ^{238}U, the enrichment of reprocessed U is performed using the MARC model instead of simple binary mixture enrichment calculation. ERU is originally enriched to 5.0 wt% ^{235}U.
3. Simulated the burnup of a single fuel assembly with the same condition as the initial step but with the ERU applied as fuel. The irradiation is continued until the k-effective reaches close to unity. After burnup and 5-year cooling period, the Pu composition of the discharged ERU is estimated in order to verify the concentration of ^{238}Pu, which has a goal

of 6.2% by mass. During the entire MCNP simulation process, the relative stochastic errors, the inherent behavior of the methodology, are kept below 1%.

4. Repeated the U reprocessing, re-enrichment, and fuel burnup steps to examine the change in the Pu and U compositions. In addition to the compositions, separative works and RepU feed per 1 kg of ERU product is estimated simultaneously.
5. Evaluated the weight fraction of ^{238}Pu and even-number Pu isotopes, and analyzed the potential advantage of using reprocessed U as a source of energy at an LWR.
6. Estimated the maximum possible ^{235}U enrichment using RepU. Recorded the total cascade flow rate and the amount of U feed. Compared the results with that of utilizing natural U.

2. MATCHED ABUNDANCE RATIO CASCADE

Natural U contains ^{234}U, ^{235}U, and ^{238}U. The most abundant isotope ^{238}U is present in the amount of 99.2742 at% and the principal nuclide utilized in the fission process, ^{235}U, is present in the amount of 0.7204 at%. The trace amounts of ^{234}U exist in U, which is about 0.0054 at%. The function of a U enrichment plant is to increase the ^{235}U content to a level that can sustain a controlled nuclear chain reaction for long periods of time in a nuclear reactor. This separation process takes advantage of differences in the behavior of isotopic molecular species. In general, elementary separation effects are very small. Thus, the elementary separation processes are repeated several times to obtain the desired product concentration. Therefore, using the minimum number of the elementary units to enrich ^{235}U in U to the intended concentration is of great interest in the separation process. An ideal countercurrent cascade, which is generally used to estimate the binary ^{235}U enrichment, gives a simple solution to the question. In the case of a multicomponent mixture, MARC provides a general solution. The aspects of the binary and multicomponent separation theory are elaborated in Appendix A, which were developed and covered by Cohen [49], S. Villani [50], B. Brigoli [51], de la Garza [34, 35], Von Halle [36], H. Wood [37], and G.A. Sulaberidze [52]. Based on the MARC theory, a python code is written to carry out multicomponent mixture enrichment problems and the efforts on verification of the code is presented in Appendices B and C.

2.1 Binary and Multicomponent Mixture Separation

An ideal countercurrent cascade, applied to a binary mixture separation, is known to have the minimum number of separating elements meaning it is the most cost-effective cascade. The term “countercurrent” indicates that the depleted stream of U at each stage is fed to the next lower

stage. It allows the greater recovery of the target isotope extracted from a given quantity of feed. The ideal cascade is a type of tapered cascade that theoretically uses the least number of elements to achieve the required separation. This is achieved by adjusting the flow rate so that two streams from different stages have the same composition at the merge point. The ideal condition, or non-mixing condition can be explained with the following equation,

$$\frac{x_n}{1-x_n} = \frac{x''_{n+1}}{1-x''_{n+1}} = \frac{x'_{n-1}}{1-x'_{n-1}}, \tag{2.1}$$

where x_n is the isotopic concentration at stage *n*, and single and double quotation marks stand for the stage enriching and depleting streams, respectively.

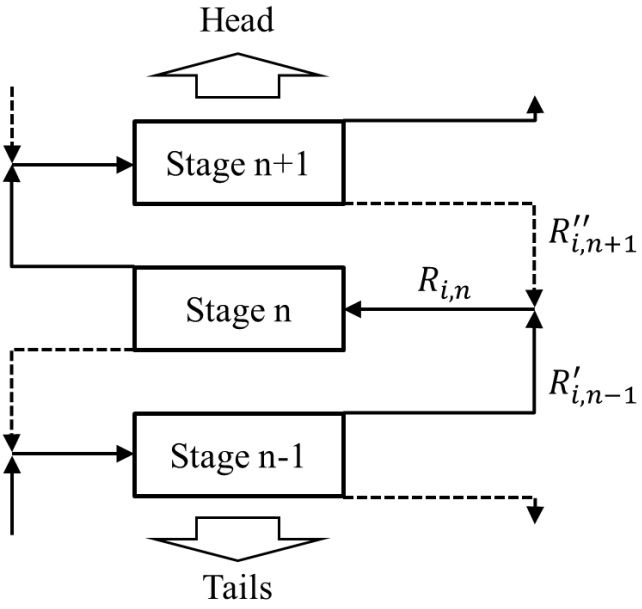

Figure 2.1. Schematic diagram of a MARC for multicomponent mixture separation.

A MARC, which is analogous to the ideal countercurrent cascade, is also known to be the most efficient cascade considering its minimum loss of separating power. Instead of the non-mixing condition specified in Eq. 2.1, MARC assumes that only the ratio of the two main components has a non-mixing condition and the other components are enriched along with the

main components. The non-mixing condition of a MARC is depicted in Fig. 2.1 and the abundance ratio equations are as follows:

$$R_{i,n} = \frac{x_i}{x_k},\ i = 1, \cdots, m \tag{2.2}$$

$$R_{i,n} = R''_{i,n+1} = R'_{i,n-1}, i = j \tag{2.3}$$

$$R_{i,n} \neq R''_{i,n+1} \neq R'_{i,n-1},\ i \neq j, \tag{2.4}$$

where $R_{i,n}$ in equations 2.2, 2.3, and 2.4 is the abundance ratio between i^{th} and k^{th} components. The k^{th} and j^{th} component are named as key and target component, respectively.

A feature found with MARC is that the product and waste stream are same for an arbitrary separation factor as long as the external parameters are consistent. This is critical because it makes MARC provide a reasonable solution for the multicomponent mixture enrichment problem. The separation factor varies depending on the feed rate. Moreover, separation factors may vary from one enrichment facility to another. Difference in separation factor would result in difference in the internal parameters such as the total number of stages, number of parallel elements in a stage, and stage cuts but not the external parameters which are the amounts and compositions of product, waste, and feed.

The purpose of modelling an ideal countercurrent cascade or a MARC is to build a cost-effective cascade. A cost-effective cascade is a cascade that requires the minimum amount of feed and separative work to produce a material at a designated enrichment. The equations for the optimum ideal countercurrent cascade are,

$$C_P = C_F f_{F/P}(x_W) + C_U f_{SWU/P}(x_W), \tag{2.5}$$

$$f_{F/P}(x_W) = \frac{1}{P}\frac{x_P - x_W}{x_F - x_W}, \tag{2.6}$$

$$f_{SWU/P}(x_W) = V(x_P) + \frac{W}{P}V(x_W) - \frac{F}{P}V(x_F), \tag{2.7}$$

$$V(x) = (2x - 1)\ln\frac{x}{1-x}. \tag{2.8}$$

where C_P, C_F, and C_U are the total cost per product, the cost per feed, the cost per separative work respectively; x_P, x_W, and x_F are the product, tails, and feed enrichment respectively; and $V(x)$ is a value function. Similarly, the equations for the MARC are as follows:

$$C_P = C_F f_{F/P}(x_W) + C_U f_{SWU/P}(x_W, M^*), \tag{2.9}$$

$$f_{F/P}(x_{j,W}) = \frac{1}{P}\frac{x_{j,P} - x_{j,W}}{x_{j,F} - x_{j,W}}, \tag{2.10}$$

$$f_{SWU/P}(x_{j,W}, M^*) = V_P + \frac{W}{P}V_W - \frac{F}{P}V_F, \tag{2.11}$$

$$V = \frac{(\gamma_j - 1)}{(\gamma_j + 1)}\sum_{i=1}^{m}\frac{(\gamma_i + 1)}{(\gamma_i - 1)}x_i \ln\frac{x_i}{x_k}, \tag{2.12}$$

$$\gamma_i = q_0^{M^* - M_i}, \tag{2.13}$$

$$M^* = \frac{M_k + M_j}{2}. \tag{2.14}$$

where q_0 is the overall stage separation factor per unit mass difference; M^* is the arithmetic mean of the molecular weights of the two main components, jth and kth components; and M_i is the molecular weight of the i^{th} component. Both of these sets of optimization equations assume that product and feed parameters remain constant.

If the tails enrichment x_W is reduced, the amount of feed will be reduced since the cascade is recycling greater amount of the material. On the other hand, it will impose more separative work to the cascade. M^* only affects separative work per product.

2.2 Enrichment of Reprocessed Uranium

For natural U, the process is a binary separation between ^{235}U and ^{238}U isotopes. However, in the case of the enrichment of reprocessed U, the multicomponent separation should be applied due to the existence of increased amount of ^{234}U, and additional isotopes generated during burnup: ^{236}U, ^{233}U, and ^{232}U. The optimization of a U enrichment cascade shows a distinctive feature from other materials. M^* does not vary over the different external parameters when the target isotope is ^{235}U. The total flow rate of a cascade always has a minimum value when M^* is around 236.55u (see Fig. 2.2). That being said, ^{238}U is always the key component of the cascade [53 - 55]. This makes the MARC optimization simple by reducing the variable to only the tails enrichment.

There have been several enrichment technologies developed, and among them, the two methods that are commercially used for large-scale U enrichment are gaseous diffusion and gaseous centrifuge. As of 2020, gas centrifuge plants are the only workhorse in the U enrichment industry. Although both methods rely on the mass difference between the lighter and heavier $^{235}UF_6$ gas molecules, their separation principles are different. Gaseous diffusion depends on the differential effusion speed through a membrane between the two molecules whereas gas centrifuge involves the different centrifugal force between the two molecules to facilitate separation. This difference, as a result, brings the difference in the stage separation factor. The stage separation factor of the gaseous diffusion method between ^{235}U and ^{238}U is less than 1.004. It can be expressed as the square root of the ratio of the molecular weights which is described in Eq. 2.15. On the other hand, the gas centrifuge method involves much larger stage separation factor which is more than 1.3 [56]. For a gas centrifuge, the stage separation factor is a function of the difference in the molecular weights (see Eq. 2.16).

$$q_i^{diffusion} = \sqrt{\frac{M_{^{238}UF_6}}{M_{\ ^{i}UF_6}}} = \sqrt{\frac{352}{114 + M_{U_i}}}, \tag{2.15}$$

$$q_i^{centrifuge} = \exp\left[\frac{\left(M_{^{238}U} - M_i\right)V^2}{2RT}\right] = \exp\left[\frac{\Delta M_i}{M}A^2\right] \tag{2.16}$$

where V is the peripheral speed of the rotor, M is molecular weight, R is the universal gas constant, T is the absolute gas temperature, ΔM is the difference in molecular weight. A^2 is the stratification parameter.

When M^*, proposed by von Halle, is used for both gaseous diffusion and gas centrifuge plants, the composition of the product and waste stream will be same and only difference will be the number of the stages. Hence, H. Wood suggested that the stage separation factor used in MARC should be modified in accordance with its separation method [49, 50]. Using a Taylor series, the separation factor of a gas centrifuge plant may be expressed as,

$$q_i^{centrifuge} = \frac{\Delta M_i}{3}\left(q_{^{235}U}^{centrifuge} - 1\right) + 1. \tag{2.17}$$

The comparison of the separation factors is listed in Tables 2.1 and 2.2. The difference is noticeable for a gas centrifuge plant.

Table 2.1. Comparing the separation factors for a gas centrifuge plant

Separation factor	**^{232}U**	**^{233}U**	**^{234}U**	**^{235}U**	**^{236}U**	**^{238}U**
MARC	2.56	2.19	1.87	1.60	1.37	1.00
H. Wood	2.20	2.00	1.80	1.60	1.40	1.00
Percentage difference (%)	15.00	8.90	3.79	0	2.38	0

Table 2.2. Comparing the separation factors for a gaseous diffusion plant

Separation factor	^{232}U	^{233}U	^{234}U	^{235}U	^{236}U	^{238}U
MARC	1.0086	1.0072	1.0057	1.0043	1.0029	1
H. Wood	1.0087	1.0072	1.0057	1.0043	1.0029	1
Percentage difference (%)	3.71E-3	2.06E-3	8.22E-4	0	4.09E-4	0

In addition to the M^* introduced in Eq. 2.14, $M^*_{diffusion}$ for a gaseous diffusion plant may be derived as given by Eq. 2.19. Using the $M^*_{diffusion}$, one can also prove that the optimum U separating cascade is when ^{235}U and ^{238}U are the two main components (see Fig. 2.2). Like M^*, any component lighter than $M^*_{diffusion}$ is enriched and heavier than $M^*_{diffusion}$ is depleted.

$$\gamma_i^{diffusion} = \frac{q_i}{\sqrt{q_j}} = \frac{\sqrt{M_k/M_i}}{\sqrt[4]{M_k/M_j}} = \sqrt{\frac{\sqrt{M_k M_j}}{M_i}} = \sqrt{\frac{M^*_{diffusion}}{M_i}}, \tag{2.18}$$

$$M^*_{diffusion} = \sqrt{M_k M_j}. \tag{2.19}$$

Also, $M^*_{cetrifuge}$ for a gas centrifuge plant may be derived as given by Eq. 2.21 which is same as M^*. The approximation using a Taylor series cannot be applied to this equation because $\gamma_i^{centrifuge}$ of a component heavier than $M^*_{cetrifuge}$ will become a negative value. Since Eq. 2.20 is analogous to the definition of γ_i (see Eq. A.63), the same total flow minimization process may be applied.

$$\gamma_i^{centrifuge} = \frac{q_i}{\sqrt{q_j}} = \exp\left[\left(\frac{M_k + M_j}{2} - M_i\right)\frac{A^2}{M}\right] = \exp\left[\left(M^*_{centrifuge} - M_i\right)\frac{A^2}{M}\right], \tag{2.20}$$

$$M^*_{centrifuge} = \frac{M_k + M_j}{2}. \tag{2.21}$$

Lastly, the cascade optimization equation must be adjusted to reflect the cost of RepU feed per ERU product. C_F^{RepU} is substituted to C_F, and separative work to a total flow in Eq. 2.9:

$$C_P^{RepU} = C_F^{RepU} f_{F/P}(x_W) + C_L f_{\sum L/P}(x_W). \quad (2.22)$$

The estimation of the value of C_F^{NatU}, C_F^{RepU}, and C_L is described in Appendix D.

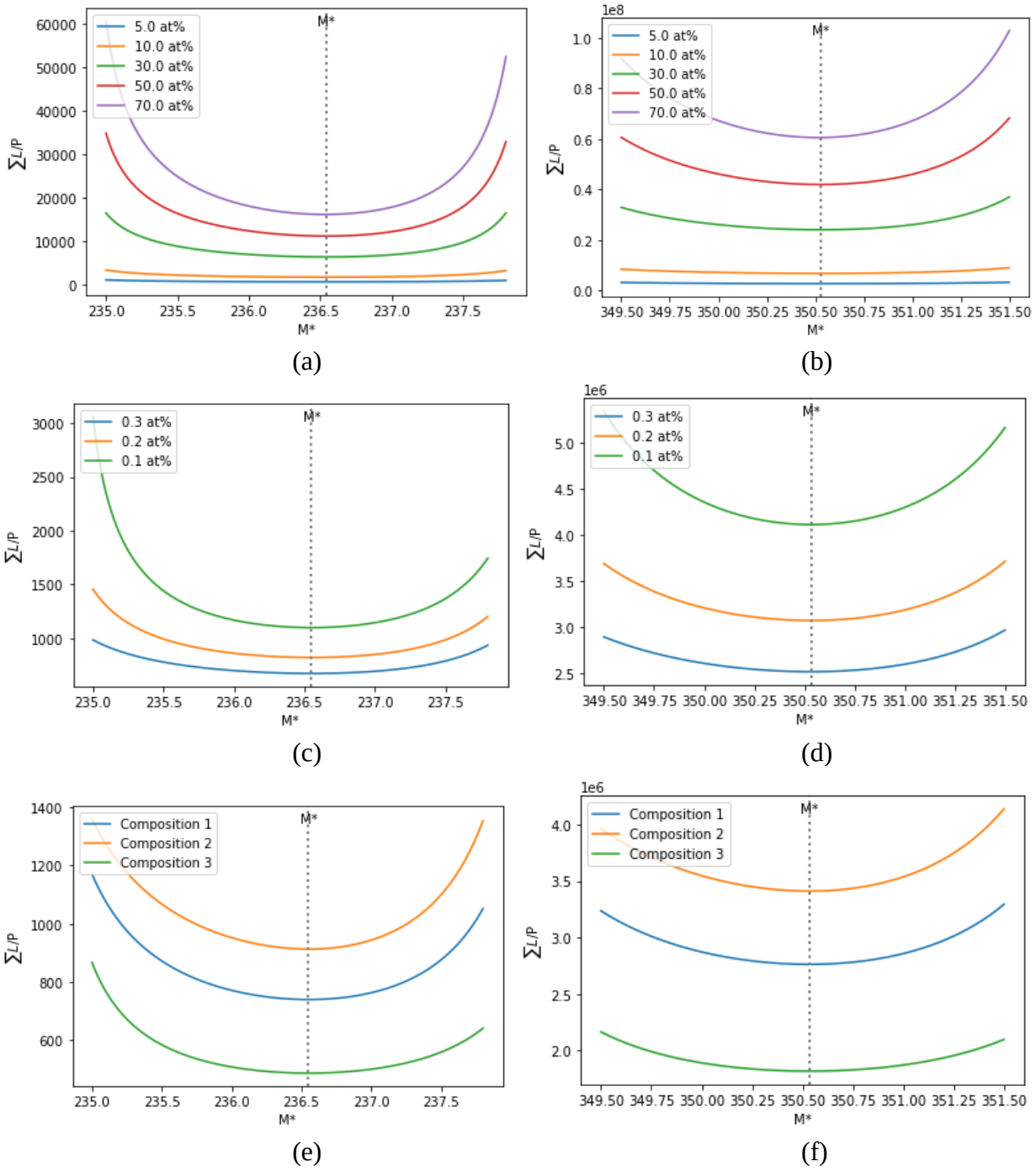

Figure 2.2. Optimization of matched-abundance cascade. Various ^{235}U enrichments for (a) gas centrifuge and (b) gaseous diffusion; Various ^{235}U concentrations in waste flow for (c) gas centrifuge and (d) gaseous diffusion; Various feed compositions for (e) gas centrifuge and (f) gaseous diffusion. ^{235}U and ^{238}U are always the two main separation components for both separating methods. The corresponding M* of each methods are calculated as $M^*_{centrifuge} = \left(M_{^{235}U} + M_{^{238}U}\right)/2 = 236.55u$ and $M^*_{diffusion} = \sqrt{M_{^{235}U} M_{^{238}U}} = 350.53u$, respectively.

3. PLUTONIUM BUILDUP IN USED FUEL

3.1 Effect of Three Factors on Reactor Neutron Population

Following the enrichment process of reprocessed U discussed in Chapter 2, it is important to investigate the factors that altered the used fuel composition, particularly Pu isotopes. This thesis study narrows down the factors that affect the concentration of Pu in used fuel to three factors (1) the initial concentration of ^{235}U, (2) the initial concentration of ^{236}U in fresh fuel, and (3) the discharge fuel burnup. Initially, three different types of U fuels are compared to analyze their effective neutron multiplication factor (k-effective) and average neutron flux values and they are shown as a function of burnup in Fig. 3.1. The compositions of each fuels are listed in Table 3.1 as well as their initial k-effective and average neutron flux values. The reactor power assumed is 3400MWth.

First, the average neutron flux values are compared with each other. As shown in Table 3.1, Type C fuel has the lowest neutron flux whereas Type B fuel has the highest neutron flux. This is due to the difference in ^{235}U atomic density. If a fuel contains less ^{235}U, it will need relatively higher flux to have the same power. The relationship between the neutron flux and ^{235}U atomic density can be explained using the power density formula:

$$P_f = \left[\left(E_{f,^{235}U} \cdot \sigma_{f,^{235}U}\right) V \cdot N_{^{235}U} \downarrow \cdot \phi \uparrow\right]_{Type\ A} = \left[\left(E_{f,^{235}U} \cdot \sigma_{f,^{235}U}\right) V \cdot N_{^{235}U} \uparrow \cdot \phi \downarrow\right]_{Type\ C} \quad (3.1)$$

where P_f is fission power; $E_{f,^{235}U}$ is energy released per fission event of ^{235}U; $\sigma_{f,^{235}U}$ is ^{235}U fission cross section; V is fuel volume; $N_{^{235}U}$is ^{235}U atomic density; and ϕ is neutron flux.

Moreover, Type B fuel has a higher neutron flux than Type A fuel even though Type A and B fuels has the same amount of ^{235}U. This is because of the ^{236}U neutron poison effect in Type B fuel; ^{236}U absorbs neutrons which otherwise would have been absorbed by ^{235}U.

Lastly, Type C fuel has the smallest increasing rate of neutron flux. As shown in Eq. 3.1, The neutron flux largely depends on the atomic density of ^{235}U and the reactor power. Thus, the depletion rate of ^{235}U decided the increasing rate of neutron flux. The depletion by decay is omitted due to its long half-life, 700 million years, and only the depletion by neutron absorption is considered. Since Type C fuel started off with the lowest neutron flux, it has the lowest depletion rate (see Eq. 3.2).

$$\frac{d}{dt}N_{^{235}U}(t) = -\sigma_{a,^{235}U}\int_0^t \phi(t')dt'. \tag{3.2}$$

The effective multiplication factor (k-effective), values can be easily explained with the analysis of the neutron flux values. Although Type A and C fuels has statistically the same k-effective value at the beginning, Type C fuel ended up having higher k-effective value than Type A fuel. For a thermal reactor, k-effective decreases as it keeps operating mostly due to the depletion of ^{235}U. As Type C fuel has the lowest ^{235}U depletion rate, it has the lowest reduction rate of k-effective. Additionally, the ^{236}U neutron poison effect can be verified with the difference in the k-effective values. Type B fuel, containing 1 at% of ^{236}U, has the lowest k-effective value. When ^{236}U absorbs a neutron, it is most likely to capture a neutron and become ^{237}U rather than fission. This results in the decrease of the k-effective value.

Table 3.1. Fuel Type A and B contain 5 at% ^{235}U but Type B contains extra 1 at% ^{236}U. Fuel Type C contains same amount of ^{236}U as Type B but has additional amount of ^{235}U in order to have equivalent k-effective as Type A.

Fuel Type	**^{235}U (at%)**	**^{236}U (at%)**	**^{238}U (at%)**	**Initial k-effective**	**Initial neutron flux (n·cm^{-2}·s^{-1})**
A	5.00	0.00	95.00	1.40662 ± 0.00044	2.770E+14
B	5.00	1.00	94.00	1.38464 ± 0.00045	2.803E+14
C	5.73	1.00	93.27	1.40636 ± 0.00046	2.712E+14

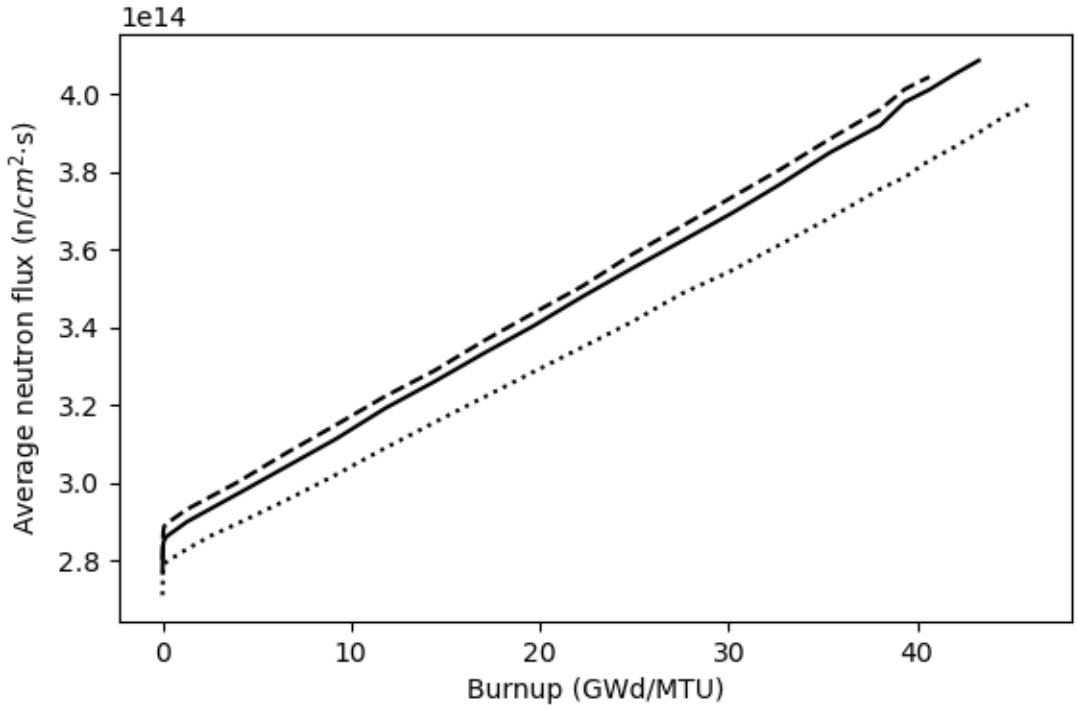

(a)

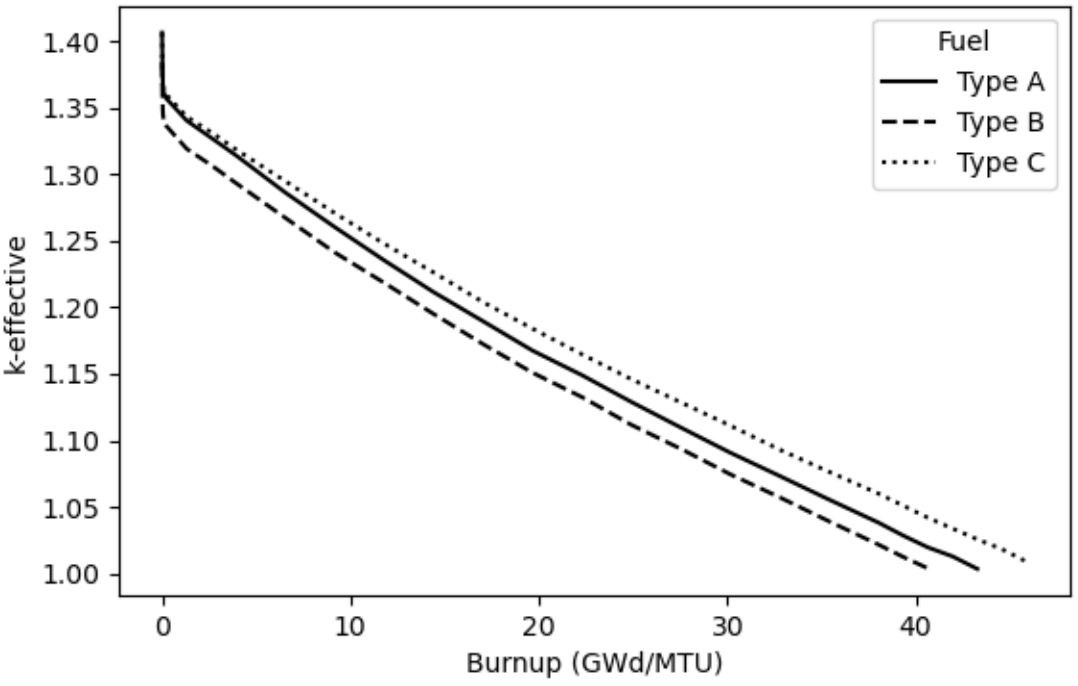

(b)

Figure 3.1. (a) Neutron flux and (b) k-effective values of three different types of fuels.

3.2 Effect of Three Factors on Plutonium Production

To identify the effect of three factors on Pu production, each factor is analyzed by changing one by one while the other factors are controlled. The benchmark is a ^{235}U at 5 at% that did not contain minor isotopes including ^{236}U. The benchmark fuel is then burned up to 42 GWd/MTU without an intermediate refueling. The results are shown in Figs. 3.4 through 3.6.

Firstly, the fuel burnup is studied from 0 to 45 GWd/MTU. Among the Pu isotopes, the buildup of ^{239}Pu stands out at the start but slows down after 20 GWd/MTU: As ^{235}U depleted, ^{239}Pu started to participate in the energy production around the burnup of 20 GWd/MTU. ^{238}Pu, on the other hand, exponentially increased. Initially, ^{238}Pu is produced from its precursors, ^{235}U and ^{236}U. As burnup increased, ^{241}Pu gradually contributed to the production of ^{238}Pu. Figs. 3.2 and 3.3 compare two different sources of ^{238}Pu production. Consequently, the weight fraction of ^{238}Pu increased as a function of fuel burnup.

Next, ^{235}U concentration was varied from 4 at% to 10 at%. The fuel with higher concentration of ^{235}U consumed less amount of ^{239}Pu for energy production. Additionally, ^{235}U hardened the neutron spectra meaning that the thermal neutron population decreased, and the fast neutron population increased. In turn, ^{235}U and ^{236}U, having the capture cross section at thermal region, produced less amount of ^{238}Pu, whereas the production chain from ^{238}U to ^{239}Pu was enhanced by the neutron spectrum hardening. Moreover, the production of heavier Pu isotopes was reduced since the absorption cross sections lie at thermal region. As a result, the weight fraction of ^{238}Pu decreased as a function of ^{235}U concentration.

Lastly, ^{236}U concentration was varied from 0 at% to 3 at%. Other than ^{238}Pu, the production of Pu isotopes did not have a significant change. ^{236}U directly contributed to the production of ^{238}Pu.

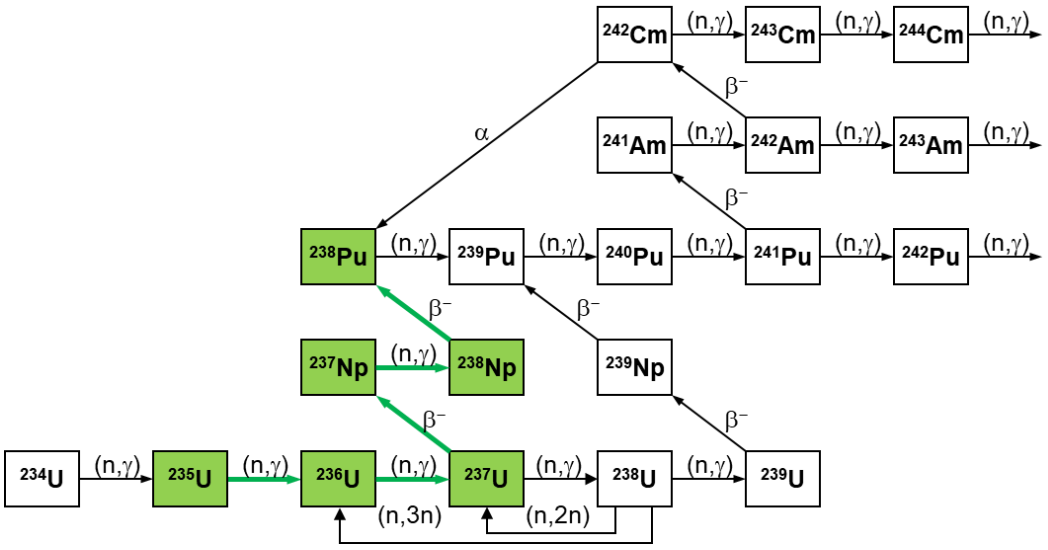

Figure 3.2. Chain of isotopic transformation from ^{235}U to ^{238}Pu in U-Pu nuclear fuel cycle.

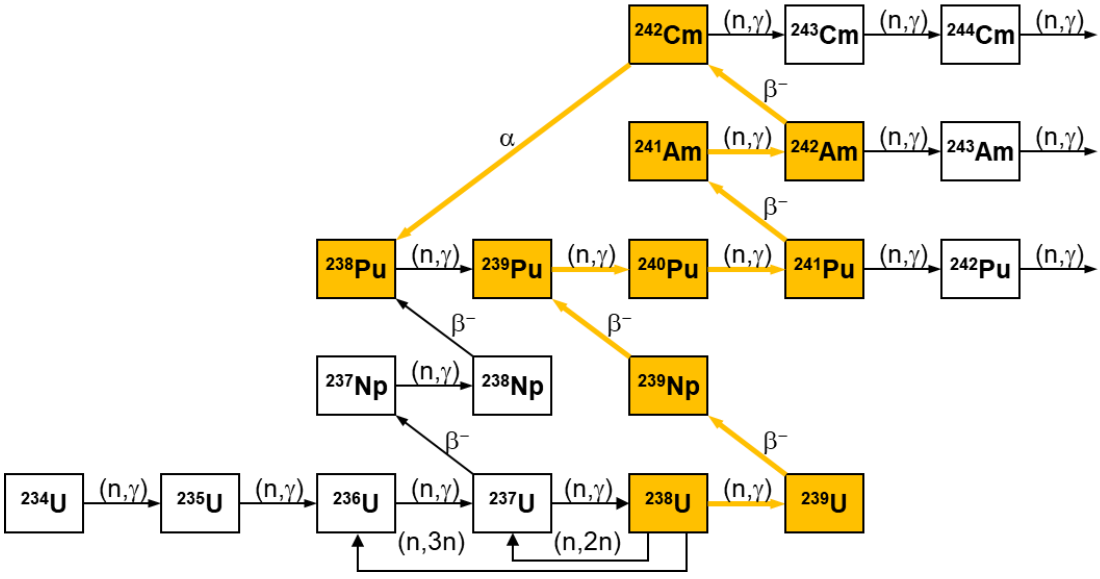

Figure 3.3. Chain of isotopic transformation from ^{238}U to ^{238}Pu in U-Pu nuclear fuel cycle.

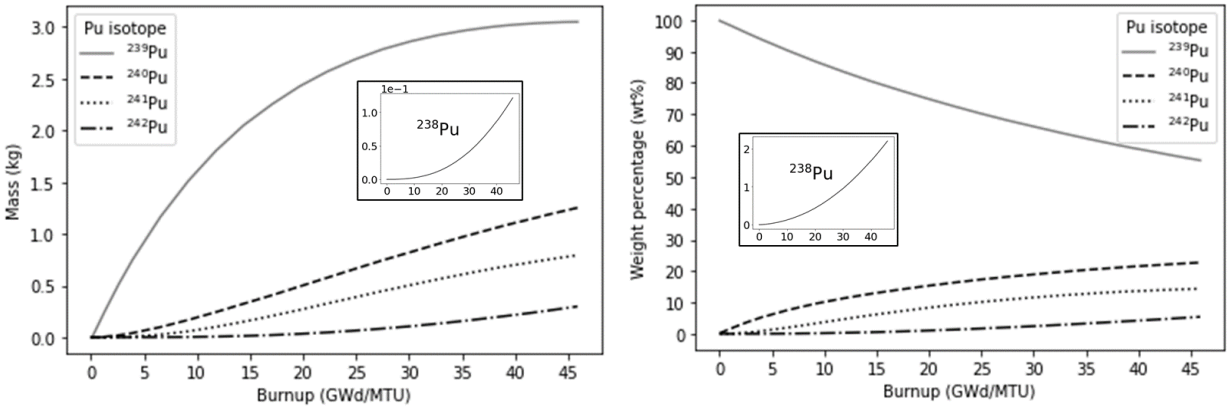

(a) **(b)**

Figure 3.4. Pu buildup by (a) mass and (b) weight percentage. Fuel burnup is varied while ^{235}U and ^{236}U concentration are fixed at 5 at% and 0 at%, respectively.

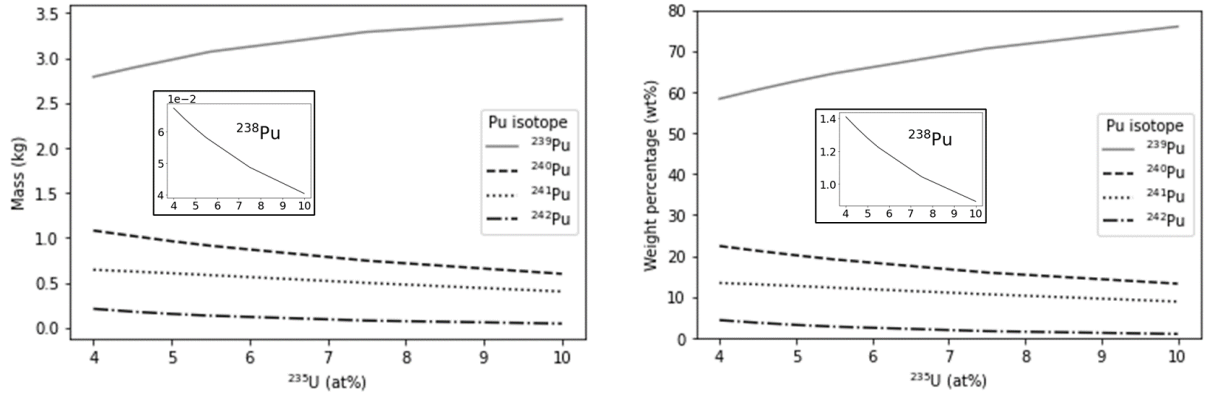

(a) **(b)**

Figure 3.5. Pu buildup by (a) mass and (b) weight percentage. ^{235}U concentration is varied while ^{236}U concentration and fuel burnup are fixed at 0 at% and 42 GWd/MTU.

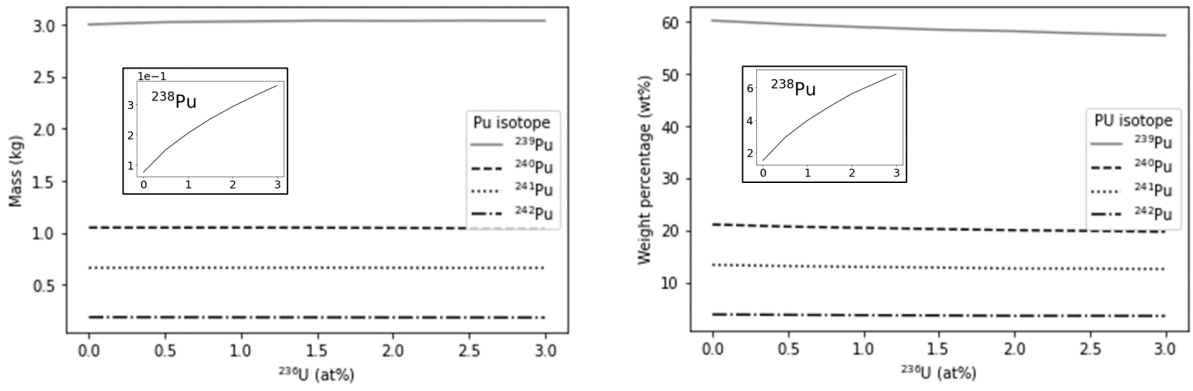

(a) **(b)**

Figure 3.6. Pu buildup by (a) mass and (b) weight percentage. ^{236}U concentration is varied while ^{235}U concentration and fuel burnup are fixed at 5 at% and 42 GWd/MTU.

In summary, the higher buildup of ^{238}Pu can be achieved with the fuel containing more ^{236}U and less ^{235}U and it must be irradiated up to the highest burnup possible. Three different types of fuel are compared again in Fig. 3.7. Type B and C fuels have more ^{238}Pu than Type A fuel at discharge. An interesting point in Fig 3.7 is that Type B fuel has higher fraction of ^{238}Pu than Type C fuel before it is discharged. However, Type C fuel when irradiated after Type B fuel was discharged, and in the end, got the highest ^{238}Pu fraction.

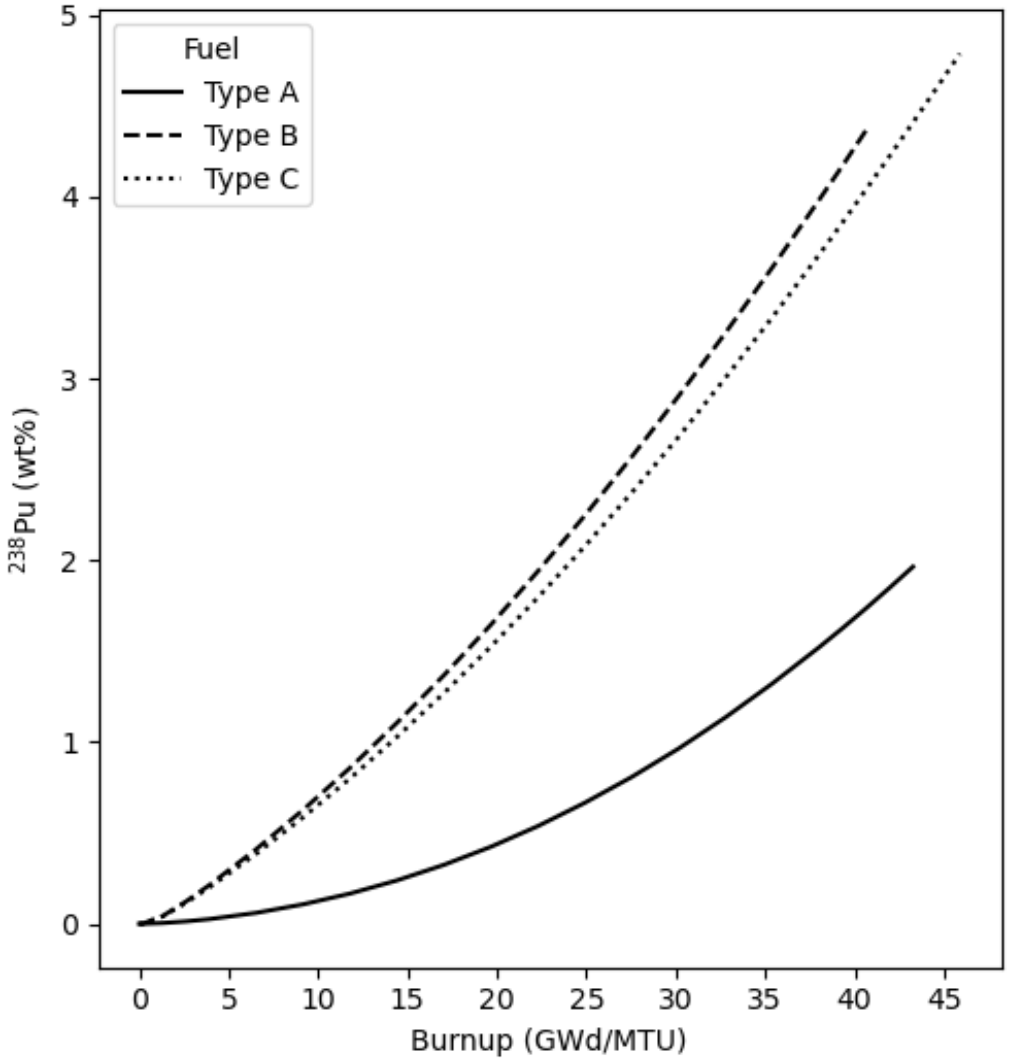

Figure 3.7. Comparison of ^{238}Pu buildup in the different fuel types.

4. PROTECTED PLUTONIUM PRODUCTION

The least concentration of ^{238}Pu to denature the Pu is proposed by G. Kessler [59]. He assumed a hypothetical nuclear explosive device (HNED) made from reactor grade Pu (RGPu) which contains 19% or more of ^{240}Pu. From his study, Pu containing more than 9% ^{238}Pu would limit the production of HNED due to the specific decay heat. The excessive decay heat will lead to the dissolution of the surrounding material such as a high-explosive lens. Therefore, a nuclear explosive device (NED) with such denatured Pu would be molten or self-ignited.

However, the Kessler's criterion does not account for the variation of other even-numbered isotopes such as ^{240}Pu and ^{242}Pu. The criterion proposed by Y. Kimura *et al*, on the other hand, counts in the even-numbered isotopes [15]. ^{240}Pu and ^{242}Pu contribute to decay heat and also increase the critical mass of the Pu core in a NED. This increases the absolute quantity of ^{238}Pu and in turn increases the decay heat. As listed in Table 4.1, ^{238}Pu, ^{240}Pu and ^{242}Pu are all measured to determine the proliferation resistance of Pu.

Table 4.1. Scientific limit for HNED

Technology class	Limit of sum of even-mass number Pu isotopes
Low	1.9 wt% = ^{238}Pu (wt%) + 0.02 × [^{240}Pu (wt%) + ^{242}Pu (wt%)]
Medium	6.2 wt% = ^{238}Pu (wt%) + 0.05 × [^{240}Pu (wt%) + ^{242}Pu (wt%)]
High	15.0 wt% = ^{238}Pu (wt%) + 0.11 × [^{240}Pu (wt%) + ^{242}Pu (wt%)]

The technology class was determined by the capacity of successfully handling the decay heat. The difference in ^{238}Pu concentrations comes from the technological advancements and the practical experience with NED manufacturing. For a medium-technology HNED, 6.2% ^{238}Pu is

sufficient to produce denatured Pu whereas more than 15.0% ^{238}Pu is needed to denature the Pu for a high-technology HNED.

4.1 Westinghouse AP1000 Modeling

The burnup simulations of ENU and ERU fuels are done employing MCNP code using a model of Westinghouse AP1000 LWR [60 - 62]. MCNP is a general-purpose, continuous-energy, generalized-geometry, time-dependent, Monte Carlo radiation-transport code designed to track many particle types over broad ranges of energies [47]. MCNP burnup and depletion calculation is a linked process between MCNP6 and CINDER90, a nuclear inventory code for reactor irradiation calculations. First, MCNP6 runs steady-state calculation to determine values of k-eff, neutron flux, neutron reaction rates, fission multiplicity, and energy per fission (Q-values). Next, CINDER90 takes the values (one group neutron interaction cross-sections derived by dividing neutron reaction rates by neutron flux) from MCNP6 and carries out the fuel depletion calculation to generate the new material atom densities for the next fuel burnup time step simulation by MCNP. This tandem process is repeated until after the final fuel burnup time step. MCNP treats any arbitrary geometry in 3D and hence useful for creating a proper reactor model for the fuel burnup simulations.

The model utilized to complete the ^{238}Pu production analysis is that of a Westinghouse AP1000 fuel assembly. Westinghouse AP1000 is a two-loop pressurized water reactor (PWR) which is a type of a light water reactor (LWR) [62]. This model is a 17 × 17 fuel array which consists of UO_2 fuel pins without integral fuel burnable absorber (see Fig. 4.1). It is assumed that empty guide tubes are inserted, and the assembly is filled with borated water in its gaps. The detailed specifications are listed in Table 4.2. The model used reflective boundary conditions on the surfaces perpendicular to x and y axis. Reducing the size of the model to a single assembly,

instead of a whole core, was useful for performing various fuel burnup calculations due to the less computational effort required. It should be noted that a reactor core, in reality, operates with multiple batch refueling scheme. Unlike the model – once loaded, burned without a shutdown – a typical PWR has a 3-batch core meaning that the reactor is regularly shutdown (in about 16 to 18 months) to refuel one-third of the core. The batch refueling scheme has an advantage for better uranium utilization and is 1.5 times better for a 3-batch refueling scheme than a single batch core as shown in Eq. 4.1,

$$BU_N(T) = \frac{2N}{N+1} BU_1(T), \tag{4.1}$$

where N is the number of batches and $BU(T)$ is the final obtainable burnup of fuel. Moreover, a core consists of assemblies with different U enrichments and fuel rod configurations so that it can be controlled in a manner to achieve maximum efficiency using the same amount of U.

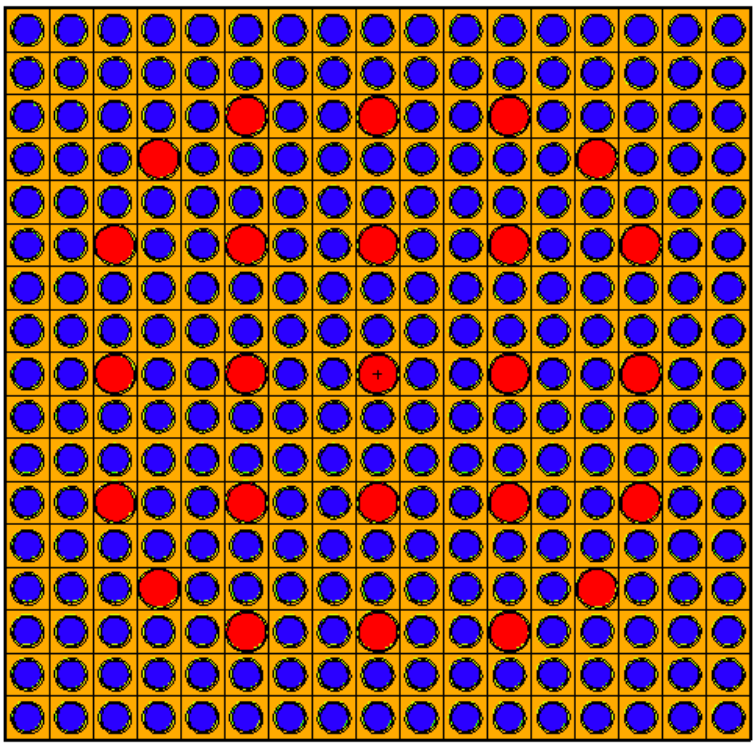

Figure 4.1. Westinghouse 17 × 17 fuel array scheme. The blue circles represent UO_2 fuel pins, and the red circles represent empty guide tubes.

Table 4.2. Westinghouse AP1000 fuel assembly specifications [60 - 62]

Parameter	AP1000
Thermal capacity	3400 MWth
Electrical capacity	1200 MWe
Rod pitch	1.25984 cm
Assembly pitch	21.50364 cm
Active core height	426.72 cm
Cladding outside diameter	0.474980 cm
Cladding inside diameter	0.417830 cm
Pellet outside diameter	0.409575 cm
Guide/instrument tube outside diameter	0.61214 cm
Guide/instrument tube inside diameter	0.56134 cm
Array size	17 × 17
Number of fuel rods	264
Number of guide/instrument tubes	25
Cladding	ZIRLO™
Initial Boron concentration	1184 ppm

4.2 Fuel Burnup and Depletion

Using the AP1000 fuel assembly model, ENU is first irradiated and cooled for 5 years to generate a used fuel. Referring to the analysis made in Chapter 3, the fuel used in the simulation is enriched to ^{235}U at 5.0 wt% in order to achieve higher fuel burnup. Next, the degree of burnup is selected according to the actual average discharge burnup data. From the references [63, 64], the maximum discharge burnup of ENU with 5.0 wt% ^{235}U is approximately 62 GWd/MTU. Applying Eq. 4.1, the maximum discharge burnup for a single batch core was estimated to be 42 GWd/MTU. After the burnup and cooling procedure, the RepU, extracted from the used fuel, was re-enriched to produce an ERU fuel.

For every U recycle, ERU fuels are re-enriched to have the same ^{235}U weight fraction as the preceding ENU fuel, 5 wt%. As U recycling was repeated, separative work and feed per unit product decreased due to the residual ^{235}U (see Fig. 4.2). Additionally, the maximum possible burnup constantly reduced because of the accumulation of ^{236}U. The ratio between ^{236}U and ^{235}U in Fig. 4.3 shows the negative effect of accumulated ^{236}U to burnup.

4.3 ^{238}Pu and Other Even-Numbered Pu Buildup

The record of Pu composition in used fuels is reported in Table 4.3. From Figs. 4.3 and 4.4 it can be inferred that ^{238}Pu buildup was boosted by the presence of ^{236}U. PR for low technology NED was instantly achieved with ENU. With ENU fuel, the PR for medium technology NED was achieved with the 1st recycled ERU. It is an encouraging result that the PR for low and medium technology NEDs can be attained after first recycling. Nevertheless, ^{238}Pu was not sufficient to deter a high technology NEP expert group from manufacturing a HNED until the 5th recycling. ^{236}U, the ^{238}Pu precursor, kept on increasing but the maximum burnup decreased accordingly. For

this reason, U should be recycled 5 or more times to denature Pu for obtaining desired PR against high technology NED.

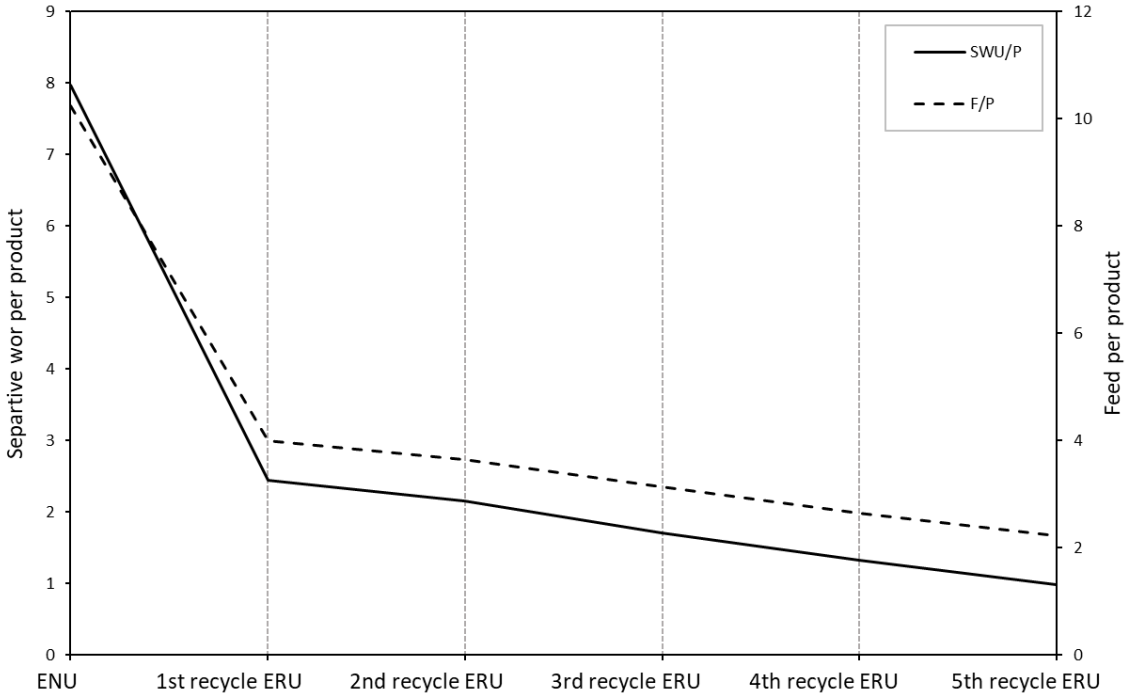

Figure 4.2. Separative work and feed per product as a function of U cycle.

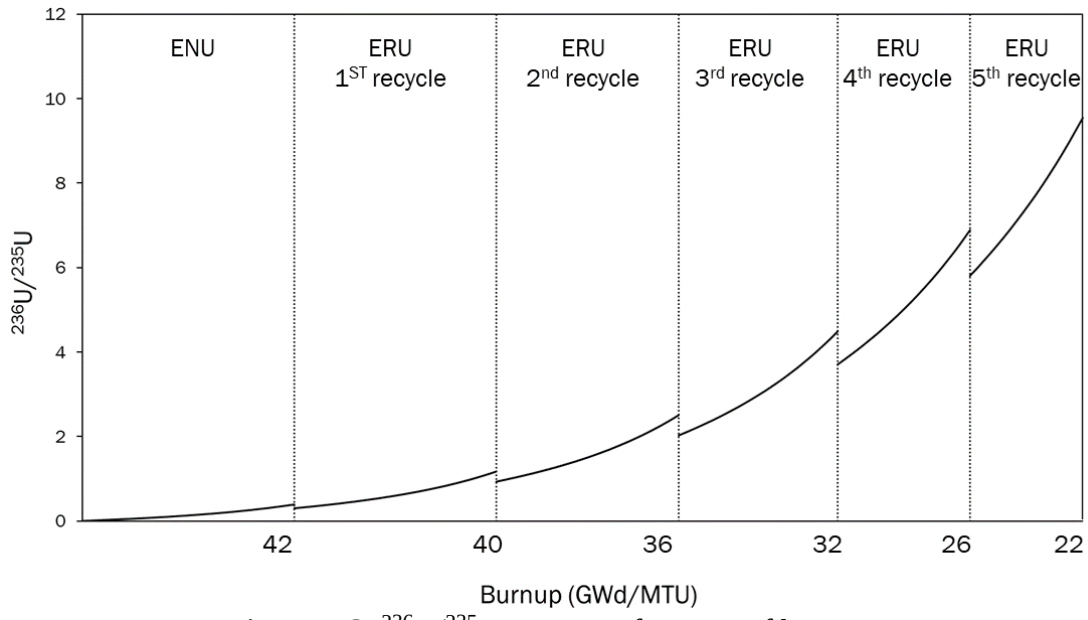

Figure 4.3. $^{236}U/^{235}U$ ratio as a function of burnup.

Table 4.3. Plutonium mass concentration in used fuel.

Cycle	^{238}Pu (wt%)	^{239}Pu (wt%)	^{240}Pu (wt%)	^{241}Pu (wt%)	^{242}Pu (wt%)
ENU	1.81	60.18	22.26	11.14	4.60
ERU 1st recycle	5.13	59.61	20.83	10.47	3.96
ERU 2nd recycle	7.82	60.46	19.02	9.59	3.11
ERU 3rd recycle	10.23	61.72	17.14	8.60	2.31
ERU 4th recycle	12.08	63.78	15.12	7.44	1.57
ERU 5th recycle	14.02	65.03	13.42	6.43	1.11

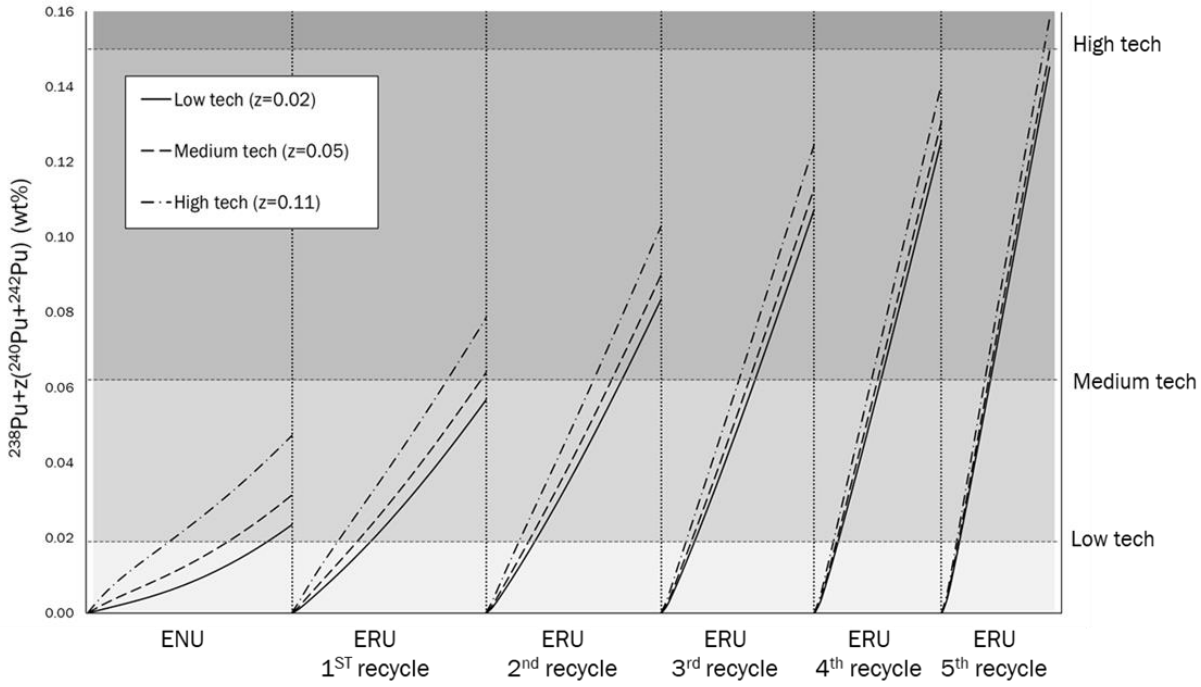

Figure 4.4. The buildup of even-numbered plutonium during each fuel cycle.

In conclusion, it was feasible to produce denatured Pu using ERU owing to the increased amount of ^{236}U in it. Nevertheless, the maximum possible burnup dramatically decreased leading to frequent refueling. To ensure the maximum possible burnup of ERU close to that of ENU, ERU must be enriched with excess amount of ^{235}U to offset the ^{236}U neutron poison effect [18 - 26]. However, the excess amount of ^{235}U would bring about the ^{235}U enrichment above American Society for Testing and Materials (ASTM) product specification and Nuclear Regulatory Commission (NRC) license for the ^{235}U enrichment limit, 5 wt % [65 - 67]. Even if the U were enriched above the limit, it would become impossible to reach equivalent k-effective value after several repetitive recycling. The more problems associated with applying ERU to energy production is further discussed below.

4.4 Constraints Associated with Enriched Reprocessed Uranium

Besides the rise in ^{236}U neutron poison effect, the radiological hazardous increases after each recycle. The daughter products of ^{232}U and ^{234}U are the strong gamma emitters, thus the feed U must contain less than the ASTM limit, 5E-7 wt% and 0.048 wt%, respectively. As shown in Fig. 4.5, ^{234}U exceeded the ASTM limit at 1st recycling and ^{232}U at 2nd recycling. They were consumed during the burnup but were generated from the alpha decay of ^{236}Pu and ^{238}Pu during the following cooling period. Then both isotopes were further enriched in a gas centrifuge enrichment plant owing to their lighter molar masses than ^{235}U. Therefore, the significant presence of ^{232}U and ^{234}U leads to the radiological contamination of an enrichment facility and increases the risk of radiation exposure to workers.

Additionally, the composition of RepU varies depending on the fuel burnup, reactor, power, cooling period, etc. The cascade configuration must be fine-tuned to the feed, and the different feed at each recycling will bring about a huge workload for an enrichment facility.

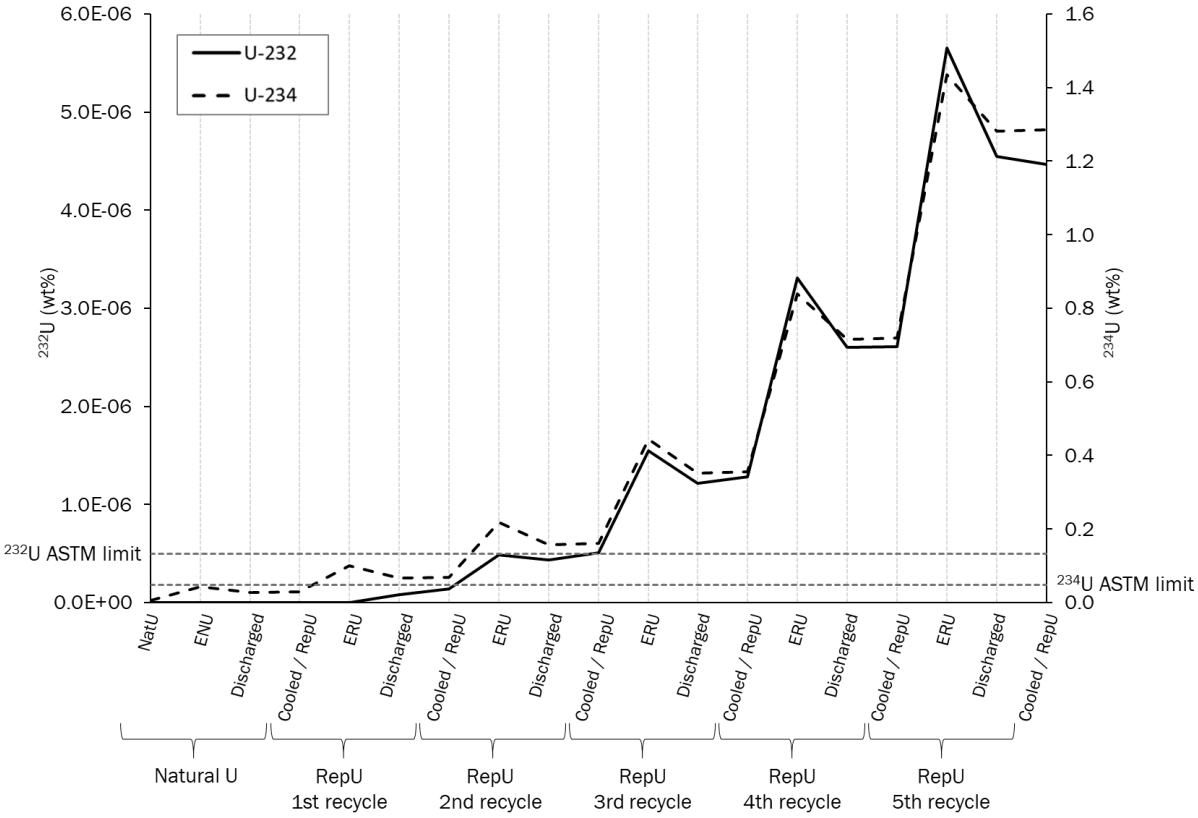

Figure 4.5. ^{232}U and ^{234}U inventories at each recycling step. The ASTM limits for ^{232}U and ^{234}U are 5E-7 wt% and 0.048 wt%, respectively.

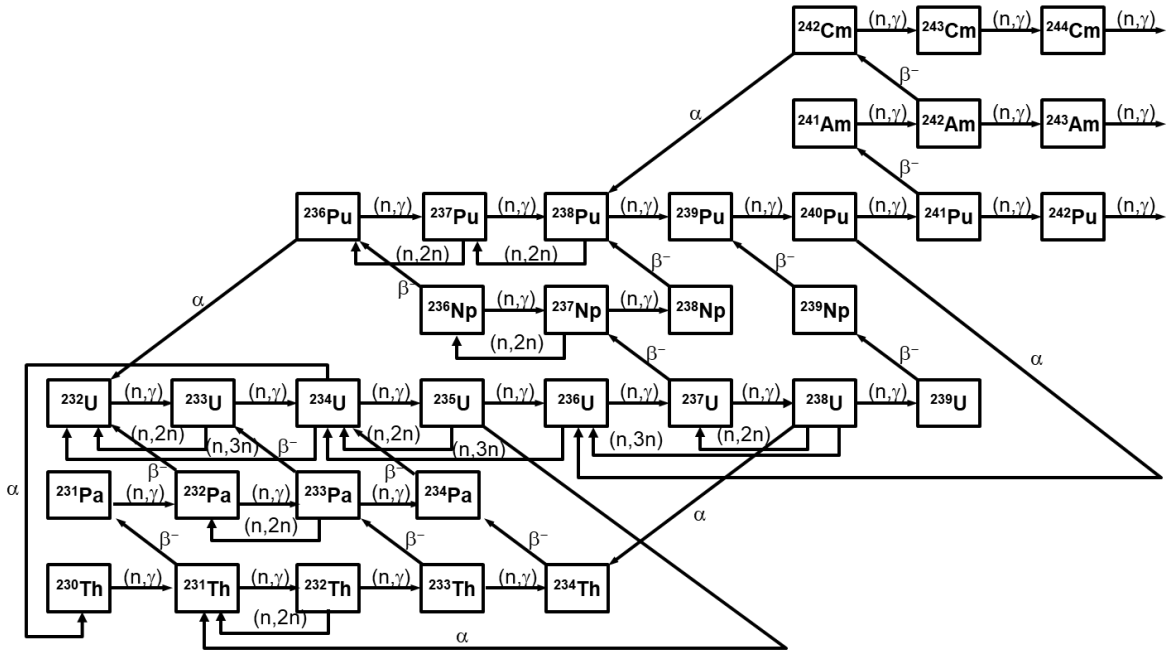

Figure 4.6. Chain of isotopic transformation from ^{235}U and ^{238}U to minor U in U-Pu nuclear fuel cycle.

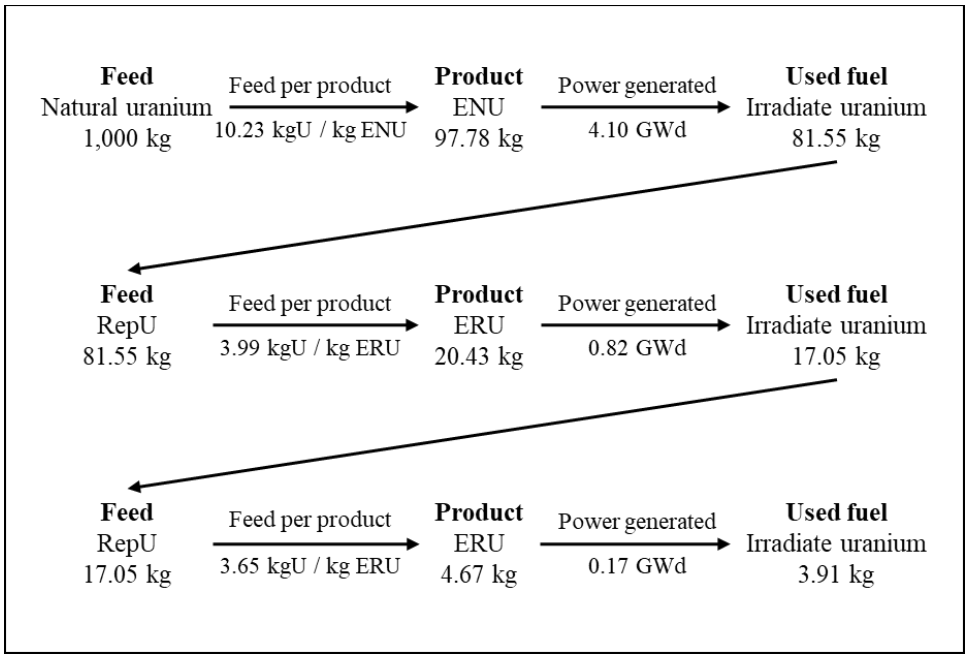

Figure 4.7. Uranium source recycling chain. The enrichment was assumed to be done at a gas centrifuge enrichment plant with separation factor of 1.3.

Moreover, the U source recovery is minimal. One metric ton of natural U feed was assumed at the first place. After two recycling, the remaining U and the generated thermal power noticeably shrunk (see Fig. 4.7). The repeated direct reuse of U is not practical. In turn, the constrains associated with ERU call for a solution: A solution to successfully dilute minor U isotopes from RepU while maintaining its merit as a proliferation resistant fuel.

Several possible solutions were proposed by Russian researchers [60 - 65]. Most of them involves mixing or blending RepU with different types of U such as natural U, ENU, or depleted U. If RepU were to be solely regenerated for energy production, a double-cascade strategy may be applied [74, 75]. However, this strategy involves significant drawbacks: radiation contamination of both cascades; intermediate product exceeding 20% ^{235}U; and high consumption of RepU per unit ERU product. Therefore, the use of natural U source and additional separative works are inevitable to regenerate or dilute RepU.

The good aspect about the dilution techniques is that even if the dilution techniques are applied to regenerate RepU, minor U isotopes will still be present in ERU. Coleman *et al.* [43], Del Cul *et al.* [44], and Smirnov *et al.* [45], evaluated that the diluted ERU still possess sufficient ^{236}U producing relatively large amount of ^{238}Pu than ENU.

5. PROTECTED URANIUM PRODUCTION

5.1 Weapon-Grade Uranium Production from Natural U

If a proliferating group is pursuing a U-based NED, they will undertake every effort to get produce HEU containing ^{235}U above 93 wt%, or so-called weapon-grade uranium (WgU). Whereas, low enriched uranium (LEU, <20 wt% ^{235}U) is not an appealing material for a weapon due to its large critical mass, the corresponding neutron emission rate, and the slow assembly process [76]. Thus, the primary motivation of proliferators is to produce HEU by some means. They can either misuse a declared U enrichment facility or build a clandestine facility to enrich U. Another possibility comes from a combination of two scenarios, which is to produce LEU at the declared facility and further enrich it at the clandestine facility [77]. Either way, the proliferators will be confronted with a hurdle, which is they must acquire sufficient amount of WgU.

To reduce the time and feed requirement, the proliferators are likely to choose to divert enriched U than natural U. As shown in Fig 5.1, the time and feed quantity dramatically drop as a function of the initial ^{235}U enrichment of the feed. Even with 5 wt% ^{235}U feed, the time is reduced by 3-fold and the feed quantity by 14-fold compared to natural U feed. Once the proliferators acquired U, they will preferably apply the most efficient enrichment strategy. Among the possible enrichment strategies, the cascade interconnection is the most efficient and time saving strategy, which has been historically used by nuclear weapon states to produce WgU [78 - 80]. Several cascades are interconnected in parallel and series to achieve enough material flow and for efficient use of separative power to produce WgU.

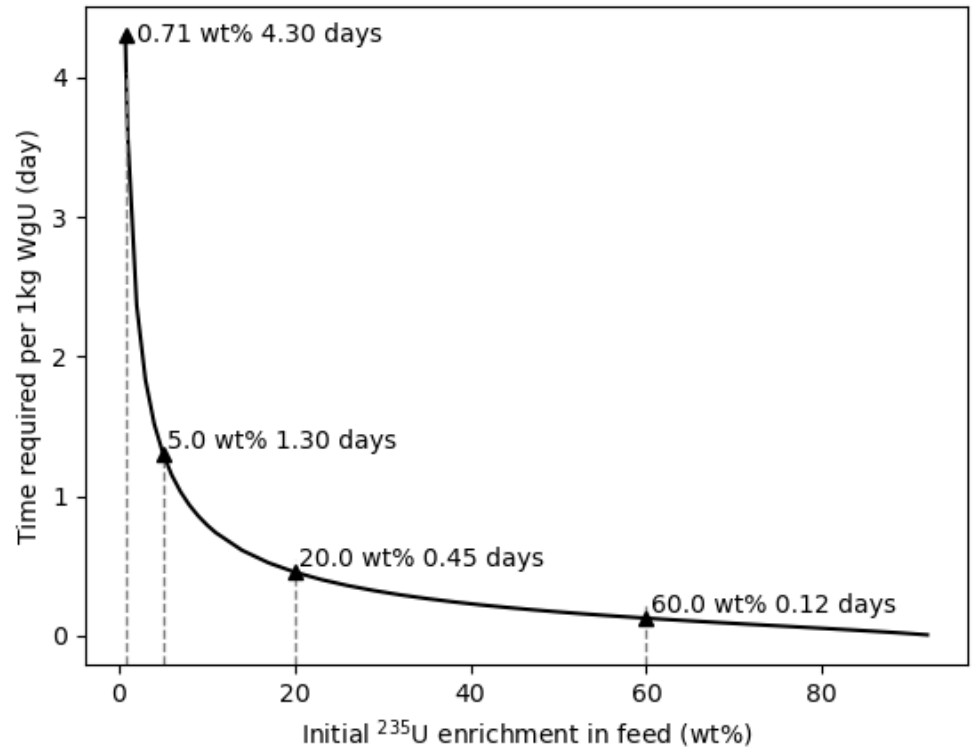

(a)

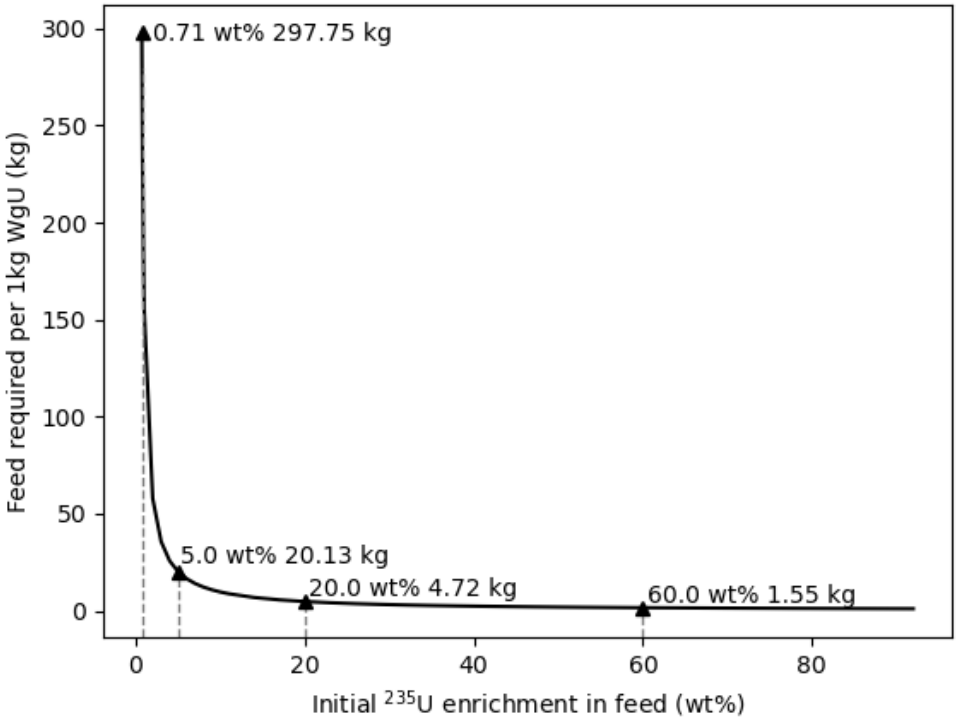

(b)

Figure 5.1. (a) Time and (b) feed required to produce 1 kg WgU as a function of initial ^{235}U enrichment in feed (wt%). The separative capacity was assumed to be 15,000 kg-SWU/yr [81].

Figure 5.2 depicts 4 different cascade interconnection strategies, all of which have same separative capacity and require same amount of feed to product 1kg of WgU. Distributing the separative works to several smaller cascades is better than having one giant cascade to produce WgU since the giant cascade will need a huge stage flow to start off with. Nevertheless, the loss of separative work may happen at the interconnecting point and so 3-4 cascades are the appropriate to interconnect. When estimating the total separative work, it is not required to know the cascade interconnection configuration. They can be calculated using the final product, waste, and external feed. The actual values will be lower than the calculated value due to the loss of separative work and pipe holdup.

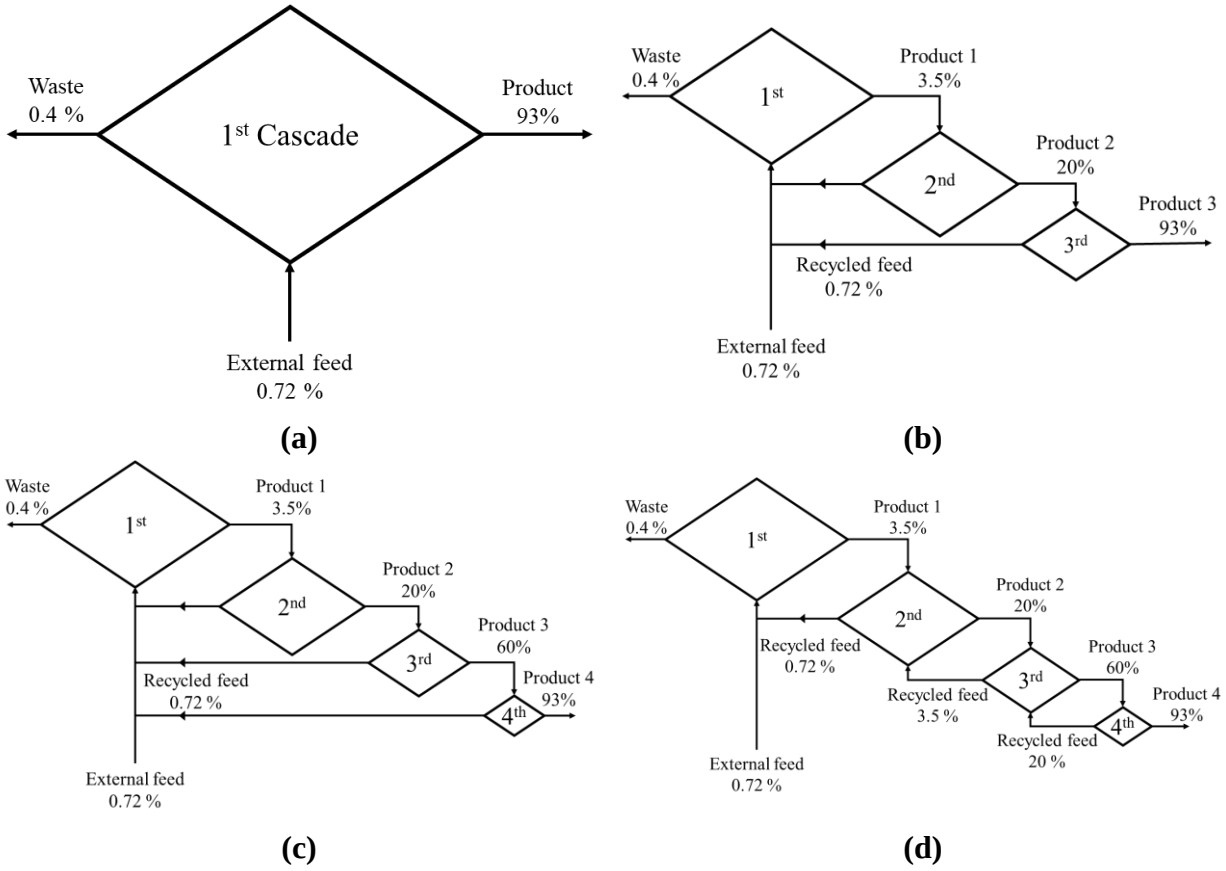

Figure 5.2. Diagrams of 4 different enrichment strategies: (a) single cascade; (b) cascade interconnection with 3 steps; (c) cascade interconnection with 4 steps; and (d) cascade interconnection with alternative recycling structure. From strategy (a) to (c), the sum of stages increases but each stage flow decreases. Compared to strategy (c), strategy (d) has smaller number of stages and its stage flows are more evenly distributed throughout the cascades.

5.2 Weapon-Grade Uranium Production from Reprocessed U

The classic example of denatured U is ^{235}U diluted with ^{238}U meaning the U diluted with more than 80% ^{238}U cannot sustain a fast chain reaction with a small critical mass [9]. Diluting U with ^{234}U and ^{236}U complements the denaturing process because their molar masses are only one unit different from that of ^{235}U making the selective enrichment of ^{235}U impracticable.

RepU, having more than 1 wt% of ^{235}U, seemingly a preferable U to divert than natural U. Nonetheless, RepU contains minor U isotopes as well, which degrade the ^{235}U enrichment process and reduce the fission yield. In Chapter 2, it was proven that the MARC operates with the least separative power when M* is 236.5. It will not be possible to enrich RepU over 93% if M* is fixed at 236.5. In this case, the M* should be adjusted lower than 236.5 but higher than 235, and accordingly the total flow rate and separative work will increase. ^{236}U will be depleted along with ^{238}U while ^{232}U, ^{233}U, and ^{234}U will be still enriched. Contrary to protected Pu production, which is largely influenced by ^{236}U, the protected U production depends on the concentration of lighter isotopes such as ^{232}U and ^{234}U.

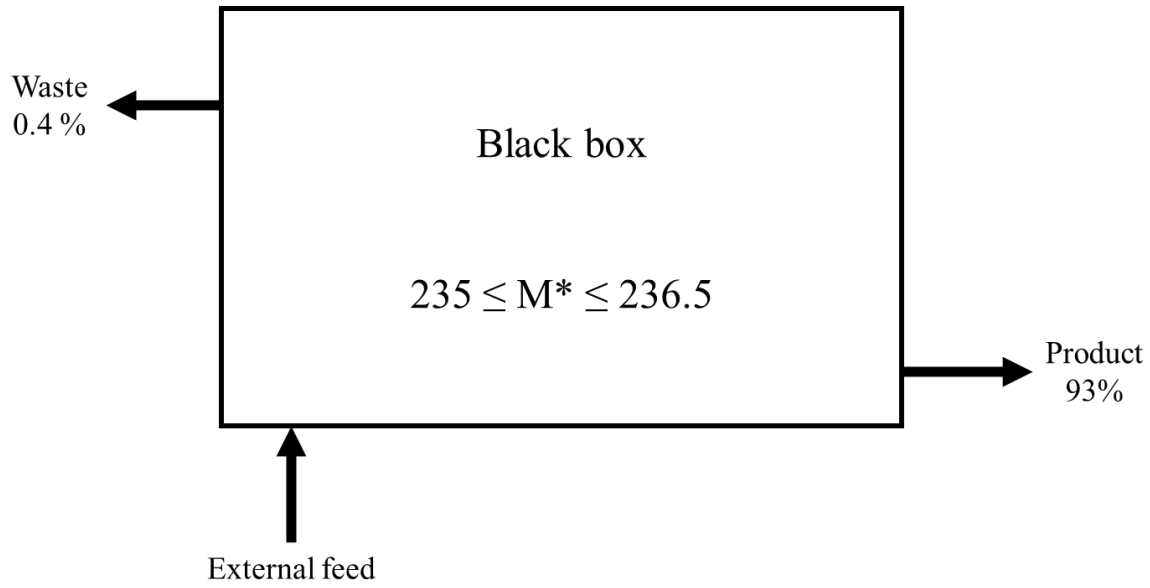

Figure 5.3. Simplified WgU producing strategy.

To simplify the calculation for WgU production, the enrichment strategy was approximated as shown in Fig. 5.3. Inside the black box, it was assumed that the multiple cascades are interconnected but their exact configuration is not known. The external parameters and M* are altered to verify the viability of producing WgU. The stage separative factor is assumed to be 1.3. The goal was to enrich to 93 wt% ^{235}U. The effect of ^{233}U was neglected because of its presence is only in trace amounts in RepU.

Even though the cascade configuration was simplified, the optimization of WgU production is still not as simple as ERU production. The independent variables are same as ERU, ^{235}U tails enrichment and M*. However, the dependent variables are weapon characteristics (critical mass, lead time, prompt neutron decay constant, and probability of a spontaneous-fission-free millisecond) as well as production characteristics (feed and total cascade flow rate per product). The goal of optimization is to promptly produce weapon-usable uranium at a minimum risk of detection.

Since the effect of ^{235}U tails enrichment on the dependent variables are small, it was fixed at 0.4 wt%. After multiple trials of various M*, production of WgU using RepU is found to be possible. The results of the calculation are listed in Tables 5.1 and 5.2. The main components of WgNU and WgRU are plotted in Fig. 5.4. The required amount of feed kept on reducing after each recycle due to the increase of the remaining ^{235}U in used fuel. On the other hand, the total cascade flow rate kept on increasing after each recycle because of the presence of ^{236}U in the feed. After 3rd recycle, not only did the total cascade flow rate become greater than that of natural uranium, but also the maximum possible ^{235}U enrichment dropped below 93 wt%. This is due to the increased concentration of ^{234}U which is more preferably enriched than ^{235}U.

Table 5.1. Characteristics of WgU made from natural U and RepU.

Fuel	M*	Feed per product	Total flow per product	Relative lead time[1]	Critical mass[2] (kg)	α (s^{-1})	Probability[3]
NatU	236.5	297.37	20355.66	100.00 %	51.24 kg	1.11E-12	94.29 %
RepU 1st recycle	236	74.80	17080.73	81.13 %	49.55 kg	1.26E-12	96.82 %
RepU 2nd recycle	235.8	67.22	21403.10	99.30 %	48.40 kg	1.07E-12	96.94 %
RepU 3rd recycle	235.7	55.09	26326.41	120.46 %	47.73 kg	1.32E-12	96.60 %
RepU 4th recycle	235.5	42.74	29565.92	139.74 %	49.31 kg	1.06E-12	95.03 %
RepU 5th recycle	235.6	31.89	26756.47	133.77 %	52.16 kg	1.05E-12	92.77 %

[1] Relative time required to produce one bare critical mass of WgU.
[2] Critical mass of a bare U metal sphere. Its density is 19.1g/cc.
[3] Probability of a spontaneous-fission-free millisecond in one bare critical mass of WgU

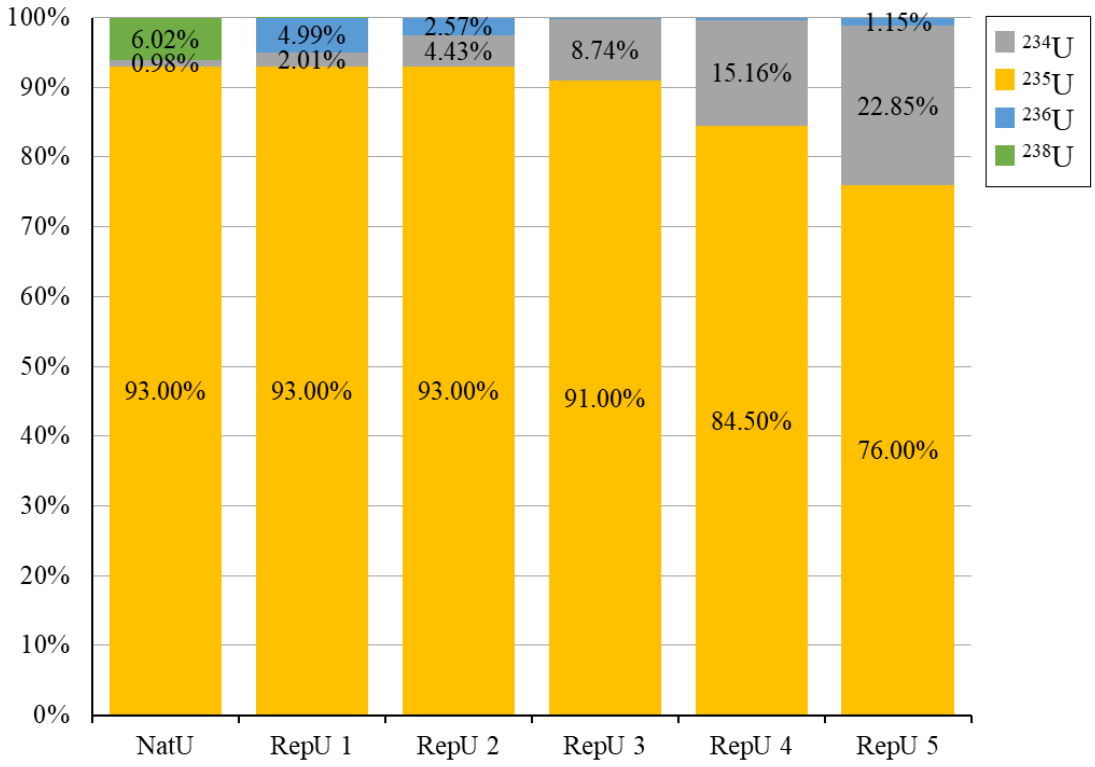

Figure 5.4. Main components of WgU made from natural U and RepU.

Table 5.2. Comparing the compositions of WgU produced from natural uranium and RepU. F, P, and W denote feed, product, and waste, respectively.

Fuel	^{232}U (wt%)			^{233}U (wt%)			^{234}U (wt%)		
	F	**P**	**W**	**F**	**P**	**W**	**F**	**P**	**W**
NatU	0	0	0	0	0	0	0.01	0.98	2.0E-3
RepU 1st recycle	0	0	0	6.5E-7	4.8E-5	8.1E-9	0.03	2.01	1.6E-3
RepU 2nd recycle	1.4E-7	9.2E-6	7.7E-11	2.0E-6	1.4E-4	8.4E-9	0.07	4.43	2.1E-3
RepU 3rd recycle	5.1E-7	2.8E-5	5.3E-11	4.9E-6	2.7E-4	6.3E-9	0.16	8.74	2.6E-3
RepU 4th recycle	1.3E-6	5.5E-5	1.7E-12	1.1E-5	4.5E-4	7.2E-10	0.36	15.46	1.2E-3
RepU 5th recycle	2.6E-6	8.3E-5	1.0E-11	2.1E-5	6.6E-4	2.7E-9	0.72	22.85	3.2E-3

Fuel	^{235}U (wt%)			^{236}U (wt%)			^{238}U (wt%)		
	F	**P**	**W**	**F**	**P**	**W**	**F**	**P**	**W**
NatU	0.71	93.00	0.40	0	0	0	99.28	6.02	99.60
RepU 1st recycle	1.64	93.00	0.40	0.64	4.99	0.58	97.69	1.2E-5	99.01
RepU 2nd recycle	1.78	93.00	0.40	2.08	2.57	2.08	96.07	3.5E-9	97.52
RepU 3rd recycle	2.05	91.00	0.40	5.14	0.26	5.23	92.65	5.0E-16	94.36
RepU 4th recycle	2.38	84.50	0.41	10.68	0.34	10.93	86.59	1.5E-11	88.67
RepU 5th recycle	2.78	76.00	0.41	19.15	1.15	19.73	77.35	9.2E-12	79.86

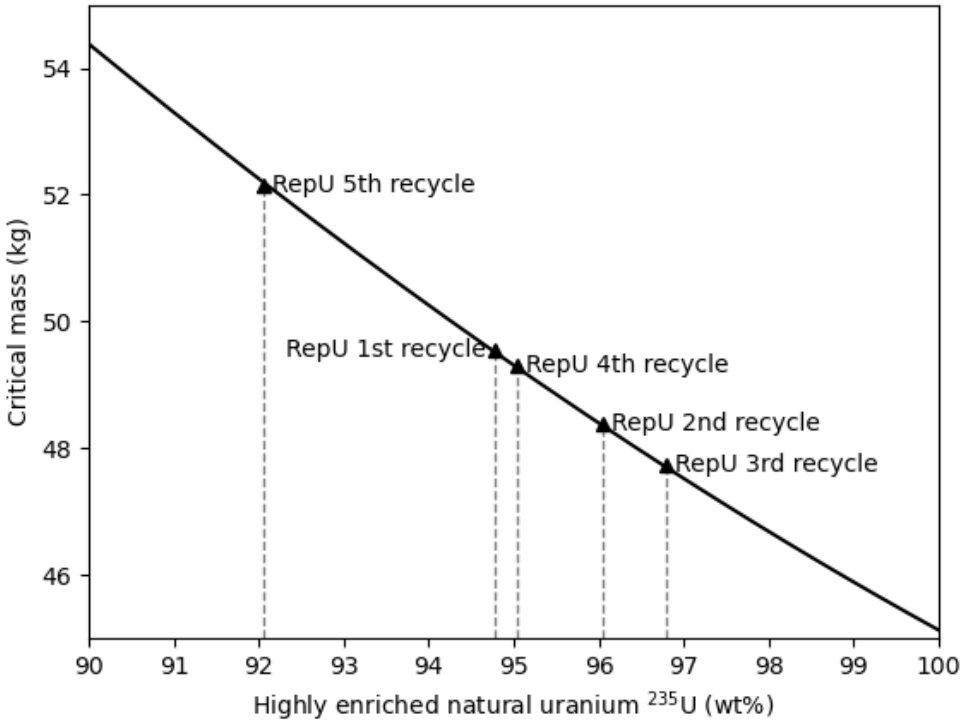

Figure 5.5. Comparing the critical mass of RepU to that of natural U.

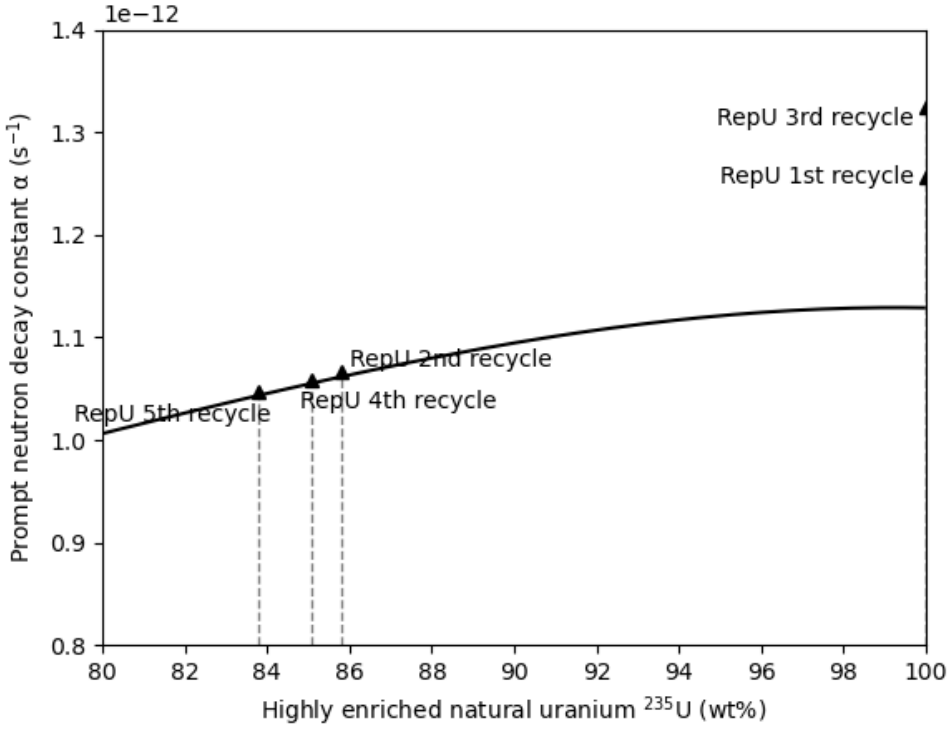

Figure 5.6. Comparing the initial prompt neutron decay constant of RepU to that of natural U.

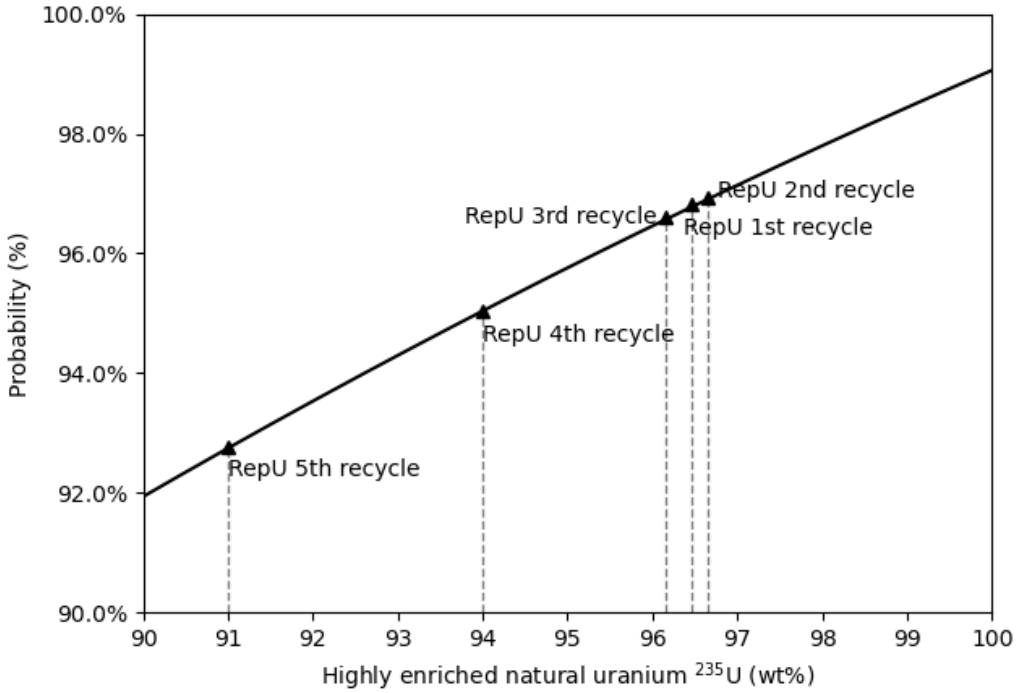

Figure 5.7. Comparing the probability of a spontaneous-fission-free millisecond in one bare critical mass of RepU to that of natural U.

In addition to ^{235}U enrichment, other characteristics of WgU to weapon-usability were estimated and are listed in Table 5.1. The results are plotted in Figs. 5.5 through 5.7. As aforementioned, critical mass and neutron emission rate are the two important characteristics of WgU [76]. Interestingly, the critical masses of Weapon-grade reprocessed uranium (WgRU) are close to or smaller than that of Weapon-grade natural uranium (WgNU). This is because the average number of neutrons released from fission and the fission cross section of minor U isotopes are larger than those of ^{238}U. The critical masses of U isotopes are compared in Fig 5.8 and Table 5.3 and they clearly show that the presence of minor U reduces the critical mass. The neutron emission rate can be examined with the probability of no spontaneous fission event in a millisecond. High probability of neutron-free millisecond can indicate low probability of pre-detonation. Except for ^{232}U, minor U isotopes have smaller spontaneous fission neutron rates than ^{238}U and therefore the probabilities of neutron-free millisecond are all close to 100%. Beside the two

important characteristics of WgU, A. Glaser suggested analyzing the initial prompt neutron decay constant α_0. Higher α_0 is preferred because the chain-reaction proceeds more quickly. Again, WgRU and WgU have similar α_0 values.

There are two significant differences between WgU and WgRU, which are feed per product and total cascade flow rate per product. The relative lead time to produce one bare critical mass of WgU can be estimated by multiplying the total cascade flow rate per product with the critical mass. The 1st and 2nd recycled RepU hold advantage over natural U in terms of relative lead time and feed per product. After 3rd recycle, the relative lead time becomes greater than that of natural U.

It is clear that presence of ^{234}U and ^{236}U complicate the enrichment process by increasing the total cascade flow and reducing the maximum possible enrichment. ^{232}U is also a troublesome isotope for proliferators. Kryuchkov et al. proposed that ^{232}U can function as a denaturing isotope if more than 0.1% ^{232}U is doped to U [27]. The gaseous uranium hexafluoride used for U enrichment will be ionized and destroyed by α-radiation. This α-radiation arises mostly from ^{232}U. Besides the α-radiation, the daughter products of ^{232}U, ^{238}Ti and ^{212}Bi, emit high-energy γ-radiation that improve the detectability and increase the difficulty of handling the U. Even if it were possible to manufacture a NED with denatured U, the daughter products of ^{232}U would build up in the nuclear weapon and thereby the decay heat and neutron emission rate would gradually exceed above the practical value [82]. Nevertheless, more than 0.1% ^{232}U cannot be achieved by solely enriching RepU. Even the 5th recycled RepU contains 8.32E-5 wt% ^{232}U after it has been enriched to 76 wt% ^{235}U.

To sum up, denatured U can be achieved with ^{234}U and ^{236}U both of which have one-unit mass difference from ^{235}U. The proliferation resistance of RepU comes from the lead time which is the only drawback. Proliferators can potentially overcome the hindrance by adding SWU.

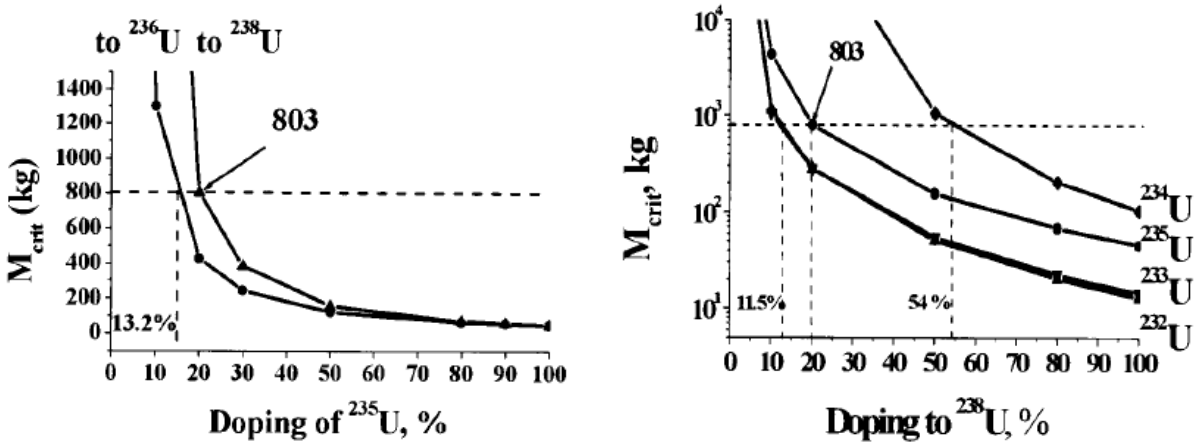

Figure 5.8. Critical masses of uranium compositions (a) doping of ^{235}U to heavy U isotopes and (b) doping of light U isotopes to ^{238}U (metal forms) [10].

Table 5.3. Properties of U isotope.

Isotope	Half-life[1] (yr)	Spont. fission neutrons rate[1] ($n \cdot g^{-1} \cdot s^{-1}$)	Alpha yield rate[1] ($\alpha \cdot g^{-1} \cdot s^{-1}$)	Alpha energy[1] (MeV)	Critical mass[2] (kg)
^{232}U	71.7	1.3	8.0E+11	5.30	12.8
^{233}U	1.59E+5	8.60E-4	3.5E+8	4.82	14.4
^{234}U	2.45E+5	5.02E-3	2.3E+8	4.76	103.4
^{235}U	7.04E+8	2.99E-4	7.9E+4	4.40	45.6
^{236}U	2.34E+7	5.49E-3	2.3E+6	4.48	∞
^{238}U	4.47E+9	1.36E-2	1.2E+4	4.19	∞

[1] Taken from Ref. 83
[2] Taken from Ref. 10

6. SUMMARY AND CONCLUSIONS

6.1 Summary

The goal of this thesis is to verify the proliferation resistance (PR) of enriched reprocessed uranium (ERU) fuel. The results of this study are useful to support the reuse of recycled U for energy generation in the foreseeable future. Matched-abundance ratio cascade (MARC) calculations are conducted to estimate the enrichment of U with multicomponent. A gas centrifuge enrichment plant having a condition of an ideal cascade is assumed to model an optimum enrichment cascade. Because the separation factors vary by the separation methods, MARC calculations differentiated the uranium enrichment methods of gaseous centrifuge and diffusion.

Next, a single pressurized water reactor (PWR) fuel assembly was modeled using Monte Carlo N-Particle code to perform fuel burnup simulations using ERU. Specifically, a Westinghouse AP1000 fuel assembly is modelled. In the fuel assembly, 5wt% ^{235}U enriched natural uranium (ENU) is first burned for 42 GWd/MTU and cooled for 5 years. 5wt% ^{235}U ERU is then produced from the used ENU fuel. ERU is then put back into the fuel assembly and burned until k-effective gets close to unity as the fuel depletion progresses. After discharge, the used ERU fuel is cooled for 5 years and the ^{238}Pu production is estimated. The uranium recycling from re-enrichment to cooling was repeated for five times and their ^{238}Pu concentrations are compared.

Lastly, the feasibility of producing weapon-grade uranium (WgU) from RepU is verified using modified MARC code. RepU from the preceding step is used to determine the PR. Instead of simulating WgU strategies one by one, the enrichment facility configuration was left as a black box, and the external feed, final product, and final waste are exclusively considered. This simplified the calculation and allowed to estimate the ideal enrichment result. Thus, any enrichment strategy will be less efficient than the result.

6.2 Conclusion

The MARC uranium enrichment mathematical method is successfully coded using python script. MARC is optimized and modified for a gaseous centrifuge uranium enrichment plant. Following the MARC uranium enrichment calculations, the effect of three factors on Pu isotopic concentration buildup in the fuel is studied. The three factor studies are the presence of ^{235}U, ^{236}U, and fuel burnup. From the study, it is confirmed that the higher the ^{236}U concentration and the higher the fuel burnup larger is ^{238}Pu isotope buildup, which is seen as a good proliferation resistance attribute. Based on the study, the used uranium recycling scenario is determined which is to enrich RepU to 5 wt% and irradiate until effective neutron multiplication factor, k-effective drops to unity.

Uranium recycling is simulated for five recycles using MARC and MCNP codes. The proliferation resistance of reprocessed Pu was determined based on Kimura's criterion: The sum of even-numbered Pu over 1.9%, 6.2%, and 15% for low, medium, and high technology nuclear explosive device creation, respectively. Denaturing of Pu, to achieve high proliferation resistance for low and medium technology nuclear explosive device, is attained at the first U recycling period. However, denaturing of Pu for high technology nuclear explosive device is attained only after the fifth recycling period. ^{236}U is the main element contributing to the formation of ^{238}Pu. As recycling is repeated, the population of minor U isotopes continued to grow degrading the RepU's value as a source of power. Potential solutions to avoid that is to use dilution techniques for minor U isotopes, which are under research, and they are expected to still produce denatured Pu but at a slower pace.

Subsequently, the proliferation resistance of RepU itself was evaluated. As aforementioned, denaturing of Pu is possible with the heavy minor isotope, ^{236}U. Whereas denaturing of U is

possible with the lighter minor isotopes such as ^{232}U and ^{234}U as well as ^{236}U. In order to highly enrich RepU, M* was adjusted below 236 resulting in depletion of ^{236}U. The lighter minor isotopes, on the other hand, are enriched substantially preventing ^{235}U to be enriched over 93%. The first and second recycled RepU are appealing for uranium diversion since they contain significantly large amounts of ^{235}U than natural U. Nevertheless, it became less attractive to produce WgU from RepU after third recycling due to the increased lead time.

The evaluation of the proliferation resistance is summarized in Table 6.1. A notable discovery is that U is found denatured when it becomes of no value for energy production. Based on the results of this study, it is worth applying RepU for protected Pu production but applying RepU for protected U production is questionable since recycling beyond the second recycle is economically not feasible.

Table 6.1. Proliferation resistance of RepU and its value as a source of power.

Cycle	Denatured U	Denatured Pu	Energy resource*
ENU	No	No	Yes
ERU 1st recycle	No	Yes (low tech)	Yes
ERU 2nd recycle	No	Yes (medium tech)	Yes
ERU 3rd recycle	Yes	Yes (medium tech)	No
ERU 4th recycle	Yes	Yes (medium tech)	No
ERU 5th recycle	Yes	Yes (high tech)	No

* Energy resource not only indicates the value as a source of power but also the U source recovery and the feasibility of handling material in fuel cycle facilities.

6.3 Future Work

In future consideration of this work, the alteration of proliferation resistance can be studied with the application of RepU regeneration techniques. As aforementioned, the impact of minor U isotopes can be reduced by adding unirradiated U during the enrichment process, which will make the concentration of minor U isotopes to be altered as well as its proliferation resistance. One can intuitively assume that denatured Pu and U would not be able to be achieved in a short recycling period. Thus, the proliferation resistance determination process can be repeated for the diluted ERU. Additionally, proliferators may use RepU regeneration techniques to produce WgU which, in turn, will bring about the change in separative work and feed requirement. If so, the proliferation resistance will change, and the U proven to be denatured will no longer be safe from diversion. On the contrary, RepU regeneration techniques can be applied to fine-tune ERU composition so that Pu and U are less suitable and non-attractive for nuclear explosive device while they are still valuable sources of power. A future study on the impact of the U regeneration techniques will be advantageous from U and Pu protection to support nuclear safeguards.

REFERENCES

[1] Feiveson, H., Z. Mian, M.V. Ramana, and F. von Hippel., ed. “Spent Fuel from Nuclear Power Reactors: An Overview of a New Study by the International Panel on Fissile Materials.” *International Panel on Fissile Materials,* 2011.

[2] Fukuda, K., Y. Peryoga, H. Sagara, M. Saito, and M. Ceyhan. “Perspectives of inventories of secondary nuclear materials generated in the nuclear energy production and mass balance in PPP cycle.” *Progress in Nuclear Energy*, vol. 50, no. 2-6, 2008, pp. 654-659.

[3] U.S. Congress, Office of Technology Assessment. *Environmental Monitoring for Nuclear Safeguards (OTA-BP-ISS-168)*. Washington, DC: U.S. Government Printing Office, 1995.

[4] National Research Council. *Proliferation Risk in Nuclear Fuel Cycles: Workshop Summary*. Washington, DC: The National Academies Press, 2011.

[5] Presidential Documents: Gerald R. Ford, 1976 Statement by the President. 28 October 1976, https://www.nrc.gov/docs/ml1209/ML120960611.pdf. Accessed 2 Dec 2020.

[6] Nuclear Energy Agency. *Nuclear Energy Data 2019*. NEA/OECD Publishing, Paris, 2020.

[7] Tsoulfanidis, N. *The Nuclear Fuel Cycle. 1st ed.,* American Nuclear Society, 2013.

[8] Bairiot, H. “Impact of market conditions on the economics of RepU utilization.” *Use of Reprocessed Uranium*, IAEA-TECDOC-CD-1630, International Atomic Energy Agency, 2009.

[9] Devolpi, A. “Denaturing fissile materials.” *Progress in Nuclear Energy*, vol. 10, no. 2, 1982, pp. 161-220.

[10] Ezoubtchenko, A.A., M. Saito, V.V. Artisyuk, H. Sagara. "Proliferation resistance properties of u and Pu isotopes." *Progress in Nuclear Energy*, vol. 47, no. 1–4, 2005, pp. 701-707.

[11] Lloyd, C. and Goddard, B. “Proliferation resistant plutonium: An updated analysis.” *Nuclear Engineering and Design*, vol. 330, 2018, pp. 297-302.

[12] Saito, M., V. Artisyuk, A. Ezoubtchenko, and H. Sagara. “Development of methodology for plutonium categorization - The challenge of attractiveness.” *Transactions of the American Nuclear Society*, vol. 96, 2007, pp. 763-764.

[13] Kessler, G. “Plutonium Denaturing by ^{238}Pu.” *Nuclear Science and Engineering*, vol. 155, no. 1, 2007, pp. 53-73.

[14] Kessler, G., C. Broeders, W. Hoebel, B. Goel, and D. Wilhelm. “A new scientific solution for preventing the misuse of reactor-grade plutonium as nuclear explosive.” *Nuclear Engineering and Design*, vol. 238, no. 12, 2008, pp. 3429-3444.

[15] Kimura, Y., M. Saito, and H. Sagara. "Evaluation of Proliferation Resistance of Plutonium Based on Decay Heat." *Journal of Nuclear Science and Technology*, vol. 48, no. 5, 2011, pp. 715-723.

[16] Kessler, G. *Proliferation-Proof Uranium/Plutonium Fuel Cycles: Safeguards and Non-Proliferation.* Germany: KIT Scientific Publishing, 2011

[17] Wilson, P.D., ed. *The nuclear fuel cycle from ore to wastes*. Oxford University Press ,1996.

[18] NEA/OECD, *The Economics of the Nuclear Fuel Cycle, Organisation for Economic Cooperation and Development*, Paris, France, 1994.

[19] International Atomic Energy Agency. *Management of Reprocessed Uranium Current Status and Future Prospects*. IAEA-TECDOC-CD-1529, IAEA, Vienna, 2007.

[20] De La Garza, A. “Uranium-236 in Light Water Reactor Spent Fuel Recycled to an Enriching Plant.” *Nuclear Technology*, vol. 32, no. 2, 1977, pp. 176-185.

[21] Youinou, G. J. "Impact of Reprocessed Uranium Management on the Homogeneous Recycling of Transuranics in PWRs." *Nuclear Technology,* vol. 198, no. 2, 2017, pp. 202-216.

[22] Coleman, J. and Knight, T. "Evaluation of multiple, self-recycling of reprocessed uranium in LWR." *Nuclear Engineering and Design,* vol. 240, 2010, pp. 1028-1032.

[23] Proselkov, V.N., S.S. Aleshin, S.G. Popov. "Analysis of the Possibility of Using Fuel Based on Reclaimed Uranium in VVÉR Reactors." *Atomic Energy,* vol. 95, no. 6, 2003, pp. 829–834.

[24] Del Cul, G.D., L.D. Trowbridge, J.P. Renier, R.J. Ellis, K.A. Williams, B.B. Spencer, and E.D. Collins. "Analysis of the Reuse of Uranium Recovered from the Reprocessing of Commercial LWR Spent Fuel." *Oak Ridge National Laboratory,* Report no. ORNL/TM-2007/207, 2009.

[25] Wieman, J. "Thirty years of experience with reprocessed uranium management in Borssele." *Use of Reprocessed Uranium*, IAEA-TECDOC-CD-1630, International Atomic Energy Agency, 2010.

[26] Hida, K., S. Kusuno, and T. Seino, "Simultaneous Evaluation of the Effects of ^{232}U and ^{236}U on Uranium Recycling in Boiling Water Reactors." *Nuclear Technology,* vol. 75, no. 2, 1986, pp. 148-159.

[27] Kryuchkov, E.F., V.A. Apse, V.A. Yufereva, V.B. Glebov, and A.N. Shmelev. "Evaluation of Self-Protection of 20% Uranium Denatured with ^{232}U Against Unauthorized Reenrichment." *Nuclear Science and Engineering,* vol. 162, no. 2, 2009, pp. 208-213.

[28] Campbell, D.O. and Gift, E.H. "Proliferation-Resistant Nuclear Fuel Cycles." *Oak Ridge National Laboratory,* Report no. ORNL/TM-6392, 1978.

[29] Waltz, W.R., W.L. Godfrey, and A.K. Williams. “Fuel Cycle Utilizing Plutonium-238 as a “Heat Spike” for Proliferation Resistance.” *Nuclear Technology,* vol. 51, no. 2, 1980, pp. 203-216.

[30] Massey, J.V. and Schneider, A. “Role of plutonium-238 in nuclear fuel cycles.” *Nuclear Technology,* vol. 56, no. 1, 1982, pp. 55-71.

[31] Broeders, C.H.M. and Kessler, G. “Fuel Cycle Options for the Production and Utilization of Denatured Plutonium.” *Nuclear Science and Engineering,* vol. 156, no. 1, 2007, pp. 1-23.

[32] Fukuda, K., H. SAGARA, M. SAITO, and T. Mitsuhashiy. “Feasibility of Reprocessed Uranium in LWR Fuel Cycle for Protected Plutonium Production.” *Journal of Nuclear Science and Technology,* vol. 45, no. 10, 2008, pp. 1016-1027.

[33] Benedict, M., T.H. Pigford, and H.W. Levi. *Nuclear Chemical Engineering. 2nd ed.*, McGraw-Hill, New York, 1981.

[34] De La Garza, A. “A Generalization of the Matched Abundance Ratio Cascade for Multicomponent Isotope Separation.” *Chemical Engineering Science*, vol. 18, 1963, pp. 73-82.

[35] De La Garza, A. “Resolution of a Multicomponent Cascade with Two Key Weights and Multi -Feeds And Withdrawals.” *Atomic Energy Commission Combined Operations Planning*, Report no. AECOP-330, 1969.

[36] von Halle, E. “Multicomponent Isotope Separation in Matched Abundance Ratio Cascades Composed of Stages with Large Separation Factors.” *Proceedings of the 1st Workshop on Separation Phenomena in Liquids and Gases*, edited by Hochshule, T., 1987.

[37] Wood, H.G., V.D. Borisevich, and G.A. Sulaberidze “On a Criterion Efficiency for Multi-Isotope Mixtures Separation.” *Separation Science and Technology*, vol. 34, no.3, 1999, pp. 343-357.

[38] Sulaberidze, G.A. and Borisevich, V.D. “Cascades for separation of multicomponent isotope.” *Separation Science and Technology*, vol. 36, no. 8-9, 2007, pp. 1769-1817.

[39] Borisevich, V.D., G.A. Sulaberidze, and H.G. Wood. “The theory of isotope separation in cascades: problems and solutions.” *Ars Separatoria Acta*, vol. 2, 2003, pp. 107-124.

[40] Sulaberidze, G.A. and Borisevich, V.D. “Comparison of optimal and model cascades for the separation of multicomponent mixtures at arbitrary stage enrichments.” *Theoretical Foundations of Chemical Engineering*, vol. 42, 2008, pp. 347-353.

[41] Wood, H.G., A. Glaser, and J.M. Begovich. “Computational Analysis of Signatures of Highly Enriched Uranium Produced by Centrifuge and Gaseous Diffusion.” *INMM 49th Annual Meeting*, 2008.

[42] Shephard, A., B. Thomas, J. Coble, and H. Wood, "Minor isotope safeguards techniques (MIST): Analysis and visualization of gas centrifuge enrichment plant process data using the MSTAR model." *Nuclear Instruments and Methods in Physics Research Section A: Accelerators, Spectrometers, Detectors and Associated Equipment*, vol. 890, 2018, pp. 79-83.

[43] Coleman, J. and Knight, T. "Evaluation of multiple, self-recycling of reprocessed uranium in LWR." *Nuclear Engineering and Design*, vol. 240, 2010, pp. 1028-1032.

[44] Del Cul, G.D., L.D. Trowbridge, J.P. Renier, R.J. Ellis, K.A. Williams, B.B. Spencer, and E.D. Collins. "Analysis of the Reuse of Uranium Recovered from the Reprocessing of

Commercial LWR Spent Fuel." *Oak Ridge National Laboratory*, Report no. ORNL/TM-2007/207, 2009.

[45] Smirnov, A.Yu., G.A. Sulaberidze, P.N. Alekseev, A.A. Dudnikov, V.A. Nevinitsa, V.N. Proselkov, and A.V. Chibinyaev, "Evolution of isotopic composition of reprocessed uranium during the multiple recycling in light water reactors with natural uranium feed", *Physics of Atomic Nuclei*, vol. 75, no. 13, 2012, pp. 1616–1625.

[46] Weber, C.F. "Generalized Modeling of Enrichment Cascades That Include Minor Isotopes." *53rd annual meeting of the Institute of Nuclear Materials Management*, 2012.

[47] Weber, C.F., J.H. Israel, and J.P. Lefebvre. "MSTAR2019 Code Description and User's Manual." *Oak Ridge National Laboratory*, 2020.

[48] Werner, C. J., ed. "MCNP User's Manual - Code Version 6.2." *Los Alamos National Laboratory*, 2017.

[49] K. P. Cohen. *The Theory of Isotope Separation as Applied to the Large-Scale Production of* ^{235}U. National Nuclear Energy Series, Division III, vol. 1B, McGraw-Hill, NY, 1951.

[50] Villani, S., ed. *Uranium Enrichment (Topics in Applied Physics, 35)*. Springer Berlin Heidelberg, 1979, pp.1-11.

[51] Villani, S., ed. *Uranium Enrichment (Topics in Applied Physics, 35)*. Springer Berlin Heidelberg, 1979, pp.13-54.

[52] Sulaberidze, G.A., A.Y. Smirnov, V.D. Borisevich, S. Zeng, and D. Jiang. "Classification of model cascades for separation of multicomponent isotope mixtures." *Separation Science and Technology*, vol. 56, no. 6, 2020, pp. 1060-1070.

[53] Sulaberidze, G.A., D.V. Potapov, V.D. Borisevich, and Q. Xie. "Special features of the enrichment of components with intermediate mass in a quasi-ideal cascade." *Atomic Energy*, vol. 100, no.1, 2006, pp. 53–59.

[54] Sulaberidze, G.A., V.D. Borisevich, and Q. Xie. "Comparison of optimal and model cascades for the separation of multicomponent mixtures at arbitrary stage enrichments." *Theoretical Foundations of Chemical Engineering*, vol. 42, 2008, pp. 347-353.

[55] Sulaberidze, G.A., Q. Xie, and V.D. Borisevich. "On some properties of quasi-ideal cascades with losses at stages." *Ars Separatoria Acta*, vol. 4, 2006, pp.67-77.

[56] Whitaker, J.M. "Uranium Enrichment Plant Characteristics – A Training Manual for the IAEA." *Oak Ridge National Laboratory*, Report no. ORNL/TM-2019/1311, 2019

[57] Wood, H. G. "Effects of Separation Processes on Minor Uranium Isotopes in Enrichment Cascades." Science & Global Security, vol. 16, no. 1, 2008, pp. 26-36.

[58] Wood, H. G., A. Glaser, and J.M. Begovich. "Computational Analysis of Signatures of Highly Enriched Uranium Produced by Centrifuge and Gaseous Diffusion." *INMM 49th Annual Meeting*, 2008.

[59] G. Kessler. "Plutonium Denaturing by ^{238}Pu." *Nuclear Science and Engineering*, vol. 155 no.1, 2007, pp. 53-73.

[60] Darnowski, P., P. Ignaczak, P. Obrębski, M. Stępień, and G. Niewinski. "Simulations of the AP1000-Based Reactor Core with Serpent Computer Code." *Archive of Mechanical Engineering*, vol. 65, no. 3, 2018, pp. 295–325.

[61] International Atomic Energy Agency. Status report 81 - Advanced Passive PWR (AP 1000), 2011.

[62] United States Nuclear Regulatory Commission. Westinghouse AP1000 Design Control Document Rev. 19, 2011.

[63] Nuclear Energy Agency. *Very High Burn-ups in Light Water Reactors.* NEA/OECD, 2006.

[64] International Atomic Energy Agency. *Impact of High Burnup Uranium Oxide and Mixed Uranium–Plutonium Oxide Water Reactor Fuel on Spent Fuel Management*. Nuclear Energy Series No. NF-T-3.8, IAEA, Vienna, 2011.

[65] "Standard Specification for Uranium Hexafluoride Enriched to Less Than 5% 235U." ASTM Spec. C-996-20, 2020.

[66] "Standard Specification for Uranium Hexafluoride for Enrichment." ASTM Spec. C-787-20, 2020.

[67] 10 CFR 110.40 EXPORT AND IMPORT OF NUCLEAR EQUIPMENT AND MATERIAL. part 110, section 40

[68] International Atomic Energy Agency. *Use of Reprocessed Uranium: Challenges and Options*. Nuclear Energy Series No. NF-T-4.4, IAEA, Vienna, 2010.

[69] Palkin, V.A. "^{232}U, ^{234}U, ^{236}U Removal from Contaminated Waste Uranium Hexafluoride in a Double Cascade." *Atomic Energy*, vol. 124, 2018, pp. 332-337.

[70] Palkin, V.A. and Maslyukov, E.V. "Purification of Reprocessed Uranium in an Additional Product Flow of a Matched Abundance Ratio Cascade and its Enrichment in an Ordinary Cascade." *Theoretical Foundations of Chemical Engineering*, vol. 50, no. 5, 2016, pp.711–717.

[71] Smirnov, A.Yu., G.A. Sulaberidze, A.A. Dudnikov, and V.A. Nevinitsa. "Method for Enriching Reprocessed Uranium in a Cascade of Gas Centrifuges with Simultaneous

Decrease in the U-232,234,236 Content." *Physics of Atomic Nuclei*, vol. 81, no. 8, 2018, pp.1233–1236.

[72] Maslyukov, E. and Palkin, V. "Regenerated Uranium Separation in Matched Abundance Ratio Cascade with Additional Product Flow." *Journal of Physics: Conference Series*, vol. 751, no. 1, 2016.

[73] Palkin, V.A. "Reprocessed uranium purification in cascades with 235U enrichment to 5%." *Atomic Energy*, vol. 115, 2013, pp. 32–37.

[74] Smirnov, A., V. Gusev, G. Sulaberidze, and V. Nevinitsa. "A method to enrich reprocessed uranium with various initial contents of even-numbered isotopes." *AIP Conference Proceedings*, vol. 2101 ,2019.

[75] Gusev, V. E. "Multy-Cascade Enrichment Schemes for Reprocessed Uranium Recycling." *Journal of Physics: Conference Series*, vol. 1696, no. 1, 2020.

[76] Glaser, A. "On the Proliferation Potential of Uranium Fuel for Research Reactors at Various Enrichment Levels." *Science and Global Security*, vol. 14, no. 1, 2006, pp. 1-24.

[77] Samore, Gary. and International Institute for Strategic Studies. *Iran's Strategic Weapons Programmes: A Net Assessment*. Routledge London, UK, 2005.

[78] Hakkila, E.A., M.F. Mullen, C. Olinger, W.D. Stanbro, A.P. Olsen, C.T. Roche, R.R. Rudolph, A.M. Bieber, J. Lemley, and E. Filby. "The safeguards options study." *Los Alamos National Laboratory*, 1995.

[79] Bukharin, O. "U.S. - Russian Bilateral Transparency Regime to Verify Nonproduction of HEU." *Science and Global Security*. vol. 10. 2002, pp. 211-221.

[80] Glaser, A. "Characteristics of the Gas Centrifuge for Uranium Enrichment and Their Relevance for Nuclear Weapon Proliferation." *Science and Global Security,* vol. 16, no. 1-2, 2008, pp. 1-25.

[81] Jones, G.S. "Iran's Centrifuge Enrichment Program as a Source of Fissile Material for Nuclear Weapons." *Nonproliferation Policy Education Center*, 8 April 2008, http://www.npolicy.org/files/20081017-Jones-IranEnrichment.pdf. Accessed 2 Mar 2021.

[82] Lloyd, C., B. Goddard, and R. Witherspoon. "The effects of U-232 on enrichment and material attractiveness over time." Nuclear Engineering and Design, vol. 352, 2019.

[83] D. REILLY, N. ENSSLIN, and H. SMITH, Jr. “Passive Nondestructive Assay of Nuclear Materials,” Los Alamos National Laboratory, 1991.

[84] Olander, D.R. "The Theory of Uranium Enrichment by Gas Centrifuge." *Progress in Nuclear Energy*, vol. 8, no. 1, 1981, pp. 1-33.

[85] Levin, S.A., S. Blumkin, and E. Von Halle. "Use of Minor Uranium Isotope Measurements as an Aid in Safeguarding a Uranium Enrichment Cascade." *IAEA Symposium on Nuclear Material Safeguards*, 1978.

[86] Palkin, V.A. "Optimization of a Cascade with Arbitrarily Specified Separation Coefficients of the Stages." *Atomic Energy,* vol. 82, no. 4, 1997, pp. 228–293.

[87] Palkin, V.A. "Determination of the Optimal Parameters of a Cascade of Gas Centrifuges." Atomic Energy, vol. 84, no. 3, 1998, pp. 190-195.

[88] Palkin, V.A., N.A. Sbitnev, and E.S. Frolov. "Calculation of the Optimal Parameters of a Cascade for Separating a Multicomponent Mixture of Isotopes." *Atomic Energy*, vol. 92, no. 2, 2002, pp. 141–146.

[89] Sulaberidze, G.A., V.D. Borisevich, and H.G. Wood, "Ideal and Optimum Cascades", *Separation Science and Technology*, vol. 43, no. 13, 2008, pp. 3377-3392.

[90] Song, T., S. Zeng, G. Sulaberidze, V. Borisevich, and Q. Xie. "Comparative Study of the Model and Optimum Cascades for Multicomponent Isotope Separation." *Separation Science and Technology*, vol. 45, no. 14, 2010, pp. 2113-2118.

[91] Borisevich, V., M. Borshchevskiy, S. Zeng, and D. Jiang. "On Ideal and Optimum Cascades of Gas Centrifuges with Variable Overall Separation Factors." *Chemical Engineering Science*, vol. 116, 2014, pp. 465–472.

[92] Song, T.M. and Zeng, S. "On the optimity of separation cascade for a binary and a multi-component case." *The 9th international workshop on separation phenomena in liquids and gases*, 2006, pp. 132-143.

[93] Potapov, D., G. Sulaberidze, and L. Kholpanov. "Designing a rectangular sectioned cascade by approximating the separation factor." *Theoretical Foundations of Chemical Engineering*, vol. 34, 2012, pp. 129-133.

[94] Sulaberidze G.A., and Borisevich, V.D. "CASCADES FOR SEPARATION OF MULTICOMPONENT ISOTOPE MIXTURES." *Separation Science and Technology*, vol. 36, no. 8-9, 2001, pp. 1769-1817.

[95] Ying, C., E. Von Halle, and H.G. Wood. "The Optimization of Squared-Off Cascades for Isotope Separation." *Nuclear Technology*, vol. 105, no. 2, 1994, pp. 184-189.

APPENDIX A

SEPARATION THEORY

A.1 Terminology

The basic component of the enrichment plant is a separation element. A feed stream enters the element and is separated into two streams: target isotope enriched stream and target isotope depleted stream. An important feature of an element is the throughput which is the flow rate at which feed can be processed. To achieve adequate throughput, several (hundreds or thousands) separation elements are connected in parallel to form a stage. In all elements of one stage, the feed stream has the same isotopic composition and the same is true for the enriched stream and depleted stream. As the feed stream passes through each stage, a certain degree of separation occurs. The degree is measured by a parameter called the stage separation factor, q. In order to achieve the desired enrichment, the stages are connected in series to form a cascade. The stages above the feed stage are considered enriching section and the other side is stripping section. At the end of each section, the product (or head) and the waste (or tails) is obtained, respectively. The diagram of an enrichment cascade is shown in Figure A.1.

The simplest scheme to connect stages is the "simple cascade" in which the enriched stream of a stage is fed to the next upper stage whereas all depleted stream is left out. However, a "countercurrent cascade" is generally adopted due to the greater recovery of the target isotope extracted from a given quantity of feed. A countercurrent cascade recycles the depleted stream of each stage which is fed to the next lower stage. When the enriched stream goes to the next upper stage while the depleted stream is fed to the immediately preceding stage, a countercurrent cascade is termed symmetric. On the other hand, when an enriched stream from a stage s enters

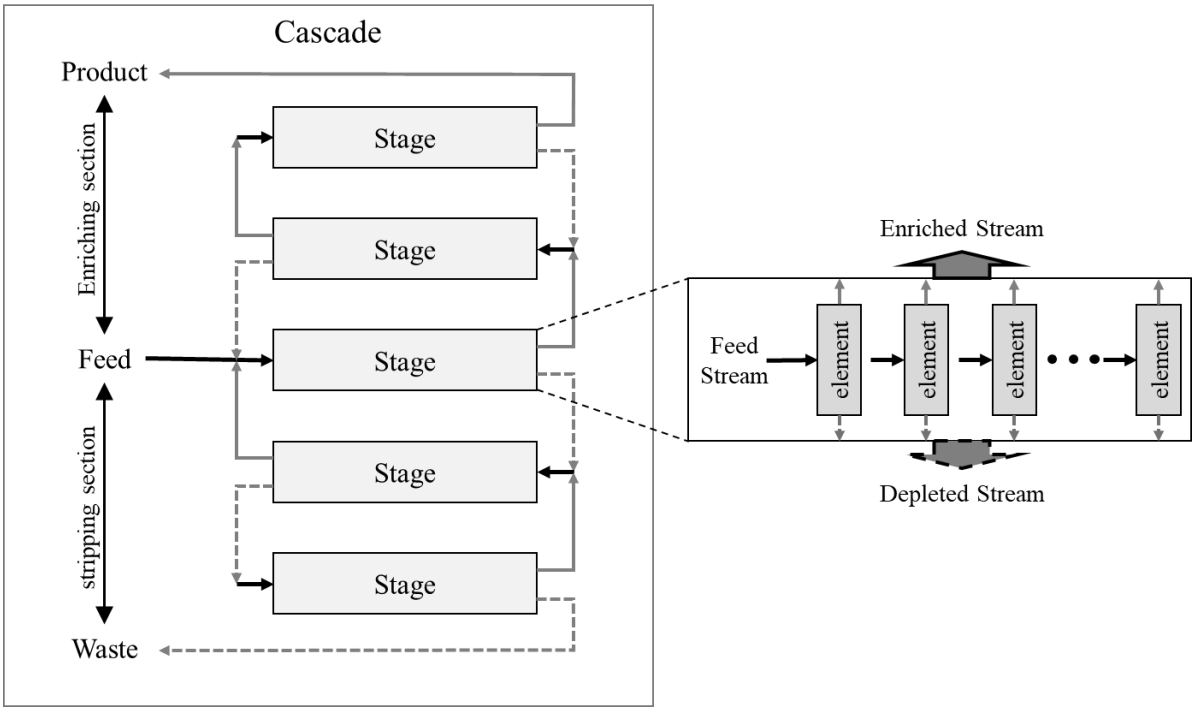

Figure A.1. Elements are connected to increase a throughput and stages are connected to multiply the separation effect.

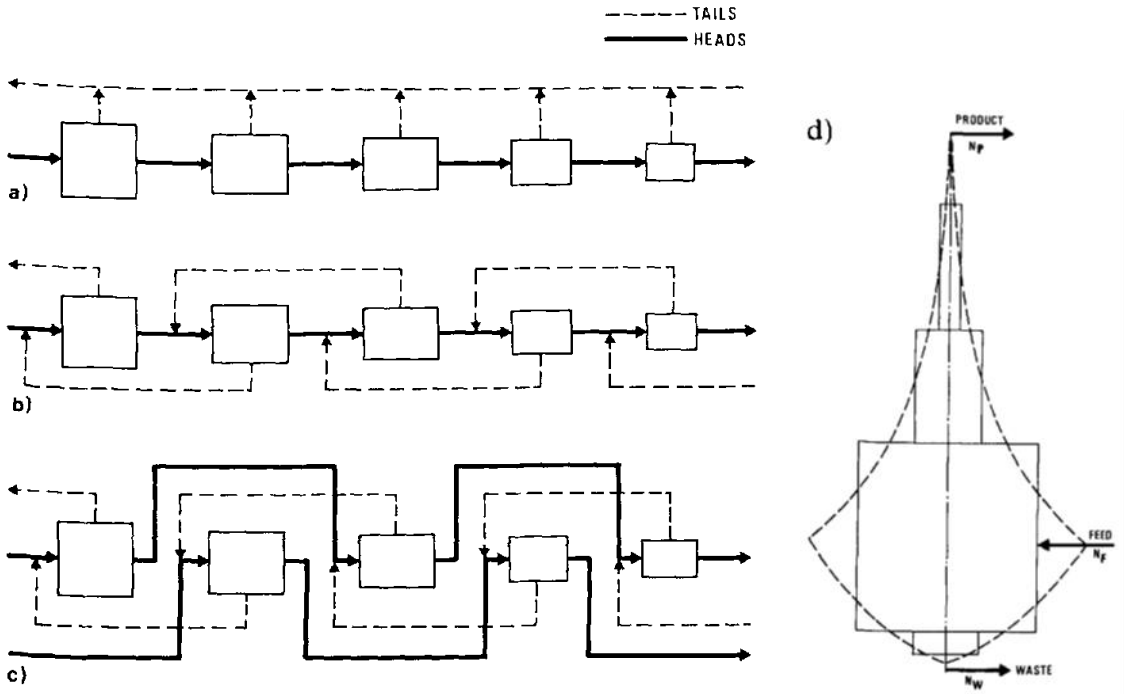

Figure A.2. Examples of cascades: (a) simple cascade; (b) countercurrent symmetric cascade; (c) countercurrent nonsymmetric cascade; (d) squared-off cascade [50].

stage $s+m$ and a depleted stream is recycled into stage s+n, (m≠n), the countercurrent cascade is called nonsymmetric. A “two-up, one-down cascade”, a common asymmetric cascade, feeds the enriched stream into the next following stage and sends the depleted stream two stages back [84]. Examples of above schemes are represented in Figure A.2.

The flow rate of one stage is the sum of the flow rate of all elements forming the stage. When the stage flow rate decreases with each stage towards the product and waste ends, this cascade is known as a tampered cascade. Whereas a square cascade has the same flow rate in all stages. Constant flow rate results in loss of separative work, and consequently square cascades are rarely used.

When the flow rates are adjusted so that the enriched and depleted streams fed to a stage have the same composition, this cascade is termed “ideal cascade” or “non-mixing cascade”. It is a type of tapered cascade introduced by Cohen[49]. Theoretically, an ideal cascade uses the least number of elements to achieve the required separation; there are no losses of separative work therefore the most efficient cascade can be built. To achieve an ideal cascade, every machine must perform the same and the stage flow rate, or stage cut, must be varied for each stage: Even slight deviation is not allowed. Furthermore, the number of stages and elements may correspond to a non-integer number because an ideal cascade is a mathematical model to have an optimized stage cut and throughput. As a result, it is not possible to build an ideal cascade. Nevertheless, it can be approximated by linking several square cascades which called a squared-off cascade (see Figure A.2 (d)).

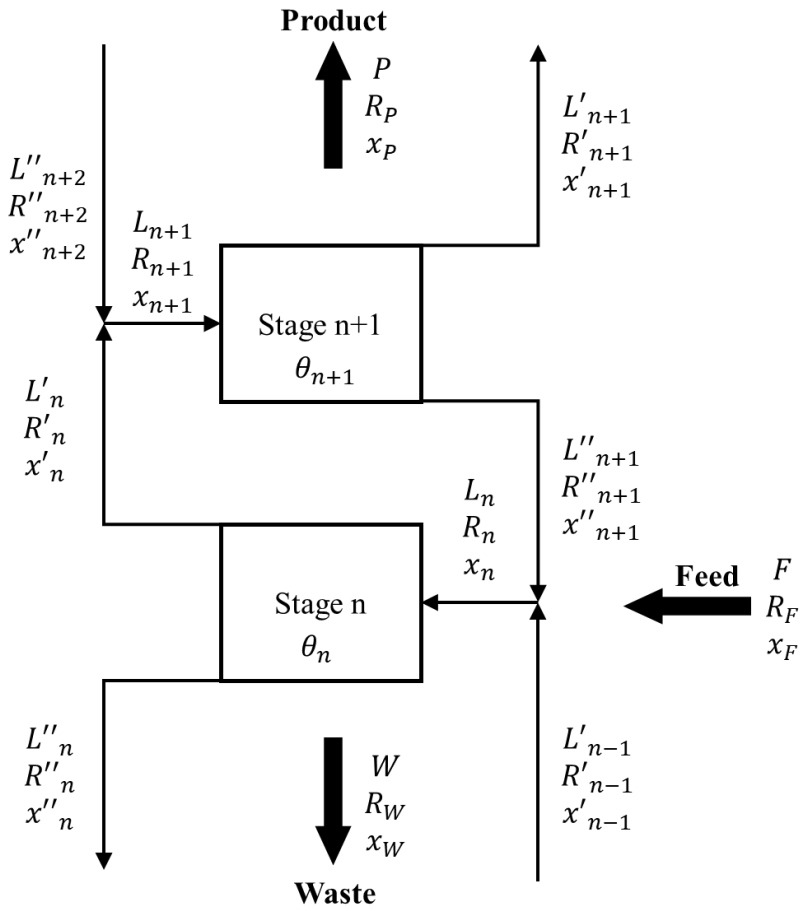

Figure A.3. Schematic diagram of an ideal cascade for binary isotope separation.

A.2 Binary Isotope Separation

The derivation of an ideal countercurrent cascade is elaborated by Cohen[49], S. Villani[50] and B. Brigoli[51]. An ideal cascade has six external variables that can be obtained without considering the internal mechanism. The flow rate of the feed, product, and waste streams are identified as F, P, and W, respectively. The target isotope composition of each stream is identified as x_F, x_P, and x_W, respectively. Stages are consecutively numbered from 1 to N and in between the top and bottom stages, the stage receiving the external feed flow is numbered as f. The internal variables of the cascade include the interstage flow rate L_n and compositions x_n. Single quotation mark denotes a quantity of the enriched stream of a stage while double quotation mark denotes a

quantity of the depleted stream of a stage. To be concrete, the flow rates and the isotopic concentrations indicate the molar flow rate and the atom fraction, respectively. For practical applications, these parameters can be expressed interchangeably in terms of the mass flow rate and the weight fraction.

It is obvious that, provided no material losses occur in the enrichment process, the total quantity of material remains constant. Not only the quantity of the material remains constant but does the quantity of each isotope component remain constant. Below equations are called the material balance equation and the isotope balance equation, respectively:

$$F = P + W, \tag{A.1}$$

$$Fx_F = Px_P + Wx_W. \tag{A.2}$$

Considering that x_F is a fixed parameter and P, x_P, and x_W are the manufacturer determined parameters, feed flow rate and waste flow rate may be calculated as function of four independent variables:

$$F = P\frac{x_P - x_W}{x_F - x_W}, \tag{A.3}$$

$$W = P\frac{x_P - x_F}{x_F - x_W}. \tag{A.4}$$

Instead of directly using the mole fraction x_n in the calculation, it is more convenient to use the relative abundance R_n defined as,

$$R_n = \frac{x_n}{1 - x_n}. \tag{A.5}$$

The stage separation factor q, which determines the concentration change across each stage, is the ratio between the relative abundance in the enriched and in the depleted streams. It may be also expressed as multiplication of the stage enrichment factor and stage stripping factor (see Eq. A.6). For an ideal cascade, the stage separation factor q is constant throughout the whole cascade. As aforementioned, an ideal cascade has non-mixing condition and is formularize in Eqs. A.7 and A.8:

$$q = \frac{R'}{R''} = \frac{R'}{R}\frac{R}{R''} = \alpha\beta, \tag{A.6}$$

$$x''_{n+1} = x_n = x'_{n-1}, \tag{A.7}$$

$$R''_{n+1} = R_n = R'_{n-1}. \tag{A.8}$$

Substituting Eq. A.8 in Eq. A.6, it can be derived that the stage enrichment and stage stripping factors are same (see Eq. A.9):

$$\sqrt{q} = \alpha = \beta. \tag{A.9}$$

It should be noted that in some literature the term "symmetric" condition refers to Eq. A.9. From the relationship above, the number of stages can be easily acquired. The desired relative abundance of the target isotope is the initial relative abundance multiplied by the stage enrichment factor α raised to the power of the number of enriching stages $N - f + 1$. Moreover, the number of stripping stages $f - 1$ may be calculated in the same manner:

$$\alpha^{N-f+1} R_F = R_P, \tag{A.10}$$

$$N - f + 1 = \frac{2}{\ln q} \ln \frac{R_P}{R_F}, \tag{A.11}$$

$$\beta^f R_W = R_F, \tag{A.12}$$

$$f - 1 = \frac{2}{\ln q} \ln \frac{R_F}{R_W} - 1. \tag{A.13}$$

A stage cut θ_n is the ratio of the feed and the enriched streams which may be written as Eq. A.14. The amount of the isotope follows the same rule as Eq. A.15:

$$L_n = L'_n + L''_n = \theta_n L_n + (1 - \theta_n) \cdot L_n, \tag{A.14}$$

$$\begin{aligned} L_n x_n = L'_n x'_n + L''_n x''_n = \theta_n L_n x'_n + (1 - \theta_n) L_n x''_n, \\ x_n = \theta_n x'_n + (1 - \theta_n) x''_n. \end{aligned} \tag{A.15}$$

The stage flow of the topmost stage N is the sum of the product flow and the stage depleted stream. Since there is no more stage above the stage N, the amount of enriched flow from stage $N - 1$ is processed at Stage N and recycled back to the stage $N - 1$ except for the amount of product flow (see Eq. A.15). It is known that all stage flows are kept constant and so Eq. 2.15 is true for all stages in the enriching section, and it can be applied to the amount of isotope as well:

$$L_N = P + L''_N = P + (1 - \theta_N) L_N = \theta_{N-1} L_{N-1}, \tag{A.15}$$

$$P = \theta_{N-1} L_{N-1} - (1 - \theta_N) L_N,$$

$$P = \theta_n L_n - (1 - \theta_{n+1}) L_{n+1}, \tag{A.16}$$

$$P x_P = \theta_n L_n x'_n - (1 - \theta_{n+1}) L_{n+1} x''_{n+1}. \tag{A.17}$$

Substituting Eq. A.16 in Eq. A.17,

$$\theta_n L_n (x'_n - x''_{n+1}) = P(x_P - x''_{n+1}). \tag{A.18}$$

Applying the non-mixing condition and eliminating θ_n and x'_n using Eq. A.6,

$$L_n = \frac{P(x_P - x_n)}{\theta_n(x'_n - x_n)} = \frac{(\alpha+1)P(x_P - x_n)}{(\alpha-1)x_n(1-x_n)}$$

$$= \frac{(\alpha+1)}{(\alpha-1)}\frac{Px_P}{R_F}\left[\alpha^{-(n-f)} - \alpha^{-(N-f+1)}\right]\left(1 + R_f\alpha^{n-f}\right). \qquad \text{(A.19)}$$

The total stage flow of the enriching section is,

$$\sum_{n=f}^{N} L_n = \frac{(\alpha+1)}{(\alpha-1)}P\left[\frac{\left(2x_p - 1\right)\ln\frac{R_P}{R_F}}{\ln\alpha} + \frac{\alpha - (\alpha+1)x_F}{\alpha - 1}\frac{x_P - x_F}{x_F(1-x_F)}\right]. \qquad \text{(A.20)}$$

Replacing P and x_P in Eq. A.19 with $-W$ and x_W, the total stage flow of the stripping section is,

$$L_n = \frac{P(x_P - x_n)}{\theta_n(x'_n - x_n)} = \frac{(\alpha+1)W(x_n - x_P)}{(\alpha-1)x_n(1-x_n)}$$

$$= \frac{(\alpha+1)}{(\alpha-1)}\frac{Wx_W}{R_F}\left[\alpha^{f} - \alpha^{f-n}\right]\left(1 + R_f\alpha^{n-f}\right), \qquad \text{(A.21)}$$

$$\sum_{n=1}^{f-1} L_n = \frac{(\alpha+1)}{(\alpha-1)}W\left[\frac{(2x_W - 1)\ln\frac{R_W}{R_F}}{\ln\alpha} + \frac{\alpha - (\alpha+1)x_F}{\alpha - 1}\frac{x_W - x_F}{x_F(1-x_F)}\right]. \qquad \text{(A.22)}$$

Therefore, the total flow of a cascade is the sum of Eqs. A.20 and A.22.

$$\sum_{n=1}^{N} L_n = \frac{(\alpha+1)}{(\alpha-1)\ln\alpha}\left[P\left(2x_p - 1\right)\ln\frac{R_P}{R_F} + W(2x_W - 1)\ln\frac{R_W}{R_F}\right]. \qquad \text{(A.23)}$$

Above equation may be written in more familiar form,

$$\sum_{n=1}^{N} L_n = \frac{P(2x_p - 1)\ln R_P + W(2x_W - 1)\ln R_W - F(2x_F - 1)\ln R_F}{\frac{(\alpha - 1)}{(\alpha + 1)}\ln \alpha}. \quad \text{(A.24)}$$

The total flow is useful in finding the whole number of separating elements n in a cascade which can be calculated as,

$$n_{cascade} = \frac{\sum L}{G}, \quad \text{(A.25)}$$

where G is the flow entering each element of a cascade. Moreover, the total number of separating elements n may be expressed in different way, which is written as,

$$n_{cascade} = \frac{\Delta U}{\delta U}. \quad \text{(A.26)}$$

where ΔU is the separation performance of a cascade and δU is the separative power of a unit and depends on separation properties of a single element. Here, the separation performance ΔU is the separation work done by a cascade per time under the condition of six external variables. It is possible to break down the separation performance ΔU of a cascade into the separative power of a stage dU_n which is a change in the value of mixture at a stage:

$$dU_n = n_{stage}\delta U = L_n\theta_n V(x_n') + L_n(1 - \theta_n)V(x_n'') - L_n V(x_n). \quad \text{(A.27)}$$

$V(x_n)$ is called value function and the word "value" in an abstract property of a quantity of material that is independent of cost and price. The sum of the separative power of a stage dU_n over all stages makes interstage flow values disappear and it only leaves the external ones. As a result,

$$\Delta U = \sum dU_n = n_{cascade}\delta U = PV(x_P) + WV(x_W) - FV(x_F), \quad \text{(A.28)}$$

From Eqs. A.25 – A.26 and A.28,

$$\Delta U = \frac{\delta U}{G}\sum L = PV(x_P) + WV(x_W) - FV(x_F), \quad \text{(A.29)}$$

$$V(x) = (2x-1)\ln R, \quad \text{(A.30)}$$

$$\delta U = G\frac{\left(\sqrt{q}-1\right)}{\left(\sqrt{q}+1\right)}\ln\sqrt{q}. \quad \text{(A.31)}$$

As shown in Eqs. A.30 and A.31, the value function depends on the isotopic composition of the material whereas the separative power of a separating element is defined by constructive and physical peculiarities which are the flow entering the element and the separation factor.

The optimization of a cascade, in other words, minimizing the cost per unit of enriched product may be done by calculating the conventional formula as follows,

$$C_{P1} = \frac{1}{P}(C_F F + C_U \Delta U), \quad \text{(A.32)}$$

where C_F and C_U are the unit feed cost and the unit separative cost, respectively. Instead of the separative performance, one may use the total flow rate in the calculation:

$$C_{P2} = C_F\frac{F}{P} + C_L\frac{\sum L}{P}. \quad \text{(A.33)}$$

For a binary separation problem, only the waste composition may affect the cost because the amount of enriched product, and the product and feed compositions are the set value. The best waste composition value x_W^{opt} is obtained putting $dC_p/dx_W = 0$, that is,

$$\frac{dC_P}{dx_W} = d\left(C_F\frac{F}{P} + C_U\frac{\Delta U}{P}\right)/dx_W = 0. \tag{A.34}$$

Substituting ΔU with Eq. A.23, and F/P and W/P with Eq. A.3 and Eq. A.4, respectively,

$$\frac{d\left\{-C_F\frac{x_P - x_W}{x_F - x_W} = C_U\left[(2x_p - 1)\ln\frac{R_P}{R_F} + \left(\frac{x_P - x_F}{x_F - x_W}\right)(2x_W - 1)\ln\frac{R_W}{R_F}\right]\right\}}{dx_W} = 0, \tag{A.35}$$

$$\frac{C_F}{C_U} = (2x_F - 1)\ \ln\frac{R_F}{R_W^{opt}} + \frac{\left(1 - 2x_W^{opt}\right)\left(x_F - x_W^{opt}\right)}{\left(1 - x_W^{opt}\right)x_W^{opt}}. \tag{A.36}$$

Finally, substituting C_F from Eq. A.36 in Eq. A.32,

$$C_P^{min} = \mathrm{C}_U\left[(2x_P - 1)\ \ln\frac{R_P}{R_W^{opt}} + \frac{\left(1 - 2x_W^{opt}\right)\left(x_P - x_W^{opt}\right)}{\left(1 - x_W^{opt}\right)x_W^{opt}}\right]. \tag{A.37}$$

The curve of product total cost, presented in Fig. A.4 (a), shows that deviation of the tails assay from the optimum x_W^{opt} does not have a great influence on the product cost. The optimum tails assay x_W^{opt} depends on the cost ratio C_F/C_U therefore it is contingent upon the economic vicissitudes (see Figure A.4 (b)). Typically, the tails assay of a normal uranium is set between 0.2 % to 0.25% whereas the tails assay of a reprocessed uranium is set between 0.25 % to 0.3 % [44].

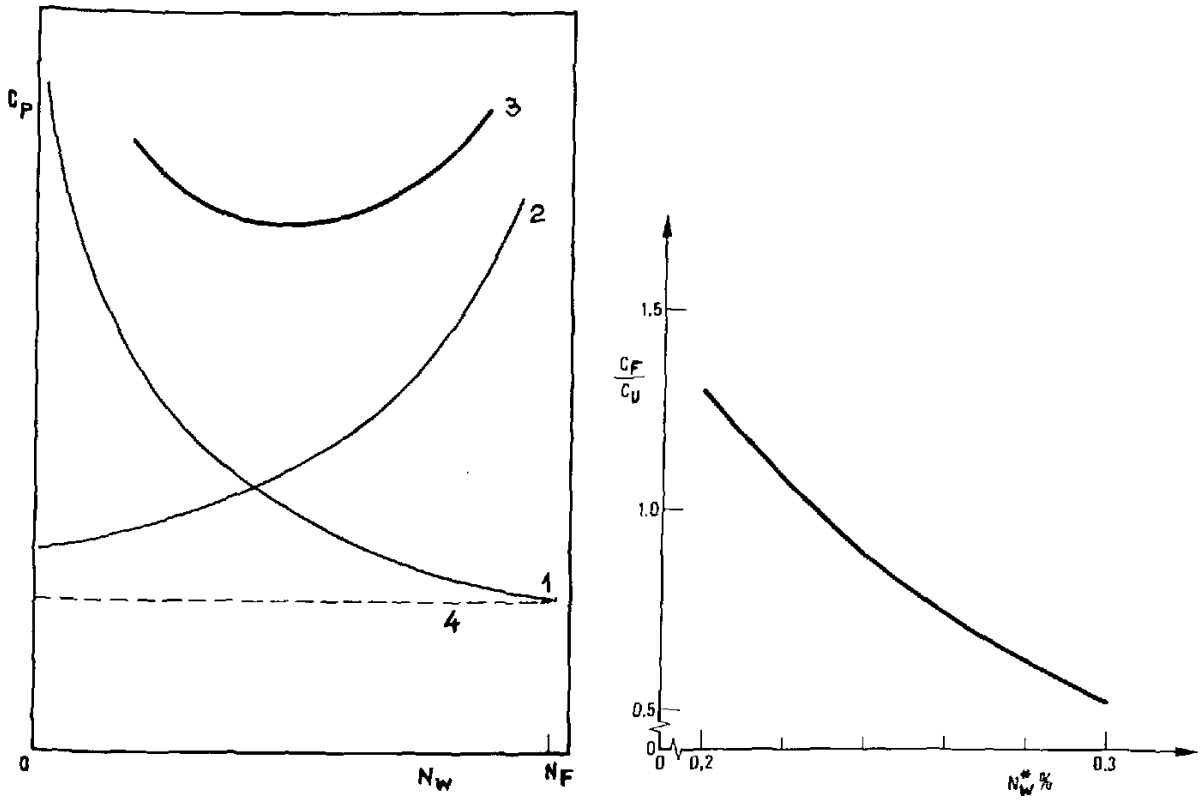

(a) **(b)**

Figure A.4. (a) Effect of waste composition on cost per unit of product: 1 cost of separative work; 2 cost of feed; 3 total cost; 4 cost of separative work in the enriching section. (b) Optimal tails assay N_W as a function of the ratio C_F/C_U. [51]

A.3 Multicomponent Isotope Separation

Matched-abundance ratio cascade, or M* cascade, developed by de la Garza[34, 35] and Von Halle[36], and refined by H. Wood[37] and G.A. Sulaberidze[52], is explained in this section. The distinguishing characteristic of the model is that it simplifies the problem by reducing to the no-mixing conditions analogous to the binary separation problem. Moreover, it is possible to select which components are enriched and which are not by modifying the key component. Finally, the total flow rate of a cascade is minimized for multicomponent mixture separation using the MARC theory. The MARC is relatively simple to code and easy to modify to serve the purpose.

Several features are distinctly different from a binary mixture. One of them is a relative abundance R introduced at Eq. A.5. The relative abundance R_i of i^{th} component is defined with respect to the concentration of k^{th} component, which is designated as the "key" component:

$$R_i = \frac{\mathrm{x}_i}{x_k}, \quad i = 1,2,\cdots,m, \tag{A.38}$$

$$q_i = \frac{\mathrm{R}_i'}{R_i''} = \frac{\mathrm{R}_i'}{R_i}\frac{R_i}{R_i''} = \alpha_i\beta_i. \tag{A.39}$$

The same principle applies to the stage separation factors of each component as the binary mixture separation. That is, q_i are independent of the stage number.

The other distinctive feature is that the non-mixing condition is only true for the target isotope, or j^{th} component:

$$\sqrt{q_i} = \alpha_i = \beta_i, \qquad i = j, \tag{A.40}$$

$$\sqrt{q_i} \neq \alpha_i \neq \beta_i, \qquad i \neq j. \tag{A.41}$$

Since it is only j^{th} component that meets the non-mixing condition, a useful variable other than the stage separation factor is introduced,

$$\gamma_i = \frac{q_i}{\sqrt{q_j}}. \tag{A.42}$$

From the definition, the stage separation factor for the key component is unity and γ_k for the key component is the reciprocal of γ_j.

Following the similar process with binary mixture yet complying with the conditions in Eqs. A.38 − A.42, one can obtain a stage flow rate, P/F ratio, and W/F ratio:

$$\mathrm{L}_{i,n}^{Enriching} = P x_{i,p} \frac{\gamma_i + 1}{\gamma_i - 1}(1 - \gamma_i^{n-N-1}), \qquad n = f, \cdots, N, \tag{A.43}$$

$$\frac{P}{F} = \frac{x_{i,F}}{x_{i,P}} \frac{1 - \gamma_i^{-f}}{1 - \gamma_i^{-N-1}} = \sum_{i=1}^{m} x_{i,F} \frac{1 - \gamma_i^{-f}}{1 - \gamma_i^{-N-1}}, \tag{A.44}$$

$$\mathrm{L}_{i,n}^{Stripping} = W x_{i,W} \frac{\gamma_i + 1}{\gamma_i - 1}(\gamma_i^{n} - 1), \qquad n = 1, \cdots, f - 1, \tag{A.45}$$

$$\frac{W}{F} = \frac{x_{i,F}}{x_{i,W}} \frac{\gamma_i^{N-f+1} - 1}{\gamma_i^{N+1} - 1} = \sum_{i=1}^{m} x_{i,F} \frac{\gamma_i^{N-f+1} - 1}{\gamma_i^{N+1} - 1}. \tag{A.46}$$

From Eqs. A.43 – A.46, the compositions of internal and external streams can be obtained:

$$x_{i,n}^{Enriching} = \frac{\mathrm{L}_{i,n}^{Enriching}}{\sum_{i=1}^{m} \mathrm{L}_{i,n}^{Enriching}} = \frac{x_{i,p} \frac{\gamma_i + 1}{\gamma_i - 1}(1 - \gamma_i^{n-N-1})}{\sum_{i=1}^{m} x_{i,p} \frac{\gamma_i + 1}{\gamma_i - 1}(1 - \gamma_i^{n-N-1})}, n = f, \cdots, N, \tag{A.47}$$

$$x_{i,n}^{Stripping} = \frac{\mathrm{L}_{i,n}^{Stripping}}{\sum_{i=1}^{m} \mathrm{L}_{i,n}^{Enriching}} = \frac{x_{i,W} \frac{\gamma_i + 1}{\gamma_i - 1}(\gamma_i^{n} - 1)}{\sum_{i=1}^{m} x_{i,W} \frac{\gamma_i + 1}{\gamma_i - 1}(\gamma_i^{n} - 1)}, n = 1, \cdots, f - 1, \tag{A.48}$$

$$x_{i,P} = \frac{x_{i,F} \frac{1 - \gamma_i^{-f}}{1 - \gamma_i^{-N-1}}}{\sum_{i=1}^{m} x_{i,F} \frac{1 - \gamma_i^{-f}}{1 - \gamma_i^{-N-1}}}, \tag{A.49}$$

$$x_{i,W} = \frac{x_{i,F} \frac{\gamma_i^{N-f+1} - 1}{\gamma_i^{N+1} - 1}}{\sum_{i=1}^{m} x_{i,F} \frac{\gamma_i^{N-f+1} - 1}{\gamma_i^{N+1} - 1}}. \tag{A.50}$$

Combining Eqs. A.38, A.39 and A.42, it can be proven that γ_k is inverse of γ_j. Therefore, the number of stages analogous to Eqs. A.11 and A.13 are obtained using Eqs. A.49 and A.50:

$$N - f + 1 = \frac{1}{\ln \gamma_j} \ln \frac{R_{j,P}}{R_{j,F}}, \tag{A.51}$$

$$f - 1 = \frac{1}{\ln \gamma_j} \ln \frac{R_{j,F}}{R_{j,W}} - 1. \tag{A.52}$$

In addition to the material balance equations, a similar equation can be obtained using either Eq. A.44 or A.46:

$$F x_{i,F} \gamma_i^{-f} = P x_{i,P} \gamma_i^{-(N+1)} + W x_{i,W}. \tag{A.53}$$

Finally, the total flow rate of a cascade is expressed in a simple equation using Eqs. A.43 and A.45,

$$\sum_{n=1}^{N} L_n = \sum_{i=1}^{m} \frac{P x_{i,P} \ln R_{j,P} + W x_{i,W} \ln R_{j,W} - F x_{i,F} \ln R_{j,F}}{\frac{(\gamma_i - 1)}{(\gamma_i + 1)} \ln \gamma_j}. \tag{A.54}$$

The total flow rate of a cascade separating multicomponent mixture is analogous to Eq. A.24. Thus, one can easily derive the separative performance, value function, and separative power:

$$\Delta U_i = \frac{\delta U_i}{G} \sum_{n=1}^{N} L_n = P V_{i,P} + W V_{i,W} - F V_{i,F}, \qquad \mathrm{i} = 1,2,\cdots,\mathrm{m}, \tag{A.55}$$

$$V_i = \delta U_i \sum_{i'=1}^{m} \frac{x_{i'} \ln R_j}{\delta U_{i'}}, \tag{A.56}$$

$$\delta U_i = G \frac{(\gamma_i - 1)}{(\gamma_i + 1)} \ln \gamma_j. \tag{A.57}$$

The separative work done on the target isotope is ΔU_j. If the mixture is composed of only two isotopes, the equations coincide with Eqs. A.29 − A.31. A further verification was done comparing the above separative work formula with the one introduced by de la Garza [34]:

$$\Delta U = PV_P + WV_W - FV_F \tag{A.58}$$

$$V = \sum_{i=1}^{m} \frac{x_i}{2k_i - 1} \ln R_j, \tag{A.59}$$

$$k_i = \frac{q_i - 1}{q_j - 1}. \tag{A.60}$$

It should be noted that the de la Garza's formula is limited for a cascade with an infinitesimal separation effect such as a gaseous diffusion plant. The verification may be simplified by proving the equation below:

$$\frac{\delta U_j}{\delta U_i} \cong \frac{1}{2k_i - 1}. \tag{A.61}$$

The result is listed in Table A.1. The average percentage difference is 0.00645 %. Especially, the main isotopes, ^{238}U and ^{235}U, have the same results for both formulas.

Table A.1. Verification of the separative work formula obtained using MARC with the separative work formula introduced by de la Garza. The separation factors are those of a gaseous diffusion plant.

Isotope	**^{232}U**	**^{234}U**	**^{235}U**	**^{236}U**	**^{238}U**
Separation factor	1.0072	1.0057	1.0043	1.0029	1
$\boldsymbol{\delta U_j/\delta U_i}$	0.427	0.599	1	3.017	-1
$\boldsymbol{1/(2k_i - 1)}$	0.426	0.598	1	3.026	-1
Percentage difference (%)	-0.205	-0.115	0	0.288	0

The optimization of MARC has an additional option other than determining the tails composition. As stated above, the relative abundance R_i and the new variable γ_i depend on the "key" component. On that account, the least cascade flow rate may be achieved by choosing the optimum key component (see Eq. A.33). The stage separation factor for a pair of the components may be expressed as a function of the difference between their molecular weight. For the case of the gas centrifuge process, the following approximation is used [36]:

$$q_i = q_0^{M_k - M_i}, \tag{A.62}$$

where q_0 is the overall stage separation factor per unit mass difference, M_k is the molecular weight of the key component, and M_i is the molecular weight of the i^{th} component. Thus, γ_i may be expressed as,

$$\gamma_i = \frac{q_i}{\sqrt{q_j}} = q_j^{\frac{M_k - M_i}{M_k - M_j}} = \gamma_j^{\frac{M^* - M_i}{M^* - M_j}} = q_0^{M^* - M_i}, \tag{A.63}$$

$$M^* = \frac{M_k + M_j}{2}. \tag{A.64}$$

For the case in which the number of stages in the enriching and stripping sections become infinitely large, it can be seen from Eqs. A.49 and A.50 that the components with lighter molecular weight than M^* is enriched and those with heavier molecular weight than M^* is depleted as the material flows through a cascade.

An interesting conclusion can be drawn that when the six external parameters are constant, the compositions of the product and waste streams will be same for different separation factors [85]. From Eqs. A.51 − A.53, it may be proven that $\left[\gamma_j^f\right]_{previous} = \left[\gamma_j^f\right]_{new}$ and $\left[\gamma_j^{N+1}\right]_{previous} =$

$\left[\gamma_j^{N+1}\right]_{new}$ are true if the molecular fractions of the target component in the feed, product, and waste streams are constant and only q_j is varied. Consequently, the concentrations of the other components will be same for different stage separation factors. This is shown in the equations below,

$$x_{i,P} = \frac{x_{i,F}\dfrac{1-\left(\gamma_j^{-f}\right)^{\frac{M^*-M_i}{M^*-M_j}}}{1-\left(\gamma_j^{-N-1}\right)^{\frac{M^*-M_i}{M^*-M_j}}}}{\sum_{i=1}^{m} x_{i,F}\dfrac{1-\left(\gamma_j^{-f}\right)^{\frac{M^*-M_i}{M^*-M_j}}}{1-\left(\gamma_j^{-N-1}\right)^{\frac{M^*-M_i}{M^*-M_j}}}}, \tag{A.65}$$

$$x_{i,W} = \frac{x_{i,F}\dfrac{\left(\gamma_j^{N-f+1}\right)^{\frac{M^*-M_i}{M^*-M_j}}-1}{\left(\gamma_j^{N+1}\right)^{\frac{M^*-M_i}{M^*-M_j}}-1}}{\sum_{i=1}^{m} x_{i,F}\dfrac{\left(\gamma_j^{N-f+1}\right)^{\frac{M^*-M_i}{M^*-M_j}}-1}{\left(\gamma_j^{N+1}\right)^{\frac{M^*-M_i}{M^*-M_j}}-1}}. \tag{A.66}$$

When it comes to a multicomponent mixture, minimizing the total flow rate per unit product in a cascade can be one of the strategies to optimize the cascade (see Eq. A.33). The total flow rate per unit product may be expressed in a simple equation without feed parameters and relative abundances:

$$\frac{\sum L}{P} = \sum_{i=1}^{m}\left(\frac{\gamma_i+1}{\gamma_i-1}\right)\times\left[x_{i,P}(N-f+1)-\frac{W}{P}x_{i,W}f\right], \tag{A.67}$$

$$\frac{W}{P} = \frac{x_{i,P}}{x_{i,W}}\frac{\gamma_i^{-f}-\gamma_i^{-N-1}}{1-\gamma_i^{-f}}. \tag{A.68}$$

Moreover, it may be also expressed without product and waste parameters:

$$\frac{\sum L}{P} = \frac{F}{P}\sum_{i=1}^{m} x_{i,F}\frac{\gamma_i + 1}{\gamma_i - 1}\left[\frac{1-(\gamma_i)^{-f}}{1-(\gamma_i)^{-N-1}}(N+1) - f\right], \tag{A.69}$$

$$\frac{F}{P} = \left[\sum_{i=1}^{m} x_{i,F}\frac{1-(\gamma_i)^{-f}}{1-(\gamma_i)^{-N-1}}\right]^{-1}. \tag{A.70}$$

Either way works and the selection of the equation depends on the variables that are handy.

A.4 Cascade Manipulation and Enrichment Limitation

At this point, it becomes of interest how M^* is manipulated. M^* is actually the numerical value to explain the phenomenon that is resulted from the manipulation of each stage cut. The stage cut θ_n, introduced in Eq. A.15 and shown schematically in Figure A.5, can be written in terms of the abundance ratios of the i^{th} component (see Eq. 2.71). Substituting x_k in Eq. A.71 with the stage material balance equation, one may obtain Eq. A.72.

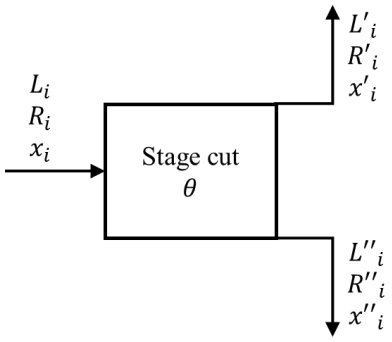

Figure A.5. A single separation stage.

$$x_k R_i = \theta x'_k R'_i + (1-\theta)x''_k R''_i, \tag{A.71}$$

$$\theta x'_k (R'_i - R_i) = (1-\theta)x''_k (R_i - R''_i). \tag{A.72}$$

Let i = jth $component$, the abundance ratio is matched in the cascade. Making use of Eq. A.39, one obtains

$$\theta = \frac{\frac{x_k''}{x_k'}}{\sqrt{q_j} + \frac{x_k''}{x_k'}} = \frac{q_i \frac{x_i''}{x_i'}}{\sqrt{q_j} + q_i \frac{x_i''}{x_i'}} = \frac{\sum_{i=1}^{m} q_i x_i''}{\sqrt{q_j} + \sum_{i=1}^{m} q_i x_i''} = \frac{\sum_{i=1}^{m} \gamma_i x_i''}{1 + \sum_{i=1}^{m} \gamma_i x_i''}. \tag{A.73}$$

Thus, the stage cut of stage n is

$$\theta_n = \frac{\sum_{i=1}^{m} \gamma_i x_{i,n}''}{1 + \sum_{i=1}^{m} \gamma_i x_{i,n}''}. \tag{A.74}$$

The concentration of i^{th} component in the stripping stream of stage *n* is

$$\left(x_{i,n}'' = \frac{\mathrm{L}_{i,n}''}{\sum_{i=1}^{m} \mathrm{L}_{i,n}''} \right)_{enriching} = \frac{x_{i,p} \frac{1 - \gamma_i^{n-N-1}}{\gamma_i - 1}}{\sum_{i=1}^{m} x_{i,p} \frac{1 - \gamma_i^{n-N-1}}{\gamma_i - 1}}, \qquad n = f, \cdots, N, \tag{A.75}$$

$$\left(x_{i,n}'' = \frac{\mathrm{L}_{i,n}''}{\sum_{i=1}^{m} \mathrm{L}_{i,n}''} \right)_{stripping} = \frac{x_{i,W} \frac{\gamma_i^{n} - 1}{\gamma_i - 1}}{\sum_{i=1}^{m} x_{i,W} \frac{\gamma_i^{n} - 1}{\gamma_i - 1}}, \qquad n = 1, \cdots, f - 1. \tag{A.76}$$

Furthermore, it is of interest to estimate the maximum enrichment of the target component since the minor isotopes are enriched as well. The solution is simple [53]. Assuming an infinite number of separation stages in the enriching section but none in the stripping section, only the isotopes lighter than M^* will be found only in the head flow.

$$x_{j,P}^{max} = \lim_{N \to \infty} \lim_{f \to 0} x_{j,P} = \frac{x_{i,F}(1 - 1/\gamma_i)}{\sum_{i=1}^{m-l} x_{i,F}(1 - 1/\gamma_i)}, \tag{A.77}$$

where l is the isotopes heavier than M^*.

A.4 Useful Equation

When the main isotopes j is enriched, the other isotopes are enriched or depleted as well. The equation for the relationship between $\Delta x_{i,P}$ and $\Delta x_{j,P}$ can be easily derived from Eq. A.49:

$$\Delta x_{i,P} = \frac{x_{i,P}\left(\frac{x_{i,P}}{x_{i,W}} - 1\right)}{\frac{x_{j,P}}{\Delta x_{j,P}}\left(\frac{x_{j,P}}{x_{j,W}} - 1\right) + \left(\frac{x_{j,P}}{x_{j,W}} - \frac{x_{i,P}}{x_{i,W}}\right)}. \tag{A.78}$$

Above equation comes handy when estimating the effect of $\Delta x_{j,P}$ to other isotopes without calculating the MARC model.

A.6 Other Calculation Options

Besides MARC theory, they exist several theories to build an optimized cascade. An optimum cascade proposed by Palkin allows the mixing of the components at the confluent points, but the value of the total flow is, in some cases, less than in corresponding MARC [86 - 92]. Also, MARC may be approximated to a squared-off cascade: It may be possible to calculate the uranium enrichment of a cascades close to an actual configuration [93 - 95]. The MARC theory, nevertheless, holds advantage over other theory: The modification is simple, and the calculation does not require a complicated computational programming. Therefore, the MARC can be considered as a golden standard of or a rough initial estimate for other enrichment theories.

APPENDIX B

MARC CODE VERIFICATION

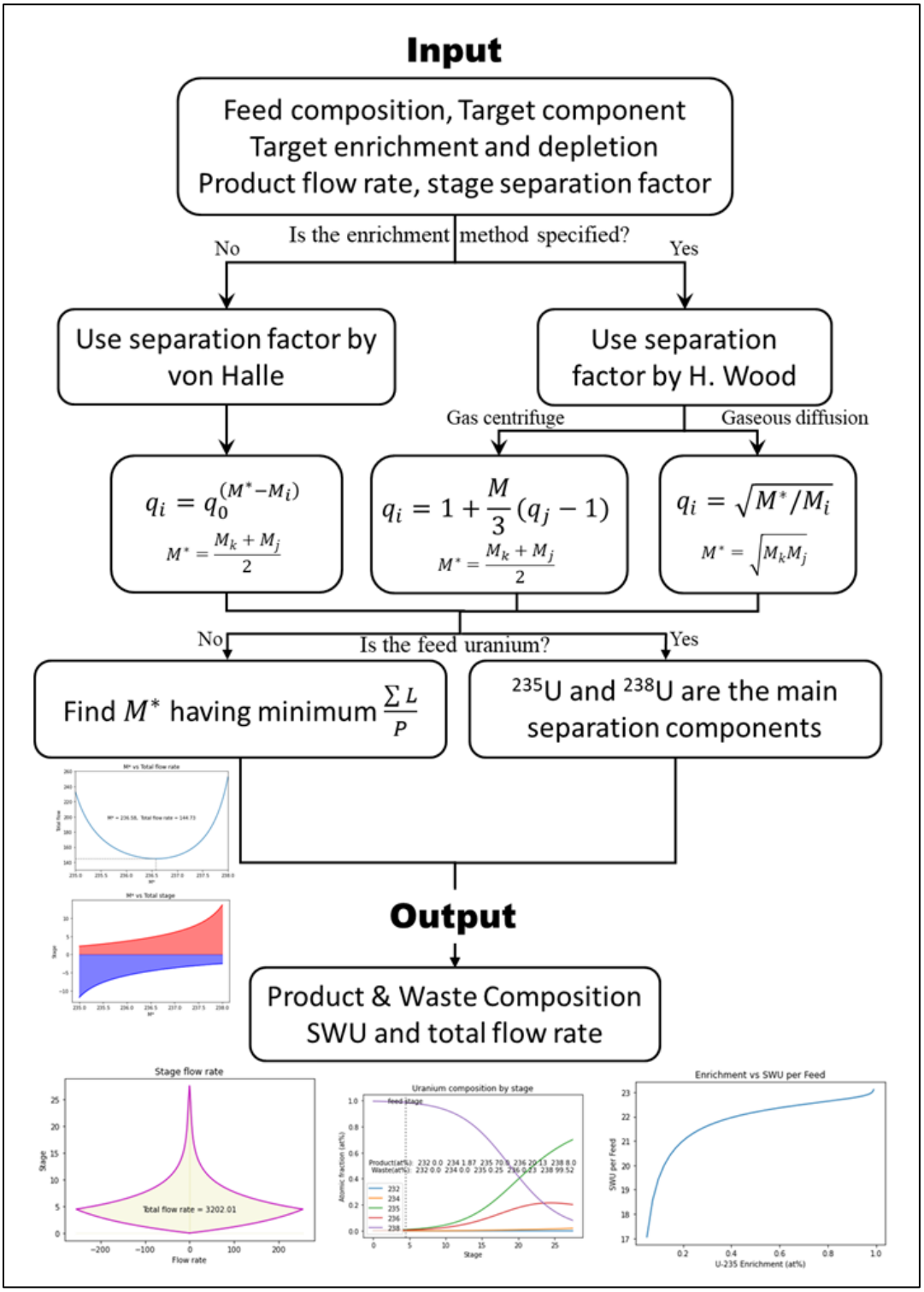

Figure B.1. MARC model flow chart.

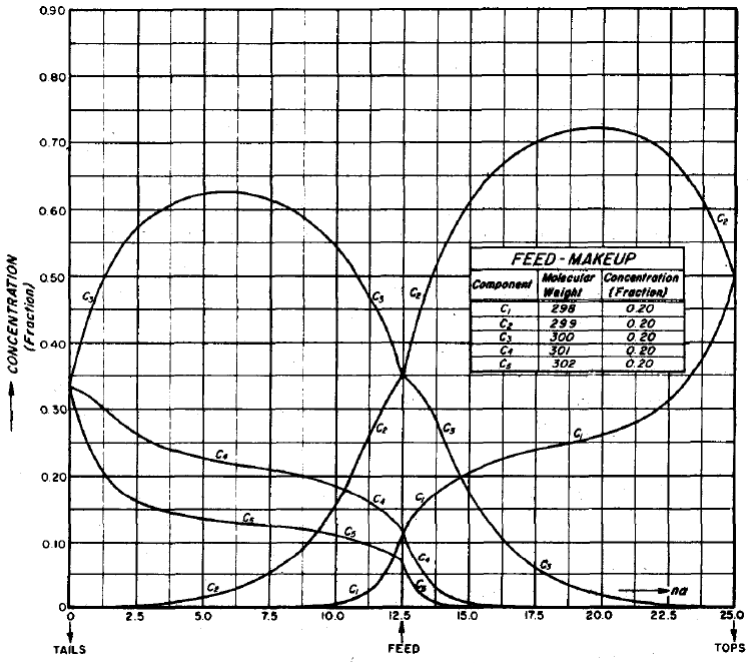

(a)

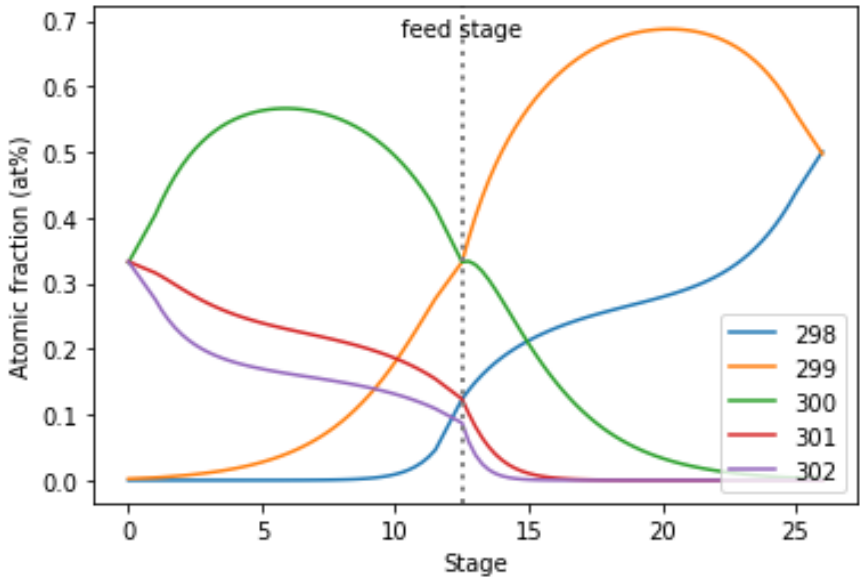

(b)

Figure B.2. Concentration gradients for cascade with M* = 299 from (a) A. de la Garza [34] and (b) MARC code. The difference in stagewise concentration between (a) and (b) comes from the different stage separation factor.

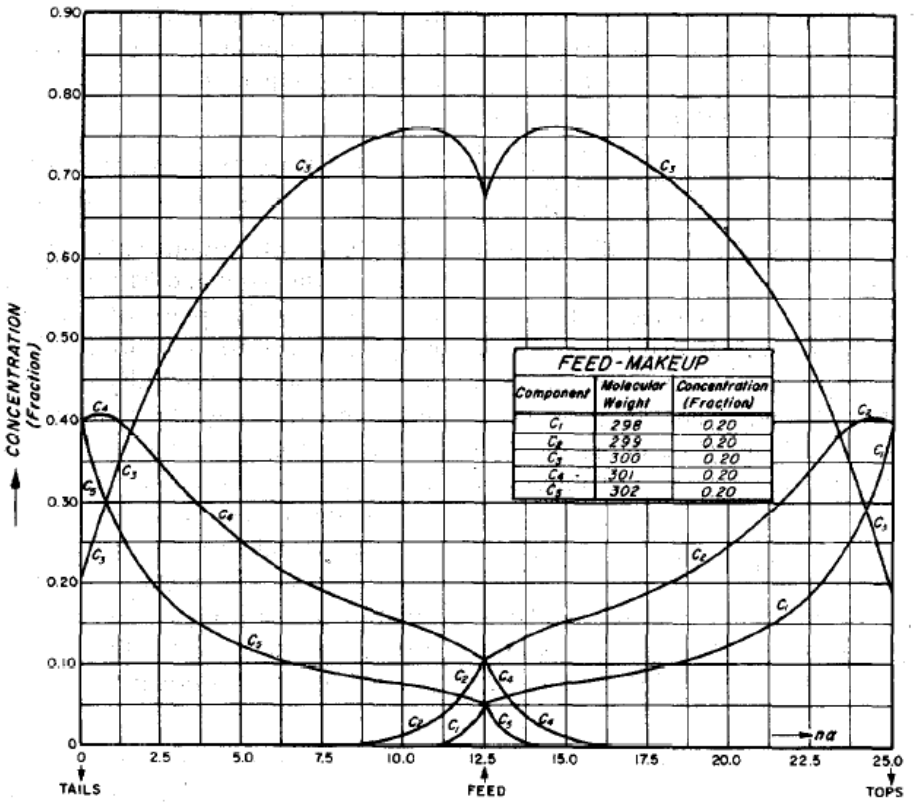

(a)

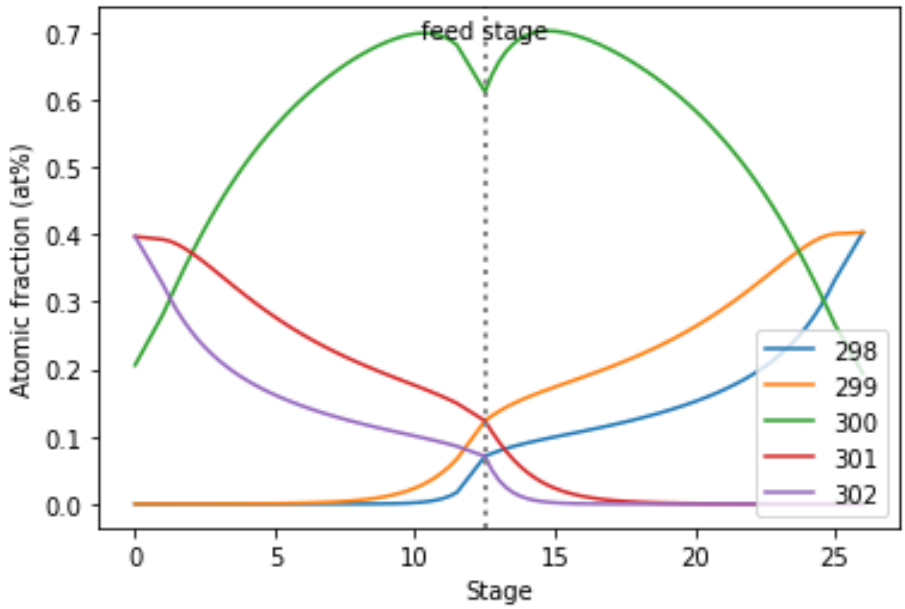

(b)

Figure B.3. Concentration gradients for cascade with M* = 300 from (a) A. de la Garza [34] and (b) MARC code. The difference in stagewise concentration between (a) and (b) comes from the different stage separation factor.

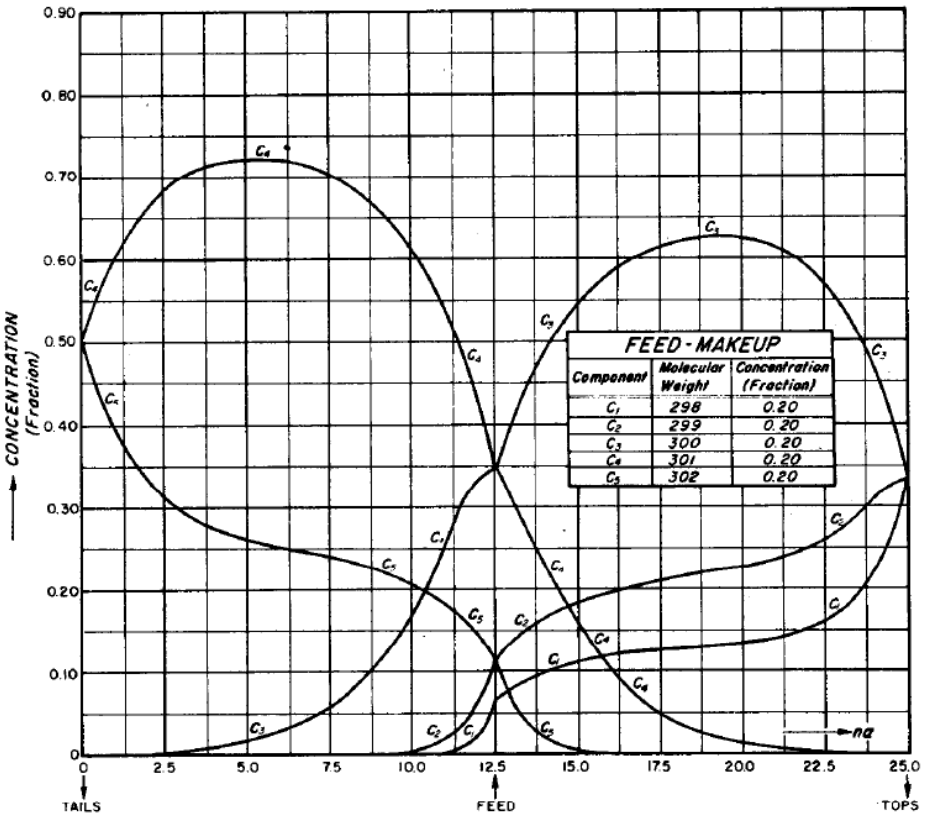

(a)

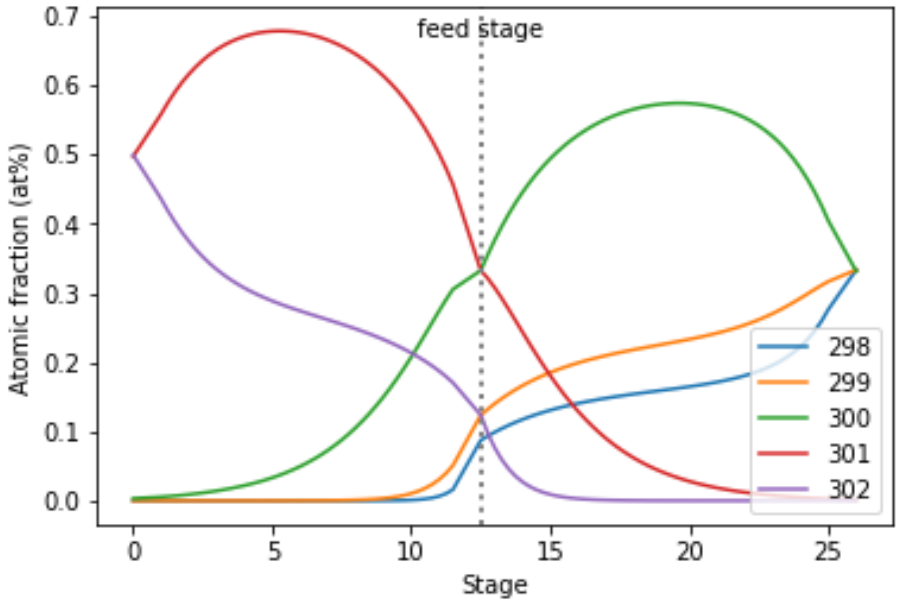

(b)

Figure B.4. Concentration gradients for cascade with M* = 300.5 from (a) A. de la Garza [34] and (b) MARC code. The difference in stagewise concentration between (a) and (b) comes from the different stage separation factor.

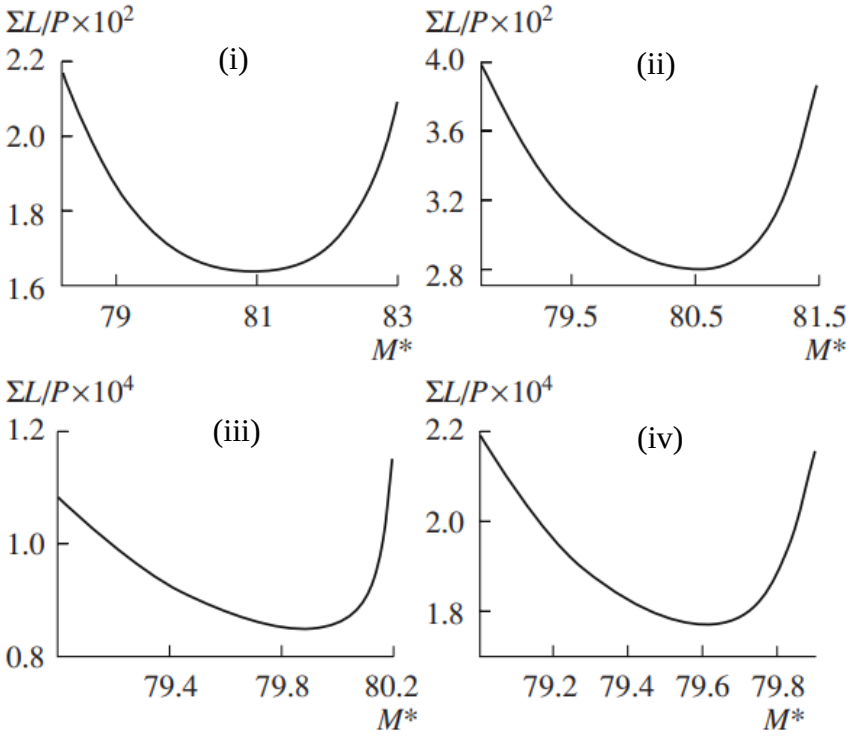

(a)

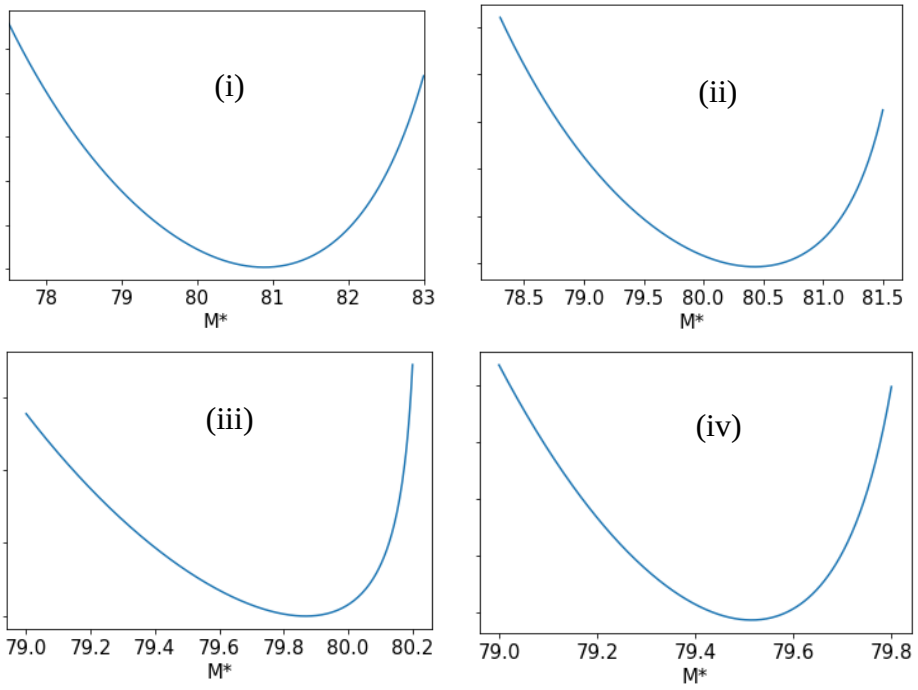

(b)

Figure B.5. Dependence of the relative total flow rate on the parameter M* for the enrichment of Kr-78 at different mole fractions of the target component in the product flow: Kr-78 at% = (i) 2, (ii) 20, (iii) 50, (iv) 90%. from (a) G. A. Sulaberidze [54] and (b) MARC code.

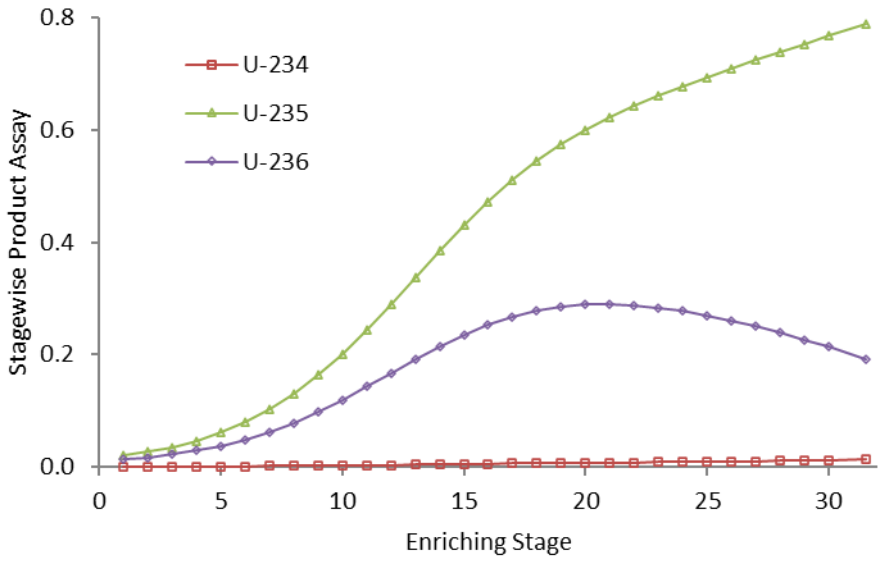

(a)

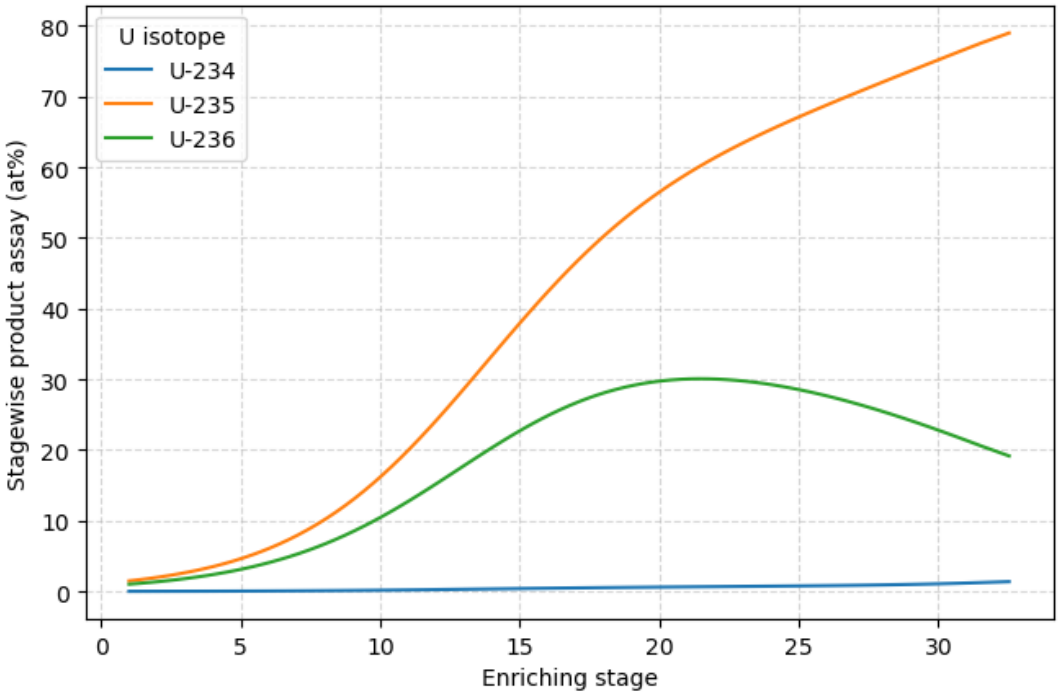

(b)

Figure B.6. Concentration gradients for cascade from (a) Weber [46] and (b) MARC code.

APPENDIX C

MINOR ISOTOPE SAFEGUARDS TECHNIQUES

The additional verification of the MARC model was carried out using the experimental data from IAEA. Instead of directly applying the model, it was modified so that the product to feed ratio was compared with the actual data. This is called the Minor Isotope Safeguards Techniques (MIST). MIST is the way of utilizing the minor isotopes for a purpose of material safeguard. The feasibility of the MIST, utilizing the ratio of ^{235}U to minor isotopes, was demonstrated by S.A. Levin et al [85]. It was further refined by A.M. Sheppard et al [42]. In this section, the MIST based on the MARC model was verified. The advantage of using MIST for material safeguard is that it reduces the input variables to $x_{^{235}U}/x_{^{238}U}$ ratio so that the inspector can compare the minor isotope composition with the actual data and estimated value. In this appendix, the estimated $x_{^{232}U}/x_{^{235}U}$, $x_{^{234}U}/x_{^{235}U}$, and $x_{^{236}U}/x_{^{235}U}$ values were compared with the experimental values obtained from IAEA [19].

The ratio of i^{th} isotope concentration to ^{235}U concentration is designated as α_i. Combining Eqs. A.65 and A.66 with Eqs. A.51 and A.52, one can easily obtain $\alpha^{Product}/\alpha^{Feed}$, $\alpha^{Waste}/\alpha^{Feed}$ and $\alpha^{Product}/\alpha^{Waste}$:

$$\frac{\alpha_i^{Product}}{\alpha_i^{Feed}} = \frac{\frac{x_{i,P}}{x_{j,P}}}{\frac{x_{i,F}}{x_{j,F}}} = \frac{\left(\frac{R_{j,W}}{R_{j,F}}\right)^{\frac{M^*-M_i}{M^*-M_j}} - 1}{\left(\frac{R_{j,W}}{R_{j,P}}\right)^{\frac{M^*-M_i}{M^*-M_j}} - 1} \frac{\frac{R_{j,W}}{R_{j,P}} - 1}{\frac{R_{j,W}}{R_{j,F}} - 1}, \tag{C.1}$$

$$\frac{\alpha_i^{Waste}}{\alpha_i^{Feed}} = \frac{\frac{x_{i,W}}{x_{j,W}}}{\frac{x_{i,F}}{x_{j,F}}} = \frac{\left(\frac{R_{j,P}}{R_{j,F}}\right)^{\frac{M^*-M_i}{M^*-M_j}} - 1}{\left(\frac{R_{j,P}}{R_{j,W}}\right)^{\frac{M^*-M_i}{M^*-M_j}} - 1} \frac{\frac{R_{j,P}}{R_{j,W}} - 1}{\frac{R_{j,P}}{R_{j,F}} - 1}, \tag{C.2}$$

$$\frac{\alpha_i^{Product}}{\alpha_i^{Waste}} = \frac{\frac{x_{i,P}}{x_{j,P}}}{\frac{x_{i,W}}{x_{j,W}}} = \frac{\left(\frac{R_{j,F}}{R_{j,W}}\right)^{\frac{M^*-M_i}{M^*-M_j}} - 1}{\left(\frac{R_{j,F}}{R_{j,P}}\right)^{\frac{M^*-M_i}{M^*-M_j}} - 1} \frac{\frac{R_{j,F}}{R_{j,P}} - 1}{\frac{R_{j,F}}{R_{j,W}} - 1}. \tag{C.3}$$

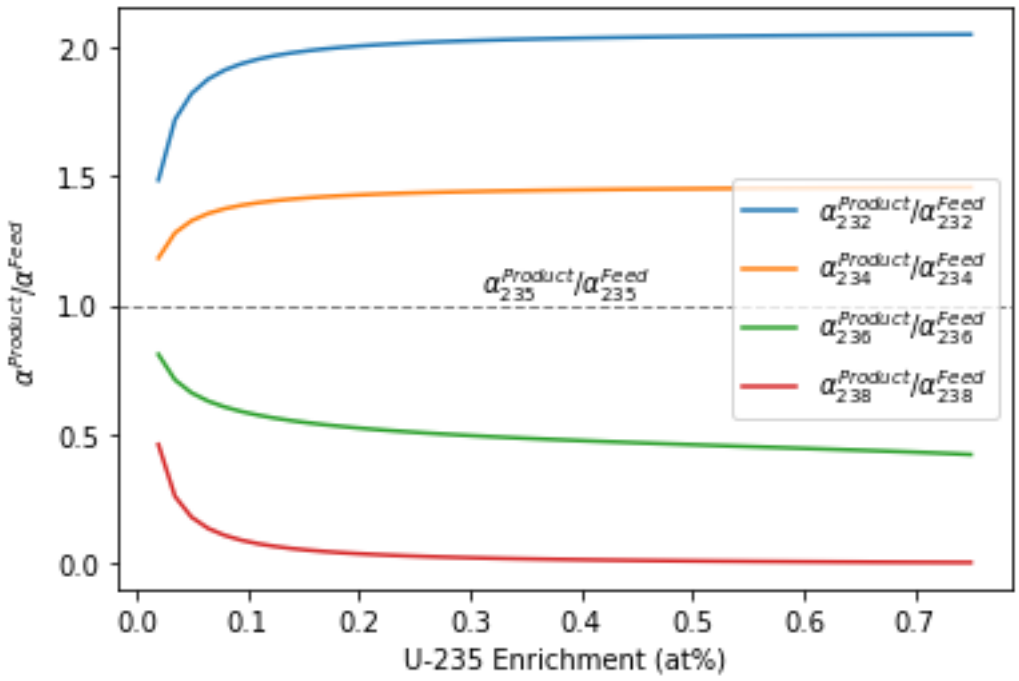

Figure C.1. $\alpha^{Product}/\alpha^{Feed}$ as a function of ^{235}U enrichment (at%) when the ^{235}U tails enrichment is kept constant.

The verification was carried out for the $\alpha^{Product}/\alpha^{Feed}$ since it is the only experimental data made public. Using the MARC model, it was able to predict that as ^{235}U enrichment increases, the $\alpha^{Product}/\alpha^{Feed}$ values of the isotopes lighter than ^{235}U increase logarithmically while the $\alpha^{Product}/\alpha^{Feed}$ values of the isotopes heavier than ^{235}U decrease exponentially. Figure C.1 shows the $\alpha^{Product}/\alpha^{Feed}$ values of each uranium isotopes when the ^{235}U tails enrichment is fixed at 0.5%.

It must be noted that the $\alpha^{Product}/\alpha^{Feed}$ values are consistent regardless of the internal parameters: This aspect makes the MIST a useful safeguard method.

Figures C.2 – C.4 compare the $\alpha^{Product}/\alpha^{Feed}$ values from the IAEA document and the MARC model. ^{238}U, ^{236}U and ^{234}U isotopes were compared respectively. ^{238}U isotope had the same value in the order of 3 decimal places. Since $(\alpha^{Product}/\alpha^{Feed})_{238}$ is γ_j^{N-f+1}, it was proven in Appendix A that γ_j^{N-f+1} is consistent as long as the external parameters are same. ^{236}U isotope also had similar values. On the other hand, the ^{234}U isotope plot displayed a noticeable difference. Eq. C.1 may account for the difference. Substituting the M_i and M^* with the actual values, below equations are obtained:

$$\frac{\alpha_{234}^{Product}}{\alpha_{234}^{Feed}} = \frac{1-\left(\frac{R_{j,W}}{R_{j,F}}\right)^{\frac{5}{3}}}{1-\left(\frac{R_{j,W}}{R_{j,P}}\right)^{\frac{5}{3}}} \frac{1-\frac{R_{j,W}}{R_{j,P}}}{1-\frac{R_{j,W}}{R_{j,F}}}, \tag{C.4}$$

$$\frac{\alpha_{236}^{Product}}{\alpha_{236}^{Waste}} = \frac{1-\left(\frac{R_{j,W}}{R_{j,F}}\right)^{\frac{1}{3}}}{1-\left(\frac{R_{j,W}}{R_{j,P}}\right)^{\frac{1}{3}}} \frac{1-\frac{R_{j,W}}{R_{j,P}}}{1-\frac{R_{j,W}}{R_{j,F}}}. \tag{C.5}$$

Since the ^{235}U tails enrichment was assumed to be between 0.3 to 0.5, the error in $R_{j,W}/R_{j,F}$ and $R_{j,W}/R_{j,P}$ that were neglectable for ^{236}U made a considerable difference in Eq. C.4. Moreover, the experiment used a squared-off cascade whereas the MARC model was based on an ideal cascade. The number of separating elements must be different.

To conclude, the MARC model was able to estimate the experimental $\alpha^{Product}/\alpha^{Feed}$ values of ^{238}U and ^{236}U but not ^{234}U. The failure to estimate the value of ^{234}U resulted from the gap between the real cascade operation and the ideal cascade operation.

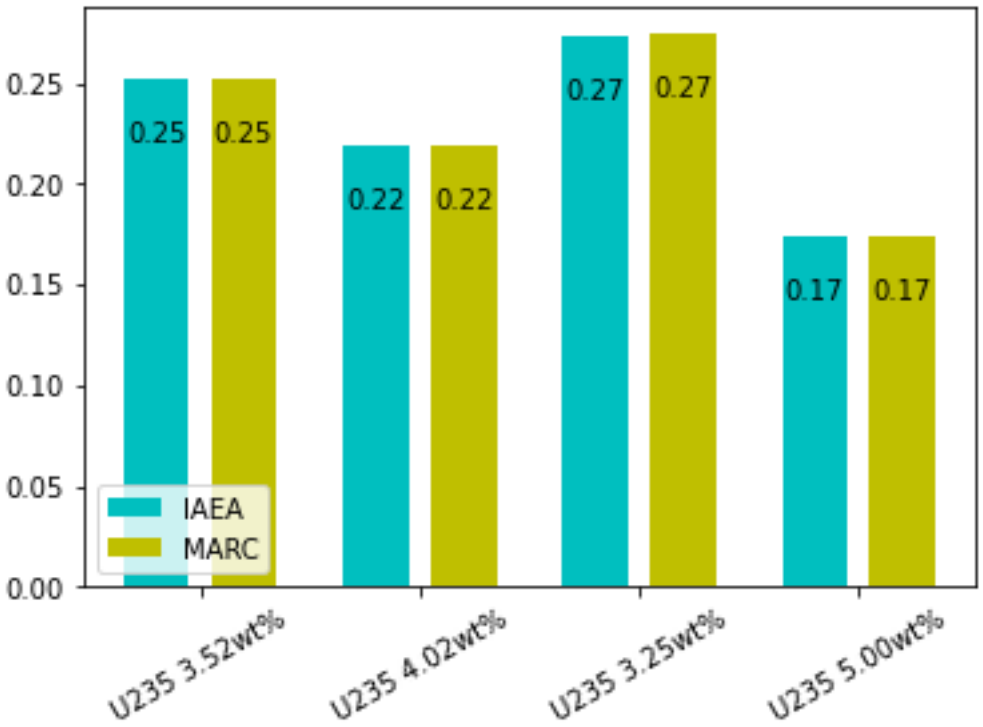

Figure C.2. Comparing $(\alpha^{Product}/\alpha^{Feed})_{238}$ values from IAEA and MARC.

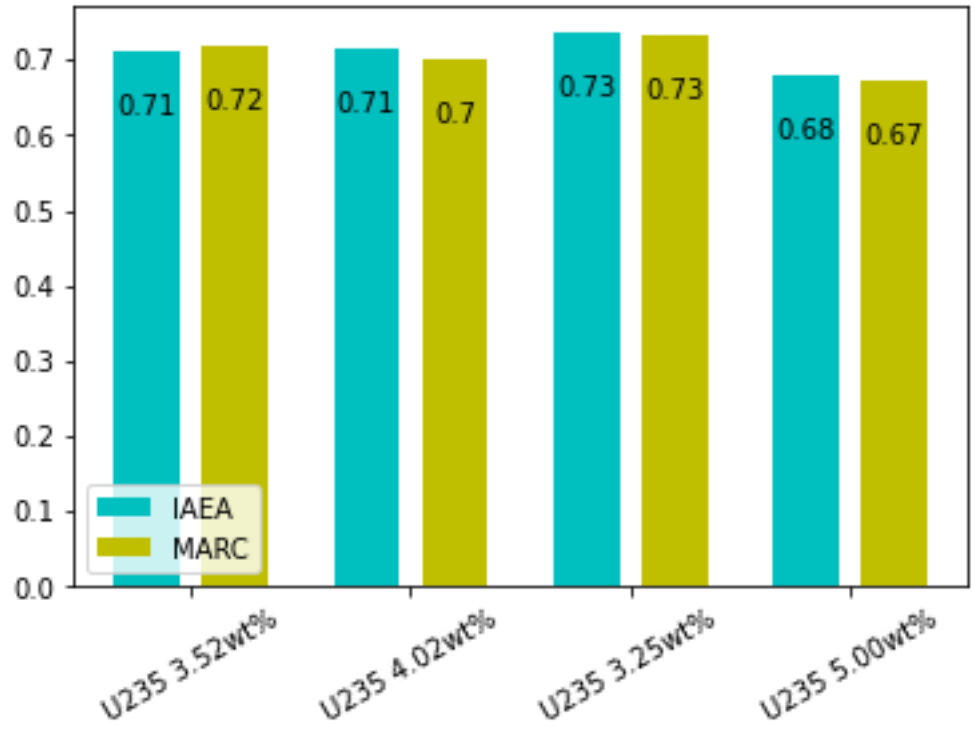

Figure C.3. Comparing $(\alpha^{Product}/\alpha^{Feed})_{236}$ values from IAEA and MARC.

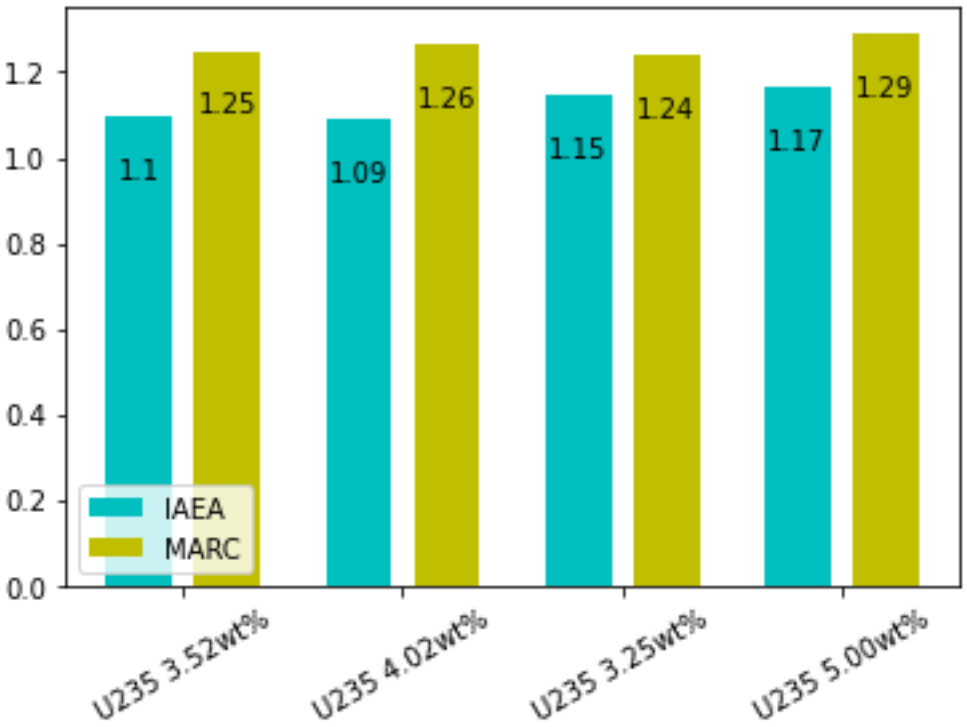

Figure C.4. Comparing $(\alpha^{Product}/\alpha^{Feed})_{234}$ values from IAEA and MARC.

APPENDIX D

CASCADE OPTIMIZATION

In this appendix, the tails enrichment optimization to build a cost-effective cascade is intensively discussed. As shown in Eqs. 2.5 – 2.14 and A.32 – A.37, the cascade optimization is to find the optimum values of x_W and M^*. However, the optimum M^* is always 236.55 as explained in Chapter 2.2 and Fig 2.1. Therefore, the tails enrichment is the solely considered for optimization. Dividing Eq. A.33 by C_F, one can get Eq. D.1:

$$\frac{C_P}{C_F} = f_{F/P}(x_{j,W}) + \frac{C_L}{C_F} f_{\sum L/P}(x_{j,W}). \tag{D.1}$$

Now, if C_L/C_F is known, the optimum tails enrichment could be estimated. Since C_U and C_F are constantly changing values depending on the world economic condition, uranium market value, etc., it is not easy to estimate C_L/C_F. Instead, C_L/C_F can be presumed to have a value that gives a minimum C_P when natural uranium is enriched to 5 wt% with the tails enrichment at 0.25 wt%:

$$\left(\frac{C_P}{C_F}\right)_{min} = f_{F/P}(x_{j,W} = 0.25\ wt\%) + \frac{C_L}{C_F} f_{\sum L/P}(x_{j,W} = 0.25\ wt\%), \tag{D.2}$$

$$\frac{C_L}{C_F} \cong 1.2417688$$

Moreover, C_F of RepU must be different and one may use the ratio between C_F^{RepU} and C_F^{NatU} to come up with the optimization equation for RepU:

$$\frac{C_P^{RepU}}{C_F^{NatU}} = \frac{C_F^{RepU}}{C_F^{NatU}} f_{F/P}(x_W) + \frac{C_L}{C_F^{NatU}} f_{\sum L/P}(x_W). \tag{D.3}$$

K. Fukuda *et al*. estimated the C_F^{RepU}: C_F^{NatU} to be 1.3:1 [32]. Finally, the optimization equations for natural uranium and RepU can be rewritten as,

$$\frac{C_P^{NatU}}{C_F^{NatU}} = f_{F/P}(x_W) + 1.24 \times f_{\sum L/P}(x_W), \tag{D.4}$$

$$\frac{C_P^{RepU}}{C_F^{NatU}} = 1.3 \times f_{F/P}(x_W) + 1.24 \times f_{\sum L/P}(x_W), \tag{D.5}$$

The results of non-waste-optimized and waste-optimized enrichment calculations are listed in Tables D.1. and D.2., respectively. For both cases, the separative work and feed per unit product reduced after each cycle. The waste-optimized case had lower separative works but higher feed requirements. Additionally, the ratio between the number of stages in the enriching section and the stripping section decreased as recycling was repeated due to the increment of minor isotopes.

It should be noted that the separative work, the amount of feed, and the number of enriching stages increase at 5th cycle. At this point, the absolute amount of ^{235}U was larger than 4th cycle but the absolute amounts of minor isotopes got over 50 % of the total amount. In turn, the weight percentage of ^{235}U became smaller than 4th cycle. Moreover, ^{236}U became one of the major isotopes in 5th cycle. M* should be reduced accordingly.

Another interesting finding was that the waste-optimized case tends to contain less amount of minor isotopes than non-waste-optimized case. Since the waste-optimized cascade send more amount of ^{236}U to the tails end, the fresh ERU fuel contained less ^{236}U. Less ^{236}U, in turn, produce less ^{232}U, ^{234}U, and ^{236}U during burnup. Therefore, at first, the waste-optimized case may seem inefficient for saving the feed. Nevertheless, as recycling is repeated, less amount of minor isotopes are formed contributing toward saving the separative work and the feed requirement, and preventing contamination of uranium.

Table D.1. Separative work per product, feed per product and the number of stages for each fuel cycle are listed in the table. The tails enrichment kept constant at 0.3 wt%.

Cycle	Waste (wt%)	SWU/P (kg-SWU/kg U)	F/P	Number of stages		Enriching and stripping ratio
				Enriching section	Stripping section	
ERU	0.25	7.97	10.23	6.72	2.58	2.60
ERU 1st recycle	0.30	3.29	3.50	8.86	12.17	0.73
ERU 2nd recycle	0.30	3.05	3.18	8.42	12.88	0.65
ERU 3rd recycle	0.30	2.54	2.61	7.41	14.39	0.52
ERU 4th recycle	0.30	2.19	2.19	6.73	16.01	0.42
ERU 5th recycle	0.30	4.67	3.33	13.07	13.73	0.95

Table D.2. Separative work per product, feed per product and the number of stages for each fuel cycle are listed in the table. The tails enrichment was optimized using Eq. D.5.

Cycle	Waste (wt%)	SWU/P (kg-SWU/kg U)	F/P	Number of stages		Enriching and stripping ratio
				Enriching section	Stripping section	
ERU	0.25	7.97	10.23	6.72	2.58	2.60
ERU 1st recycle	0.51	2.45	4.00	8.85	7.93	1.12
ERU 2nd recycle	0.56	2.15	3.65	8.37	7.93	1.06
ERU 3rd recycle	0.66	1.70	3.13	7.52	7.94	0.95
ERU 4th recycle	0.79	1.32	2.65	6.70	7.95	0.84
ERU 5th recycle	0.97	0.99	2.22	5.85	7.98	0.73

Table D.3. Uranium concentration of enriched fuels when the tails enrichment was kept constant at 0.3 wt%.

Cycle	^{232}U (wt%)	^{233}U (wt%)	^{234}U (wt%)	^{235}U (wt%)	^{236}U (wt%)	^{238}U (wt%)
ERU	0	0	4.34E-2	5.00	0	94.96
ERU 1st recycle	0	2.20E-6	0.09	5.00	1.68	93.23
ERU 2nd recycle	4.29E-9	5.92E-6	0.19	5.00	5.41	89.40
ERU 3rd recycle	1.21E-6	1.15E-5	0.36	5.00	11.96	82.68
ERU 4th recycle	2.29E-6	1.92E-5	0.63	5.00	22.26	72.11
ERU 5th recycle	7.17E-6	4.57E-5	1.52	5.00	54.05	39.43

Table D.4. Uranium concentration of enriched fuels when the tails enrichment was optimized.

Cycle	^{232}U (wt%)	^{233}U (wt%)	^{234}U (wt%)	^{235}U (wt%)	^{236}U (wt%)	^{238}U (wt%)
ERU	0	0	4.34E-2	5.00	0	94.96
ERU 1st recycle	0	2.44E-6	0.10	5.00	1.54	93.36
ERU 2nd recycle	4.85E-7	6.93E-6	0.22	5.00	4.64	90.14
ERU 3rd recycle	1.55E-6	1.45E-5	0.45	5.00	10.15	84.40
ERU 4th recycle	3.31E-6	2.65E-5	0.84	5.00	18.53	75.63
ERU 5th recycle	5.65E-6	4.34E-5	1.43	5.00	29.02	64.54